Project Report

Project Title: RDI-MOUDI-IMPROVE Intercomparison Study

Agreement number: 12-309

Project period: December 1, 2012 – August 31, 2014

Submitted to:

Mr. Leon Dolislager and Dr. Eileen McCauley
Research Division
California Air Resources Board
1001 "I" Street, 5th Floor
Sacramento, CA 95814

Phone: (916) 323-1533
E-mail: ldolisla@arb.ca.gov

Prepared by:

Prof. Anthony S. Wexler (Principal Investigator)
Dr. Peter G. Green (Co-PI)
Dr. Yongjing Zhao (Co-PI)
Dr. Michael Kleeman (Co-PI)
Dr. Chuck McDade (Co-PI)
Mr. Jose Mojica (Co-PI)
Ms. Melissa Venecek (Investigator)
Air Quality Research Center
University of California-Davis
One Shields Ave.
Davis, CA 95616-8521

Phone: (530) 754-6558
Fax: (530) 752-4158
E-mail: aswexler@ucdavis.edu

Disclaimer

The statements and conclusions in this Report are those of the contractor and not necessarily those of the California Air Resources Board. The mention of commercial products, their source, or their use in connection with material reported herein is not to be construed as actual or implied endorsement of such products.

Table of Contents

1. Report Summary 4
   Executive Summary 5
2. Introduction 7
3. Instrument Descriptions 8
   3.a.1. RDI Description 8
   3.a.2. RDI History. 10
   3.b. MOUDI Description 13
   3.c. IMPROVE Description 14
4. Site Description 16
5. Sampling Schedule 19
6. Instrument SOP Summaries 20
7. Method Detection Limits 21
8. Precision Analysis of Elements above MDL 26
   8.a. RDI-RDI. 26
   8.b. IMPROVE-IMPROVE 30
   8.c. MOUDI XRF 44
   8.d. MOUDI ICPMS 45
   8.e. MOUDI ICPMS prior observations 49
   8.f. MOUDI XRF-ICPMS 50
   8.g. RDI Stage Precision 52
9. Regression Analysis of 10 core XRF elements 61
   9.a. MOUDI vs IMPROVE 61
   9.b. RDI vs IMPROVE 63
   9.c. RDI vs MOUDI 75
   9.d. Time Series 79
   9.e. IMPROVE (PM2.5) ICP-MS vs MOUDI (PM1.8) ICP-MS 90
10. Regression Analysis of all XRF Elements 93
   10.a. Tier 1 Comparison. 94
   10.b. Tier 2 Comparison 98
   10.c. Tier 3 Comparison 101
11. RDI-MOUDI size distribution comparison 102
12. Conclusions 107
13. References 110

Appendices
A. RDI SOP A-1
B. MOUDI SOP B-1
C. ICPMS SOP C-1

1. Report Summary

Project Title: RDI-MOUDI-IMPROVE Intercomparison Study

Project PI: Anthony S. Wexler Ph.D., Professor
Project Co-PIs: Dr. Peter Green (Co-PI)
Dr. Yongjing Zhao (Co-PI)
Dr. Michael Kleeman (Co-PI)
Dr. Chuck McDade (Co-PI)
Mr. Jose Mojica (Co-PI)
Ms. Melissa Venecek (Investigator)

Contact Information: Air Quality Research Center
University of California
One Shields Ave
Davis, CA 95616

E-mail: aswexler@ucdavis.edu
Phone: (530) 754-6558
Fax: (530) 752-4158

Project Deliverables: Comparison of the RDI, IMPROVE, and MOUDI Samplers

Project Period: December 1, 2012 to August 31, 2015

Project Funds: $153,812

Brief Summary: The Rotating Drum Impactor (RDI) is designed to collect particle size and temporally resolved airborne particle samples. Although several generations of RDI instruments have been used for a wide range of atmospheric field studies, to date there has not been a study to characterize its performance. This study was designed to characterize the performance of the latest generation of the RDI sampler. Airborne particulate matter was collected at the IMPROVE sampling station on the roof of Ghausi Hall, UC Davis, during the winter and summer of 2013. Two RDI samplers, two IMPROVE samplers, and two MOUDI samplers were deployed for both seasons. The RDI samples were scanned using synchrotron X-rays from the Advance Light Source (ALS), Lawrence National Berkeley Laboratory, to obtain X-ray Fluorescence (XRF) spectra. IMPROVE samples were analyzed using Panalytical XRF instruments using the IMPROVE protocol, then analyzed using ICPMS. One set of the MOUDI stage samples was analyzed by XRF using the IMPROVE protocol on the same Panalytical instrument, and then analyzed by ICP/MS. Intra-instrument comparisons are provided to elucidate precision; inter-instrument comparisons are presented to show accuracy. The RDI + s-XRF analysis technique precisely measured 35-40% and 5-20% of elements above stated MDLs in winter and summer, respectively. A gap was found in the size distributions measured by the RDI; the cause is under investigation. This gap calls into question the validity of the RDI size distribution measurements. Identical gaps in both instruments indicate a design or manufacturing flaw in this version of the RDI. Assessment of RDI stage precision indicates that longer sampling times should be employed under clean conditions. The IMPROVE + XRF analysis technique precisely measured 78% of elements present above stated Minimum Detection Limits (MDLs) in winter and 42% of elements above MDL in summer. The MOUDI + XRF analysis technique precisely measured 33% and 37% of elements above stated MDLs in winter and summer, respectively. The MOUDI + ICPMS analysis technique precisely measured 62% and 91% of elements above stated MDLs in winter and summer, respectively.

Executive Summary

The Rotating Drum Impactor (RDI) is designed to collect particle size and temporally resolved airborne particles. Although several generations of the RDI instruments have been used for a wide range of atmospheric field studies, to date there has not been a study to characterize its performance. This study was designed to characterize the performance of the latest generation RDI instrument. Airborne particulate matter was collected at the IMPROVE (Interagency Monitoring of Protected Visual Environments) sampling station on the roof of Ghausi Hall, UC Davis, during the winter and summer of 2013. Two RDI samplers, two IMPROVE samplers, and two MOUDI (Micro-Orifice Uniform Deposition Impactor) samplers were deployed for both seasons; data from only one MOUDI sampler is available, so far, for this study. The RDI samples were scanned using synchrotron X-rays from the Advance Light Source (ALS), Lawrence National Berkeley Laboratory, to obtain X-ray Fluorescence (XRF) spectra. IMPROVE samples were analyzed using Panalytical XRF instruments using the IMPROVE protocol, then analyzed using Inductively Coupled Plasma Mass Spectrometry (ICP/MS). One set of the MOUDI stage samples was analyzed by XRF using the IMPROVE protocol on the same Panalytical instrument, and then analyzed by ICP/MS. Intra-instrument comparisons are provided to elucidate precision; inter-instrument comparisons are presented to show accuracy.

The following conclusions derive from this work:

1) **RDI PM2.5**
20 elements were above the stated S-XRF MDLs for the RDI sampler in both winter and summer. The RDI3 sampler precisely measured 7 elements (35%) in the winter and 4 elements (20%) in the summer; RDI7 sampler precisely measured 8 elements (40%) in winter and 1 element (5%) in summer. The RDI has a bias for some elements in that the temporal patterns generally match those of the other instruments but the magnitudes are different and probably incorrect (e.g., Na in Figure 9d1; Si in 9d12). This difference is likely not a flow rate calibration problem because the magnitudes of other elements match quite well. Other elements are uncorrelated to IMPROVE and MOUDI.

2) **RDI Size Distributions**
Despite passing precision tests and accuracy tests for PM2.5 (see sections of the report for definitions of precision and accuracy employed here), the particle size distributions reported by the RDI were unrealistic in both the winter and summer seasons. The RDI size distribution was shown to be qualitatively implausible since size distributions with a gap around 0.2μm are generally not observed in the atmosphere. In addition, using the size-dependent deposition efficiency measurements of Raabe and coworkers (1988), it was shown that the gap in the size distribution measurements at this stage are implausible, indicating a problem associated with this stage. As of this writing, the cause of this problem is still being investigated. Since impaction on this stage is incorrect, impaction on subsequent stages is probably also in error.

3) **IMPROVE PM2.5**
The stated MDLs for the IMPROVE sampler and XRF analysis technique are optimistic. 18 elements were measured above stated MDLs in winter and 19 elements were measured above MDLs in summer. Of these, 14 elements (78%) passed precision tests between the two co-located IMPROVE samplers for the winter and 8 elements (42%) passed the precision test between the two IMPROVE samplers for the summer. This leads to the

conclusion that the actual IMPROVE sampler + XRF MDLs are greater than stated and that more elements are actually below MDL than would be expected based on the stated MDL values. XRF appears to be quite precise so the disagreement is due to sampler performance differences. This is a known shortcoming of the IMPROVE sampler (Hyslop and White, 2011).

4) **MOUDI XRF PM1.8**
18 elements were above the stated XRF MDLs for the MOUDI sampler in winter and 19 elements were above the MDLs during the summer. Of these, 6 elements (33%) passed the precision tests between a co-located MOUDI + XRF and IMPROVE + XRF sampler during the winter and 7 elements (37%) passed the precision tests between the MOUDIs + XRF and IMPROVE + XRF sampler during the summer. The MOUDI PM1.8 size fraction should be comparable to the IMPROVE PM2.5 because the elements are from high temperature sources so should have negligible mass in the 1.8 to 2.5 μm size range. This lack of agreement may reflect the need for appropriate size-resolved correction factors to account for XRF response to different particle diameters on different impactor stages (Formenti et al., 2009). No size-resolved MOUDI + XRF corrections were applied in the current study.

5) **MOUDI ICP/MS PM1.8**
13 elements were above the stated ICP-MS MDLs for the MOUDI sampler in winter and 11 elements were above the MDLs during the summer. Of these, 8 elements (62%) passed the precision tests between a co-located MOUDI + ICPMS and IMPROVE + ICPMS sampler during the winter and 10 elements (91%) pass the precision tests between a MOUDI + ICPMs and IMPROVE + ICPMS sampler during the summer. The closer agreement between the expected MDLs and the actual performance of the co-located samplers suggests that the stated MOUDI + ICP-MS MDLs are more realistic than the stated MOUDI + XRF MDLs, but still somewhat optimistic.

6) **MDLs**
Under the low concentration conditions present during this study, none of the instruments could precisely measure 100% of the elements that were above stated MDL for either XRF or ICP-MS. Investigators should assess their MDLs and consider longer collection times under low concentration conditions.

2. Introduction

Rotating Drum Impactors (RDI) and similar instruments have been used by ARB contractors and other state and federal agencies to measure the size distribution of particulate elements. These measurements have helped identify the sources of particulate matter in California and other regions of the country and abroad. Yet to date, only two published studies have characterized the RDI-style samplers (Raabe et al. 1988; Bukowiecki et al., 2009). Raabe and coworkers characterized an earlier version of the instrument, while Bukowiecki modified the drum of an RDI before characterizing. Raabe found narrow particle collection size cuts while Bukowiecki found broad particle collection size cuts. Thus, the RDI obtains near-continuous measurements of size resolved particulate metals for months at a time but the accuracy and precision of the measured size distribution is unknown. The purpose of this study is to investigate the accuracy and reliability of the RDI measurements in terms of time, size and metal quantification.

Particle collection by impaction is characterized by their cutpoint (the size where 50% deposit, called the D50) and the slope of deposition curve at this cutpoint. For particles much greater than the D50, a large fraction deposit on the collection surface and for particles much smaller than the D50, very few particles deposit (see Figure 2.1). To obtain the size distribution of particles, cascade impactors are used that have a series of impaction staged with D50 values spaced evenly over the range of particle sizes to be measured. If the spacing between adjacent stages is small compared to the slope of the collection efficiency curve, a substantial number of particles may deposit on adjacent stages instead of the designated one. The RDI size cut slopes are likely much broader than those for the MOUDI and IMPROVE samplers so these other instruments were used to characterize the RDI performance.

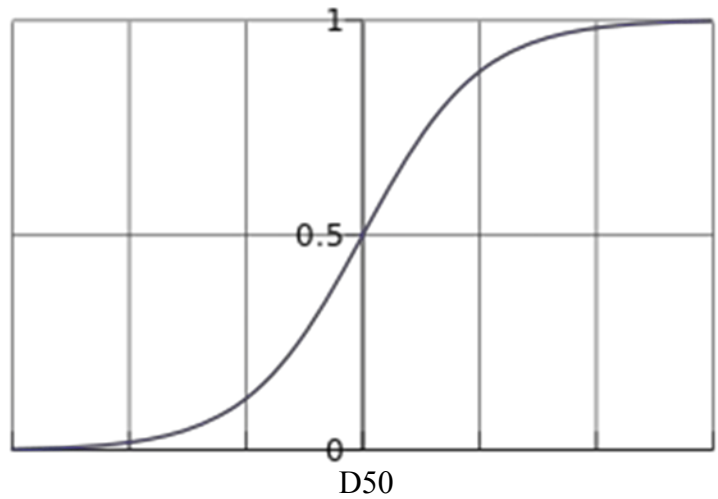

Figure 2.1. Typical deposition efficiency curve.

3. Instrument Descriptions

3.a.1. RDI Description

Rotating drum impactor (RDI) sampler: Two RDI samplers were operated side-by-side on the roof of Ghausi hall. The RDI sampler was developed and constructed at University of California-Davis (UC Davis) based on the basic design of Lundgren (1967) and has evolved significantly from the original drum impactor as described by Raabe et al. (1988). In the present study, the 4th generation design of an 8-stage RDI sampler was used to collect ambient particles. Figure 3.1 is a photo of the 8-stage RDI sampler showing the visible components inside its enclosure, including (1) power and battery backup, (2) electronic control box, (3) relative humidity and temperature (RH/T) sensor, (4) differential pressure probe between stages 2 and 3, (5) bottom part of the inlet tube, and (6) drum

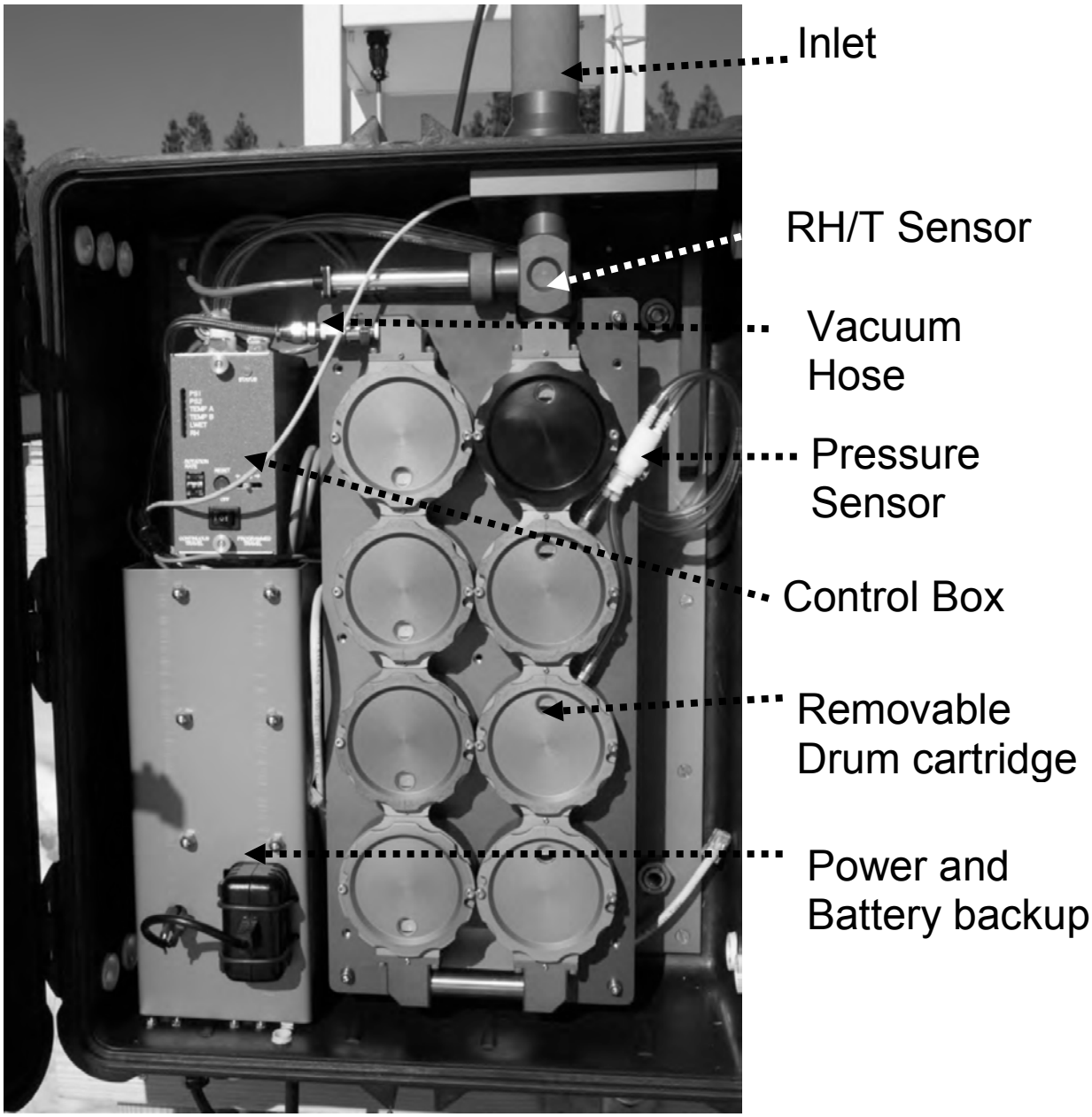

Figure 3.1. Photo of the 8-stage RDI sampler inside its enclosure.

cartridges. Behind the cartridge assembly, there is a programmed stepper motor and driving mechanism, a data-logger, and a network adapter. The data logger records inlet RH/T, differential pressure between stages 2 and 3 (sample flow rate), pressure at the external pump inlet, and drum angular position, and also controls RH by switching on/off an inlet heater. The network adapter enables connection of the RDI to external computers by which the RDI's operational status can be monitored remotely. The most important improvement of the 4th generation RDI is the sample cassette, which houses the sampling drums and sampled substrates in isolated compartments. While the driving mechanism remains within the sampler enclosure, the cassette with isolated samples is removable. This new feature is especially important because substrates are not exposed in the field (potentially contaminating them), so that sample collection and data retrieval efficiencies approach 100%.

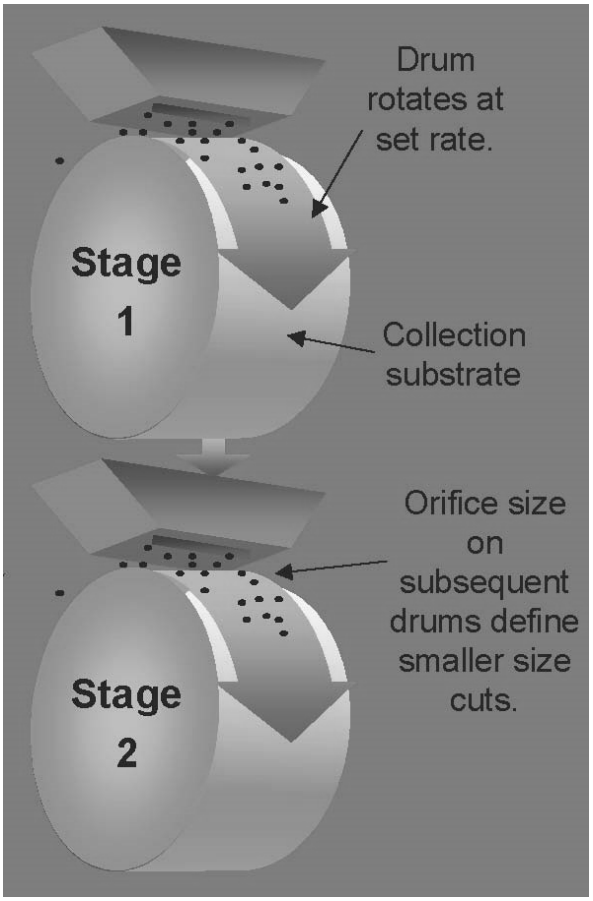

Figure 3.2. Schematic of particle collection on RDI strips.

The RDI is a cascade impactor operated at 16.7 L/min airflow rate drawn by an external pump and coupled to a 10 µm cut-point (PM10) inlet. Figure 3.2 illustrates the particle impaction on rotating drums in two consecutive stages. The geometry of the slit orifice above the drum and the airflow rate determine the particle size cut-point of each stage. Particles deposit on the collection substrate on the drum when their aerodynamic diameter is greater than the cut-point. Particles with aerodynamic diameter smaller than that cut-point enter the next stage with the air stream and undergo size selection again by the following slit orifice. The 8-stage RDI sampler collects particulates continuously on 8 drums in 8 size ranges (i.e., 10-5, 5-2.5, 2.5-1.15, 1.15-0.75, 0.75-0.56, 0.56-0.34, 0.34-0.26, and 0.26-0.09 µm) with programmable time resolution of 0.4 to 48 hours (corresponding to about 0.75 to 96 weeks sampling duration), which was preset depending on the expected particle loading. In the present study, the time resolution was 3 hours (approximately 6 weeks duration).

The RDI sampler stages were engineered, based on theoretical calculations of aerodynamic collection efficiency, to select the particle sizes. Pressure differential between stages is one quantity measured to verify compliance with the designed airflow flow rate. Multiple studies comparing results from the current RDI sampler to EPA approved PM2.5 and PM10 samplers have been published revealing less than 10% bias for PM10 and PM2.5 elements (Perry et al., 2004; Cliff, 2005). Additionally, samplers preceding the current RDI (with similar physical parameters) have been fully calibrated and published (Raabe et al., 1988) and the uniformity of the sample deposit, which relates to analytical

quality assurance, has been established (Bench et al., 2002). The current study further explores the RDI sampler performance in terms of precision and accuracy.

Synchrotron X-ray Fluorescence (XRF) analysis: The RDI samples were analyzed by XRF (Knochel, 1990) using a broad-spectrum X-ray beam generated on beamline 10.3.1 at the Advanced Light Source (ALS), Lawrence Berkeley National Laboratory. The ALS XRF system is capable of high sensitivity detection of elements ranging from sodium to uranium (Perry et al., 2004). The XRF analysis of the RDI samples provides quantitative elemental data for approximately 28 elements. Of the 28 elements analyzed in that study, approximately 18 were well-quantified due to their sufficiently high ambient atmospheric concentrations while the concentrations of the remaining 10 elements were often too low to be quantified.

The X-ray beamline was collimated prior to entry into the sample chamber and plane polarized, which greatly reduced the background signal and greatly improving the signal-to-noise ratio. Quantitative analysis was performed by calibrating with a comprehensive set of 40 single- and multi-element standards from National Institute of Standards and Technology (NIST) traceable standards (Micromatter, Inc., Vancouver, Canada). An inter-laboratory comparison between Desert Research Institute and UC Davis of ambient particulate samples showed no significant bias for major elements (i.e., those significantly above minimum detectable limit) (Cliff, 2005). Tests have shown that the sample deposit on the RDI sampler is extremely uniform orthogonal to the time axis (Bench et al., 2002). De-convolution of the raw XRF spectra is performed using WinAxil software (Canberra, Brussels, Belgium).

3.a.2 RDI History

Impaction - DRUM Samplers

(a) Early work - 1969-1979

In 1967, Dale Lundgren mated the well-characterized slotted impactor to a moving impaction substrate on a slowly rotating drum, the 5 stage high flow 110 l/min “Lundgren Impactor” (Lundgren 1967). The advantage of this scheme is that time is retained along the circumference of the drum by using a removable substrate, on the impaction medium. Mass was impossible to measure, and chemical analysis by standard methods proved difficult, but the sensitivity of proton induced x-ray emission (PIXE) allowed analysis of samples for a large suite of elements, Na through Pb. An early major use was for studies of California freeways (Feeney et al., 1975). A modification of the Lundgren impactor, the 3 stage Multiday impactor, was used for the large California Air Resources Board aerosol network, a 14 site network that, in 4 years of operation, gathered 14,400 samples in 3 size modes with full compositional analysis, 1973-1977 (Flocchini et al., 1976, Barone et al., 1978, Motallebi et al., 1992) as well as special studies (Ashbaugh et al., 1981; Flocchini et al., 1981, Barone et al., 1984).

(b) Development of Jetted DRUM Sampler - 1985-1987

In response to a growing need for size and compositionally resolved samples for the National Park Service, a new sampler was designed in 1985 (Cahill et al., 1985), modified and calibrated (Raabe et al., 1988). This sampler was based upon a single jet, and since it operated at only 1 L/min, delivered a very small amount of mass suitable only to focused analysis systems such as a PIXE milliprobe. This unit, the Davis Rotating-drum Unit for

Monitoring (DRUM) was used extensively 1986 through 1998 for studies in Los Angeles (Cahill et al., 1989), Kuwait (Reid at al,, 1995) and the national parks (Cahill and Wakabayashi, 1996, Perry et al., 1997), among other studies. Still, the very small amount of mass limited usefulness to relatively polluted conditions, while the line deposit was difficult to quantify, thereby limiting precision.

Development of Slotted DRUM Sampler - 1987 - Present

(c) RB Monitoring Sampler MSAM 1988-1990

In response to the need for small, inexpensive aerosol samplers that could monitor major parameters associated with acidic species in remote areas of California, the Modular System for Acidic deposition Monitoring, or MSAM, (MSAM, 1993) was developed using a combination of filters and a slotted 2-stage rotating drum impactor. The unit was designed, built, tested and field evaluated as part of the ARB Acid Deposition program, but was not widely deployed before the program was terminated. However, the MSAM remains both the smallest IMPROVE-protocol sampler ever built, 25 cm x 15 cm x 8 cm, and the smallest DRUM impactor. Its technical successes led, however, to the IMPROVEd DRUM (below).

(d) IMPROVEd DRUM 1992 - Present

In 1992, a new impactor was designed for visibility studies in the IMPROVE program (Malm et al., 1984). In it, three size classifications were achieved designed to match the needs of Mie Theory for visibility; 2.5 > Dp > 1.15 μm, 1.15 > Dp > 0.34 μm, and 0.34 > Dp > 0.1 μm, plus an integrating afterfilter intended to collect particles < 0.34 μm. The coarsest particles, while optically efficient, are too few in number to have much effect on visibility by the $1/r^3$ dependence on number and mass. The middle group is the heart of light scattering, with very high optical efficiency/particle proportional to $1/r^2$. In addition, this mode is the peak of the Accumulation Mode (Whitby et al., 1975) and has high mass and many particles. The finest stage normally possesses many particles, but since the 0.34 μm cut point is set where Qscat = 1.0 and dropping rapidly, the particles are highly inefficient in scattering light. This sampler, because it deposits a 6 mm wide strip instead of a line, is much easier to analyze and has far better precision than the jetted drum configurations (Cahill et al., 1995) due to the relatively homogenous deposition in the width of the deposit. Finally, the increased flow of 10 L/min gives 10 times more mass to analyze than the 1.0 L/min jetted DRUM. An example of data resulting from this instrument is found in (Perry et al. 1999) in which the increased mass allowed operation even in the very clean conditions at the NOAA Mauna Loa Observatory, at 3.4 km elevation.

(e) DELTA 8 DRUM 1999 - Present

In 1999, the DELTA Group at UC Davis began a process to convert an existing jetted 8 drum impactor to the slotted configuration building upon the IMPROVEd 3 DRUM design. Professor Otto Raabe performed aerodynamical modeling for 6 mm slots, generating cut points that better met the needs of Mie Theory than the jetted DRUM, with the increased flow to 10.8 L/min and the better precision of the IMPROVEd DRUM (Raabe, private communication).

Table 1 Parameters of the DELTA DRUM Slotted Drum Impactor

The width of the mass at full width, half maximum, W mass, represents the measured footprint of a non-rotating DRUM, accurate to about + 15%. This results in a resolution in time using a 42 day rotation period (4 mm/day) given in T (hr). The after filter was not used in this work.

Stage No.	W (s) cm	L Cm	S cm	P out kPa	Re	u out m/s	ECD ae, μm	W (d) μm	ΔTime hr
1	0.360	0.6	1.44	101.3	2231	7.7	5.0	750	4.5
2	0.163	0.6	0.65	101.1	2810	17.1	2.5	500	3.0
3	0.073	0.6	0.29	100.2	3195	38.3	1.15	300	1.8
4	0.049	0.6	0.20	98.3	3331	58.3	0.75	265	1.6
5	0.038	0.6	0.15	94.9	3416	77.4	0.56	240	1.4
6	0.026	0.6	0.11	86.8	3575	122.2	0.34	245	1.8
7	0.024	0.6	0.10	75.1	3692	156.0	0.26	180	0.9
8	0.021	0.6	0.10	39.7	4595	315.9	0.09	175	0.9
filter									

This impactor (along with an IMPROVEd DRUM) was deployed in the BRAVO study in Big Bend NP, July - October 1999, and operated with essentially no loss of samples. The time resolution was obtained by the size of the analytical beams used, and could be high as 1 hour when analyzed at the synchrotron x-ray fluorescence microprobe of the Advanced Light Source, Lawrence Berkley NL.

In 2000, at the request of ARB, for their study at the Fresno Supersite, the DELTA Group modified to directly match the 16.7 liter/min flow of standard PM10 heads. The DELTA Group accomplished this modification by extending the length of the orifice slot (i.e. make a larger rectangle) without changing any other engineering parameters. In this modification the orifice width remains constant and thus the impaction characteristics are expected to be identical to the 6mm wide orifice shown in Table 1 (Raabe, personal communication). A jetted DRUM would not allow such modification, as increasing the orifice diameter would result in both additional flow and changed cutpoints.

(f) DELTA 3-DRUM 2000 - Present

For the National Science Foundation-funded ACE-Asia program, 10 new 3 DRUM samplers were purchased from Integrity Manufacturing, Inc. (Research Triangle Park, NC) with revised parameters. The flow was raised to 23 l/min by lengthening the slots of the IMPROVEd DRUM while keeping all other parameters fixed. The flow was designed to match the IMPROVE cyclone, which was then added as a pre-cut to the sampler at 2.5 μm.

(g) Rotating DRUM Impactor Sampler 2002-present

Under National Oceanic and Atmospheric Administration and Air Resources Board funding, we developed and constructed several proprietary aerosol impaction samplers similar to that deployed at Fresno noted above. The current (4th) generation 8-Stage Rotating DRUM Impactor Sampler (8-RDI) used first in this work is a cascade impactor based on the basic design of Lundgren (1967), and evolved from the original DRUM impactor as described by Raabe et al. (1988). The 8-RDI sampler operates at 16.7 liters per minute allowing it to couple to a 10 μm cutpoint ("PM10") inlet. The aerosol sample for each stage is deposited onto a rotating drum faced with a removable greased Mylar impaction surface for s-XRF analysis. As the drum rotates, a continuous aerosol sample is laid down along the direction of rotation with density varying along the length of the substrate in proportion to the aerosol collected as the substrate rotates. By replacing the circular jets of the

original DRUM sampler with slits, the aerosol deposit is made uniform crosswise to the direction of rotation and the total deposit is spread over a known area per unit time (Bench et al., 2002). With the drums for all stages of the impactor geared together, coincident samples are collected on all eight stages. Analysis using narrow beam techniques (i.e. s-XRF) for quantitative elemental analysis produces data with time resolution proportional to the ratio of drum surface speed divided by the beam width. Typical sampling during this work allowed 42-day continuous record in 8 size bins (See Table 2) for analysis in 3-hr time steps in each sampling period. Aside from a defined cutpoint inlet and rectangular orifice, this sampler incorporates a stepper motor control, diagnostic testing for temperature, humidity, flow rate and pressure, a Campbell data-logger, and battery backup. These recorded sampler diagnostics are retrievable via direct connection during or following sampling in the field. Routine sampler audits are able to verify compliance with sampling parameters.

Table 2. Particle Size Ranges for each RDI Stage

Stage	Size Range [µm]
1	10-5
2	5-2.5
3	2.5-1.15
4	1.15-0.75
5	0.75-0.56
6	0.56-0.34
7	0.34-0.26
8	0.26-0.09

The most important feature of this sampler design is the sample cassette which houses the substrates. The sampler has a separate drive and sampling mechanism that can be removed in the field without exposing the substrates. The drive mechanism remains with the mounted sampler enclosure. The cassette is loaded with unexposed substrates in the laboratory and shipped to the sampling location with the sampler enclosure, drive mechanism and electronics remaining mounted at the site. This feature is especially important and useful for the extended sampling periods used in studies where multiple sites and/or remote locations are necessary. Since substrates are only handled in the laboratory, sample and data retrievals approached 100%. Also, because the sampling is continuous and preprogrammed for sampling duration, the sampler operates autonomously with little or no operator interaction. The sampler consists of a self-contained package of sampling cassette, drive system, diagnostics and electronics and an externally located pump.

3b. MOUDI Description

The MOUDIs are cascade impactors designed to collect samples of airborne particulate matter that are segregated according to particle size. The upper stages of the impactor have large holes in the orifice plates and lower jet velocities, thus collecting larger particles. The lower stages of the impactor have smaller holes in the orifice plates and higher jet velocities, thus collecting smaller particles. Dr. Kleeman's group at the University of California, Davis, operates the MOUDIs in a different configuration than other groups, using a 1.8 µm cyclone up front to remove coarse particles such that the MOUDI stages at 3.2, 5.6, 10 and 18 µm are inoperable. The stages used for this study had cuts at 0.18, 0.32, 0.56, 1.0, and 1.8 µm.

Two MOUDIs were used side-by-side at the IMPROVE air quality sampling shed on top of Ghausi Hall on the University of California campus in Davis, CA. One MOUDI was loaded with Teflon substrates to be analyzed by ICP-MS and XRF while the other was loaded with foil substrates to be analyzed for EC/OC. The foil substrates did not permit elemental analysis for comparison with RDI samplers, but Dr. Kleeman's group is working on an elemental analysis off the foil substrates that will enable such a comparison. Both MOUDIs ran while rotating to allow for a uniform deposit, which was required for XRF analysis – although MOUDIs are designed to rotate while collecting particles to more evenly distribute particles over the substrate surface, they can be operated without rotating for special purposes. The MOUDIs ran over a 48-hour sampling cycle, starting at 12:00pm and ending at 9:00am allowing for a 45 hour collection period and a 3 hour sample unloading and loading period.

AIHL-design cyclones were used upstream of the MOUDI to prevent larger particles from entering the instrument. Large particles tend to bounce more frequently than small particles, possibly causing contamination on lower collection stages, and plugging orifice plates in extreme cases. At the design flow rate of 30 lpm, the AIHL-design cyclones removed particles larger than 1.8 μm from the sample stream. As a result, stages 0-4 of the MOUDIs did not collect meaningful samples. These stages were loaded with unweighed foil substrates that had been baked for 48 hours at 550C. Because the stage 0-4 samples were theoretically clean, these substrates were not changed between sampling events.

A carbon vane vacuum pump was used to draw air through the MOUDI. Flow was controlled to achieve the calibrated pressure drops between stages 1-5 and 5-10 of each impactor. The exhaust of each pump was equipped with a High-Efficiency Particulate Arrestance (HEPA) filter to prevent particles in the pump exhaust from contaminating the sample. All pumps were located inside the IMPROVE shed on the rooftop of Ghausi Hall.

3c. IMPROVE Description

The sampler deployed in the IMPROVE network consists of four modules used to collect aerosol samples, labeled A, B, C, and D. In addition, a controller contains the timer, the keypad, and other electronic equipment required to operate the sampler. During a sampling period, each of the four modules collects a filter sample simultaneously. The four modules are used to collect four different types of samples.

- Module A collects $PM_{2.5}$ particles on Teflon filters. These filters are analyzed by three methods:
    a. gravimetric analysis for $PM_{2.5}$ mass,
    b. hybrid-integrating plate and sphere (HIPS) for optical absorption,
    c. x-ray fluorescence for elements ranging from sodium (Na) to lead (Pb).
- Module B collects $PM_{2.5}$ particles on nylon filters. A denuder before the nylon filter removes nitric acid and sulfur dioxide vapors. These filters are analyzed by ion chromatography for nitrate, chloride, sulfate and nitrite.
- Module C collects $PM_{2.5}$ particles on quartz filters. These filters are analyzed for organic and elemental carbon using Thermal Optical Reflectance (TOR).
- Module D collects PM_{10} particles on Teflon. These filters are analyzed by gravimetric analysis for PM_{10} mass.

In the A, B, and C modules the $PM_{2.5}$ size cut is achieved using a cyclone with a 2.5 µm cutpoint at the nominal flowrate of 23 liters per minute. The D module has no cyclone but is equipped with a Sierra-Andersen PM_{10} inlet. The D module is operated at 16.9 liters per minute.

Details of the IMPROVE sampler can be found in the IMPROVE standard operating procedures (SOPs) located on the IMPROVE website:

http://vista.cira.colostate.edu/improve/Publications/SOPs/ucdsop.asp

For the RDI intercomparison study at UC Davis, only modules A and D were used. Hence, all samples were collected on Teflon filters. Two A modules and two D modules were mounted adjacent to one another on the rooftop sampling platform. Operating duplicate sampling modules enabled an estimate of the measurement precision of the IMPROVE sampler.

4. Site Description

Measurements were performed on the IMPROVE sampler testing platform on the roof of Ghausi Hall on the UCD campus (see Figure 4.1). Inlet stacks for IMPROVE samplers are shown in Figure 4.1 (right). RDI and MOUDI inlets were placed as close to the IMPROVE sampler inlets as possible and were at similar heights to minimize artifacts due to sampling different air streams. Prevailing winds are generally from the south (bottom of Figure 4.1a, left, left side of Figure 4.1a, right) or the north (top of Figure 4.1a, left; right side of Figure 4.1a, right) but occasionally from the west (straight ahead in Figure 4.1a, right). Figure 4.1b illustrates the relative position of the samplers. A meteorological tower operated by the Department of Land, Air and Water Resources at the Campbell Tract, UC Davis, measured temperature, relative humidity, wind speed and direction during the campaign. This meteorological monitoring site is located approximately 1 mile from Ghausi Hall and samples at 10 meters above ground level. Figures 4.2ab show the meterological conditions during the measurements.

Figure 4.1a. Roof of Ghausi Hall showing the location of the IMPROVE sampling station where the method intercomparison was conducted.

	IMPROVE ROSN	West	IMPROVE RONS	
	MOUDI 214	S N	MOUDI 212	
	RDI 3	East	RDI 7	

Figure 4.1b. Instrument layout in the shelters located on the roof of Ghausi Hall.

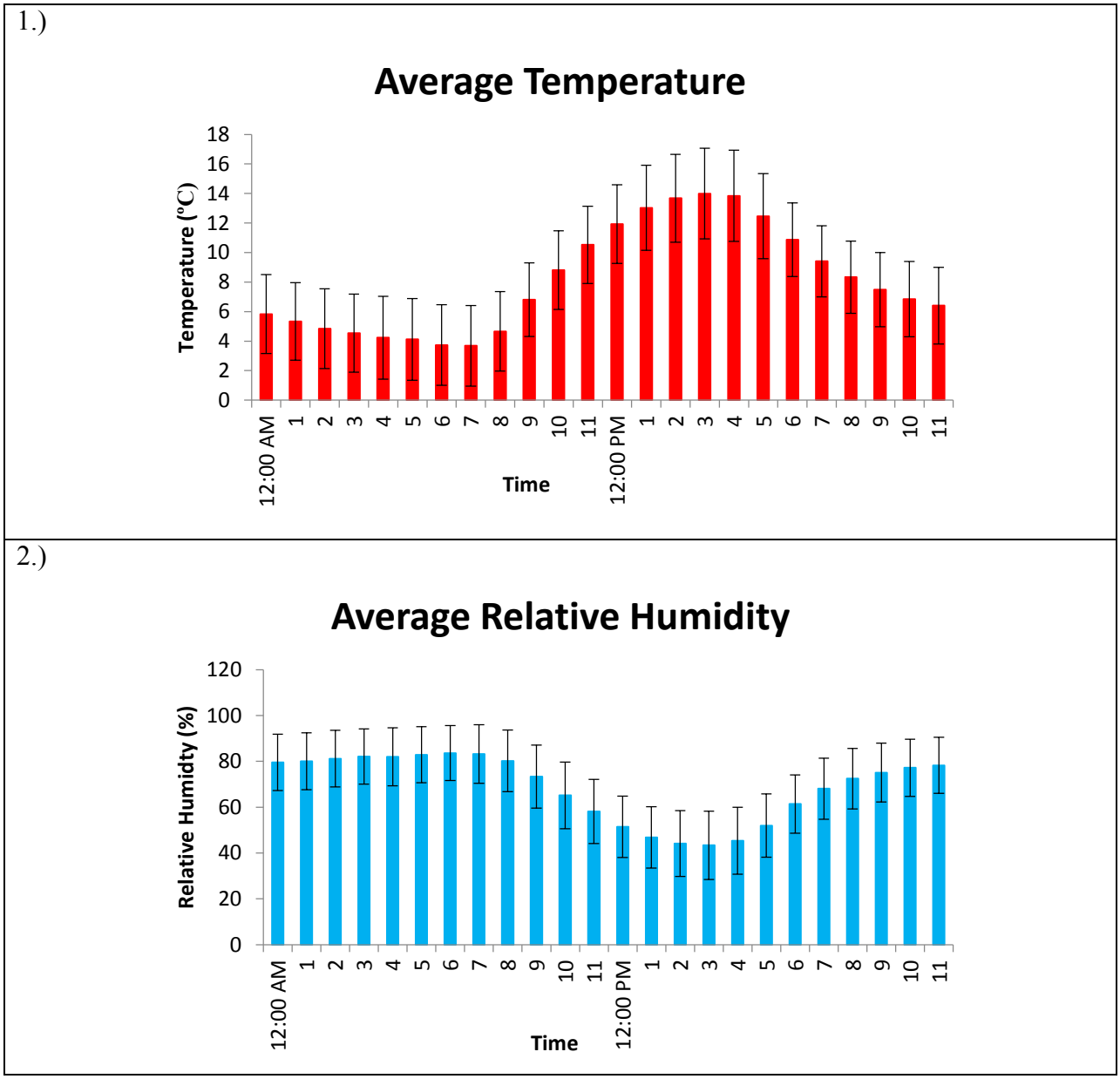

Figure 4.2a Meteorology Data for winter sampling campaign. Box 1 represents the average temperature (ºC) with standard deviation bars while box 2 represents the average relative humidity (%) for the winter sampling season (January – February 2013).

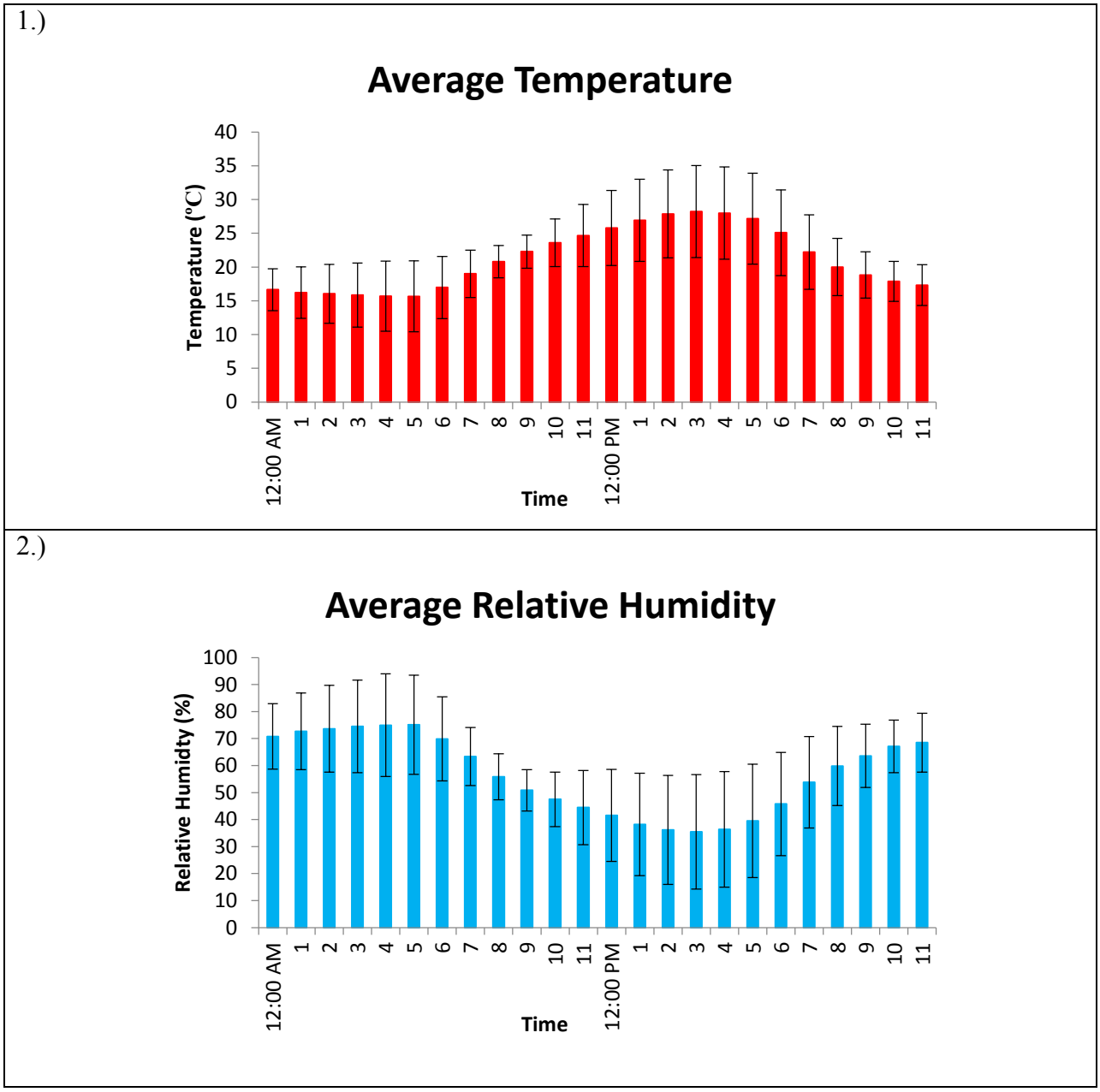

Figure 4.2b Meteorology Data for summer sampling campaign. Box 1 represents the average temperature (ºC) with standard deviation bars while box 2 represents the average relative humidity (%) with standard deviation bars for the summer sampling season (July – August 2013).

5. Sampling Schedule

A two-day average was defined as the average starting at noon on Day 1 and ending at 9am on Day 2, starting again at noon on Day 2 and ending on 9am on Day 3. Each two-day period reported was labeled by the starting day of the sample (see Figure 5.1). For each 2-day sampling period:

- IMPROVE collected two PM2.5 and two PM10 filters from noon on the first day to 9am on the next day for two consecutive days of sampling.

- MOUDI collected one filter from noon on the first day to 9am on the next, turning off the pump on the MOUDI from 9am until noon, then turning it back on again from noon on the second day until 9am on the third day.

- RDI operated continuously for the two sampling periods with 3-hour resolution, and will report total XRF elements for each size cut for the time periods that match those for the IMPROVE and MOUDI samples.

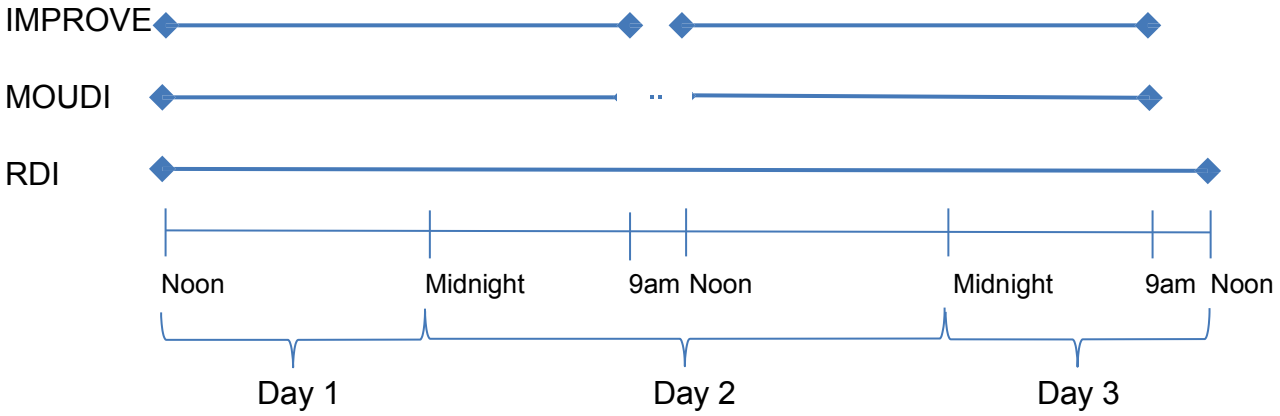

Figure 5.1. 2-day Sampling Schedule – IMPROVE two 21-hr samples; MOUDI one 45-hr sample with pump shut off for 3 hours; RDI continuous sampling analyzed as 16 3-hr samples. Diamonds indicate filter changes. Dotted line indicates MOUDI pump turned off with no filter change.

During the winter sampling period, all samplers operated from January 11, 2013 to February 11, 2013. During this sampling period, the following time periods were not usable:

RDI: A planned timing gap was inserted on January 29, 2013 18:00 to 21:00 so data for this time period are not valid. Note: since the Mylar sample collection strip may shrink or expand between sampling and analysis, such timing marks help align samples with sampling time.

IMPROVE: Due to a scheduling mistake, data were not collected on one sampler for one day starting 1/21/13 and ending 1/22/13.

MOUDI: 1/15-17/13: The MOUDI producing elemental data malfunctioned
1/25-27/13: The MOUDI producing elemental data malfunctioned
1/27-29/13: The MOUDI producing elemental data malfunctioned
1/29-31/13: Slight contamination of substrates on both samplers

During the summer sampling period, all samplers operated from July 10, 2013 to August 12, 2013. During this sampling period, the following data were not usable:

IMPROVE samplers failed July 26 to 29.

6. Instrument SOP Summaries

6a. RDI SOP

See Appendix A for the RDI SOP.

6b. MOUDI SOP

See Appendix B for the instrument SOP and Appendix C for the ICPMS SOP.

6c. IMPROVE SOP

Detailed IMPROVE SOPs are posted on the IMPROVE website at:

http://vista.cira.colostate.edu/improve/Publications/SOPs/ucdsop.asp

7. Method Detection Limits

Method detection limits (MDL) were calculated for XRF and ICP-MS using the procedure recommended by the U.S. Environmental Protection Agency (EPA, 2011). Any element found with concentration below the MDL will not be included in the comparison as any concentration below the instrument MDL is considered noise and will not provide a reliable reading.

7a. XRF MDL

The following table lists the MDL per filter for the IMPROVE sampler for the elements analyzed by the XRF. Values are the same for both seasons.

Table 7a.1 MDL for IMPROVE XRF.

Element	MDL ($\mu g/m^3$)
Na	2.79E-03
Mg	1.90E-03
Al	1.22E-03
Si	2.64E-04
P	2.71E-05
S	0.00E+00
Cl	1.78E-05
K	8.25E-05
Ca	1.76E-04
Sc	4.32E-04
Ti	4.74E-05
V	5.65E-05
Cr	6.99E-05
Mn	1.87E-04
Fe	4.83E-04
Co	4.64E-05
Ni	2.82E-05
Cu	1.00E-04
Zn	1.37E-04
As	7.55E-05
Se	1.37E-04
Br	1.23E-04
Rb	1.22E-04
Sr	7.04E-05
Zr	9.71E-04
Sn	1.01E-03
Sb	1.29E-03
Cs	9.12E-04
Ba	2.45E-03
Pb	1.48E-04

The following table lists the MDL per stage for both winter and summer seasons measured by XRF for the RDI. MDL is determined by measuring blanks for each sample, so is different for each of the two measurement periods in this study.

Table 7a.2 Winter and Summer MDL for RDI XRF.

Element	Winter RDI MDL (μg/m^3)	Element	Summer RDI MDL (μg/m^3)
Na	3.19E-02	Na	3.12E-02
Mg	1.06E-02	Mg	8.25E-03
Al	2.24E-03	Al	1.14E-02
Si	1.14E-02	Si	2.60E-02
P	1.51E-03	P	2.05E-03
S	5.20E-03	S	4.69E-03
Cl	1.17E-03	Cl	4.74E-03
K	2.42E-03	K	3.37E-03
Ca	2.95E-03	Ca	4.69E-03
Ti	5.51E-04	Ti	1.68E-03
V	3.71E-05	V	6.27E-05
Cr	3.98E-05	Cr	1.64E-04
Mn	2.32E-04	Mn	4.29E-04
Fe	2.56E-03	Fe	9.60E-03
Co	3.18E-04	Co	2.19E-04
Ni	1.04E-04	Ni	1.13E-04
Cu	3.48E-04	Cu	2.64E-04
Zn	4.39E-04	Zn	4.12E-04
Se	2.76E-04	Se	2.76E-04
Br	6.70E-04	Br	6.36E-04

The following table lists the MDL per stage measured by XRF for the MOUDI. MDLs are the same for both seasons.

Table 7a.3 MDL for MOUDI XRF.

Element	MDL (µg/m^3)
Na	2.14E-03
Mg	3.83E-03
Al	1.90E-03
Si	9.86E-04
P	2.20E-04
S	0.00E+00
Cl	1.70E-04
K	1.27E-04
Ca	1.51E-03
Ti	1.09E-04
V	1.68E-04
Cr	1.17E-04
Mn	7.61E-04
Fe	3.07E-03
Ni	1.35E-04
Cu	3.02E-04
Zn	3.30E-04
As	1.30E-04
Se	3.04E-04
Br	1.01E-04
Rb	2.37E-04
Sr	4.42E-04
Zr	1.74E-03
Pb	1.59E-03

Although XRF analysis was reported on a large suite of elements, only the following subset of 10 elements was consistently above MDL for this study:

Elements - Na, Si, S, Cl, K, Ca, Ti, Mn, Fe, Br

These elements will be the core focus for the XRF analysis in Sections 8 and 9. Section 10 will show a full tier comparison of all XRF elements for all samplers.

7b. ICPMS MDL

The ICPMS method that was used analyzes 53 elements in total. Herner et al (2006) concluded that only 21 elements found in ambient particle samples collected by the MOUDI cascade impactor could be measured with good precision and so we focus our analysis on these 21 elements. The following table lists the MDL per filter for these 21 elements analyzed by ICP-MS for the IMPROVE sampler.

Table 7b.1 MDL for IMPROVE ICPMS.

Element	MDL (µg/m3)
Li	1.99E-06
S	5.98E-05
K[a]	N/A
Ti	1.16E-04
V	1.56E-06
Mn	1.02E-06
Fe	1.98E-04
Ga	9.44E-07
Ge	4.74E-06
As	1.85E-06
Se	3.69E-05
Br	1.09E-04
Rb	2.07E-06
Sr	1.68E-06
Cd	1.52E-06
Sn	6.67E-06
Sb	1.28E-05
Ba	2.43E-06
Tl	7.48E-07
Pb	5.40E-07
Bi[a]	N/A

[a] N/A represents an element that did not have an accurate set of external standards analyzed by the ICP-MS to allow for calculation of mass.

The following table lists the MDL per filter for the 21 acceptable elements analyzed by ICP-MS for the MOUDI.

Table 7b.2 MDL for MOUDI ICPMS.

Element	MDL (µg/m3)
Li	1.63E-04
S	4.89E-02
K[a]	N/A
Ti	9.51E-04
V	1.27E-06
Mn	8.35E-07
Fe	1.62E-04
Ga	7.72E-07
Ge	3.88E-06
As	1.51E-06
Se	3.02E-05
Br	8.89E-05
Rb	1.69E-06
Sr	1.38E-06
Cd	1.24E-06
Sn	5.45E-06
Sb	1.05E-05
Ba	1.98E-06
Tl	6.12E-07
Pb	4.42E-07
Bi[a]	N/A

[a] N/A represents an element that did not have an accurate set of external standards analyzed by the ICPMS to allow for calculation of mass.

8. Precision Analysis

Before comparing the performance of different types of samplers to each other, precision analysis was performed on each type of sampler to better place the methods intercomparison in context. Two versions of each sampler type were deployed at the site for the precision analysis. Unfortunately, one of the two MOUDI samplers was loaded with a substrate suitable for OC/EC analysis, not for XRF/ICPMS analysis, so MOUDI sampler precision could not be directly assessed. The statistical parameters R^2 (the Excel RSQ correlation function), slope (the Excel slope function) and intercept/average(=mean) (the Excel intercept and average functions) were used to compare sample period results to each other. The statistical values, standard error RSQ (SE RSQ), standard error slope (SE SLOPE) and standard error of intercept divided by the mean (SE INTERCEPT/AVG), using the Excel LINEST function, are the uncertainty in the RSQ, slope, and intercept respectively.

8a. IMPROVE PM vs IMPROVE PM

Two IMPROVE samplers (RONS and ROSN, see figure 4.1b) were deployed for both the winter and summer 2013 sampling events. A duplicate XRF analysis on the IMPROVE substrates was not performed, therefore the precision of the XRF was not tested. Tables 8a.1-4 and Figures 8a.1-2 show the precision between the two samplers, which tested the combined precision of the sampler and the XRF analysis.

Table 8a.1 Winter PM10 - IMPROVE RONS vs IMPROVE ROSN.

(ROSN = f(RONS).

Element	RSQ	SE RSQ	SLOPE	SE SLOPE	INTERCEPT/AVG	SE INTERCEPT /AVG
Na	0.989	0.024	1.009	0.020	-0.005	0.038
Si	0.992	0.034	0.986	0.016	-0.013	0.019
S	0.995	0.005	1.027	0.013	-0.016	0.014
Cl	0.998	0.014	1.002	0.007	-0.016	0.019
K	0.994	0.004	1.005	0.015	-0.013	0.016
Ca	0.996	0.007	0.985	0.012	-0.011	0.015
Ti	0.981	0.002	0.974	0.025	0.010	0.029
Mn	0.941	0.001	0.956	0.044	0.038	0.052
Fe	0.993	0.013	0.996	0.016	-0.015	0.018
Br	0.923	0.000	1.012	0.054	0.011	0.060

Table 8a.2 Winter PM2.5 - IMPROVE RONS vs IMPROVE ROSN.

(ROSN = f(RONS).

Element	RSQ	SE RSQ	SLOPE	SE SLOPE	INTERCEPT/AVG	SE INTERCEPT /AVG
Na	0.979	0.017	1.180	0.032	-0.003	0.064
Si	0.959	0.006	0.895	0.034	0.043	0.042
S	0.997	0.003	1.061	0.010	-0.021	0.011
Cl	0.991	0.009	0.993	0.018	-0.006	0.044
K	0.996	0.001	1.019	0.011	0.004	0.013
Ca	0.966	0.002	0.964	0.034	-0.005	0.041
Ti	0.927	0.000	0.951	0.050	0.030	0.058
Mn	0.645	0.000	0.806	0.111	0.265	0.168
Fe	0.968	0.005	0.969	0.033	-0.001	0.038
Br	0.923	0.000	0.925	0.050	0.084	0.056

Table 8a.3 Summer PM10 - IMPROVE RONS vs IMPROVE.

ROSN (ROSN = f(RONS).

Element	RSQ	SE RSQ	SLOPE	SE SLOPE	INTERCEPT/AVG	SE INTERCEPT /AVG
Na	0.897	0.118	0.892	0.057	0.073	0.082
Si	0.844	0.224	0.948	0.077	0.046	0.079
S	0.946	0.031	0.948	0.043	0.028	0.047
Cl	0.832	0.232	0.865	0.073	0.136	0.120
K	0.906	0.017	1.065	0.065	-0.065	0.066
Ca	0.921	0.029	1.087	0.060	-0.080	0.062
Ti	0.808	0.008	0.953	0.088	0.053	0.090
Mn	0.772	0.002	1.030	0.106	0.000	0.107
Fe	0.804	0.099	0.957	0.089	0.048	0.092
Br	0.842	0.001	1.048	0.086	-0.081	0.095

Table 8a.4 Summer PM2.5 - IMPROVE RONS vs IMPROVE ROSN.

(ROSN = f(RONS).

Element	RSQ	SE RSQ	SLOPE	SE SLOPE	INTERCEPT/AVG	SE INTERCEPT /AVG
Na	0.898	0.089	0.954	0.061	0.102	0.085
Si	0.445	0.024	0.346	0.073	0.513	0.089
S	0.847	0.048	0.837	0.067	0.188	0.073
Cl	0.952	0.049	1.020	0.043	0.083	0.082
K	0.844	0.007	0.822	0.067	0.149	0.077
Ca	0.651	0.009	0.565	0.078	0.359	0.094
Ti	0.476	0.001	0.338	0.067	0.545	0.080
Mn	0.037	0.000	0.133	0.128	0.727	0.153
Fe	0.471	0.010	0.315	0.063	0.565	0.075
Br	0.808	0.000	0.830	0.076	0.163	0.086

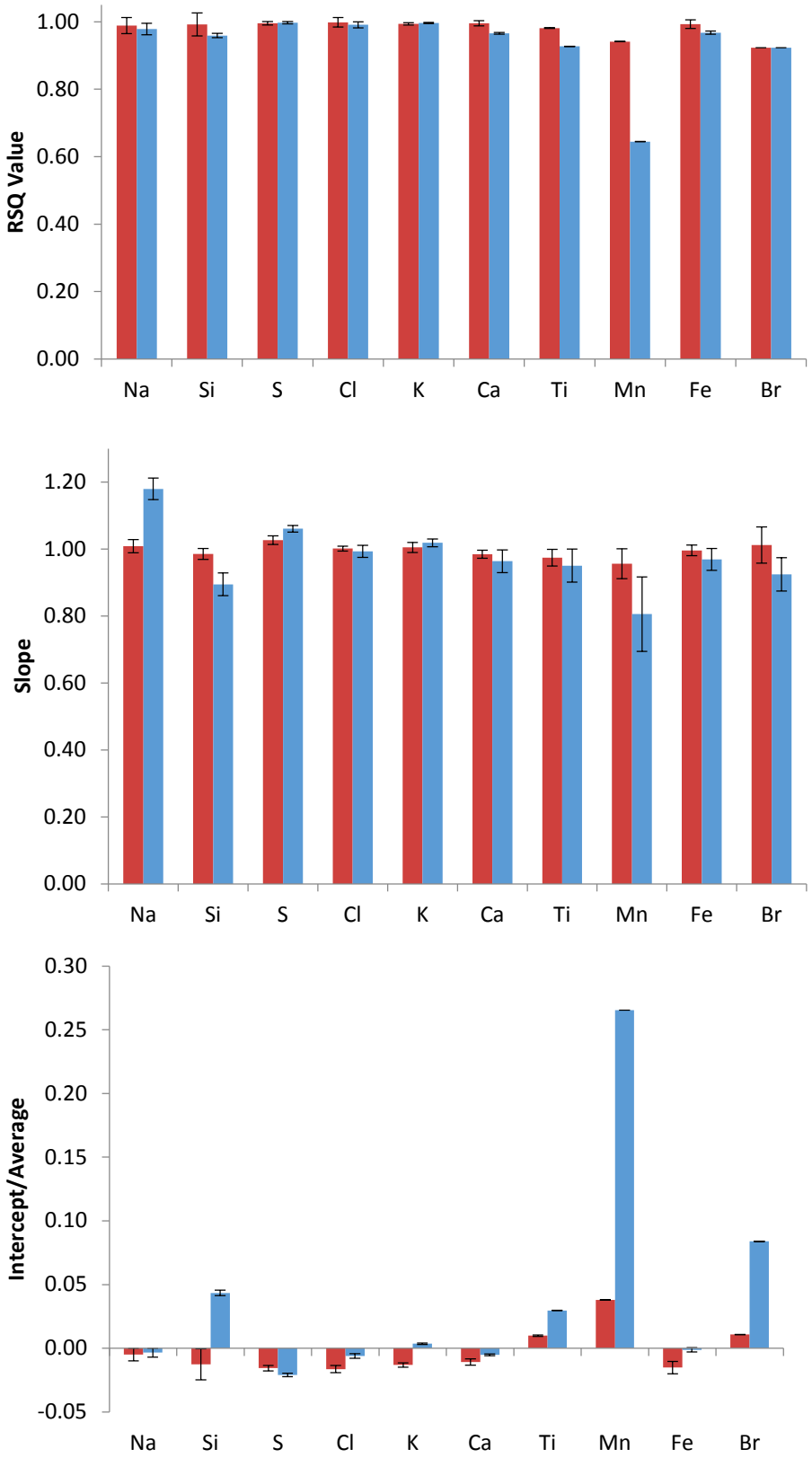

Figure 8a.1 Comparison between two IMPROVE samplers RONS and ROSN (ROSN = f(RONS)) for winter IMPROVE PM10 (red bars) and PM2.5 (blue bars) showing RSQ, slope, intercept/average and their uncertainties for each (error bars).

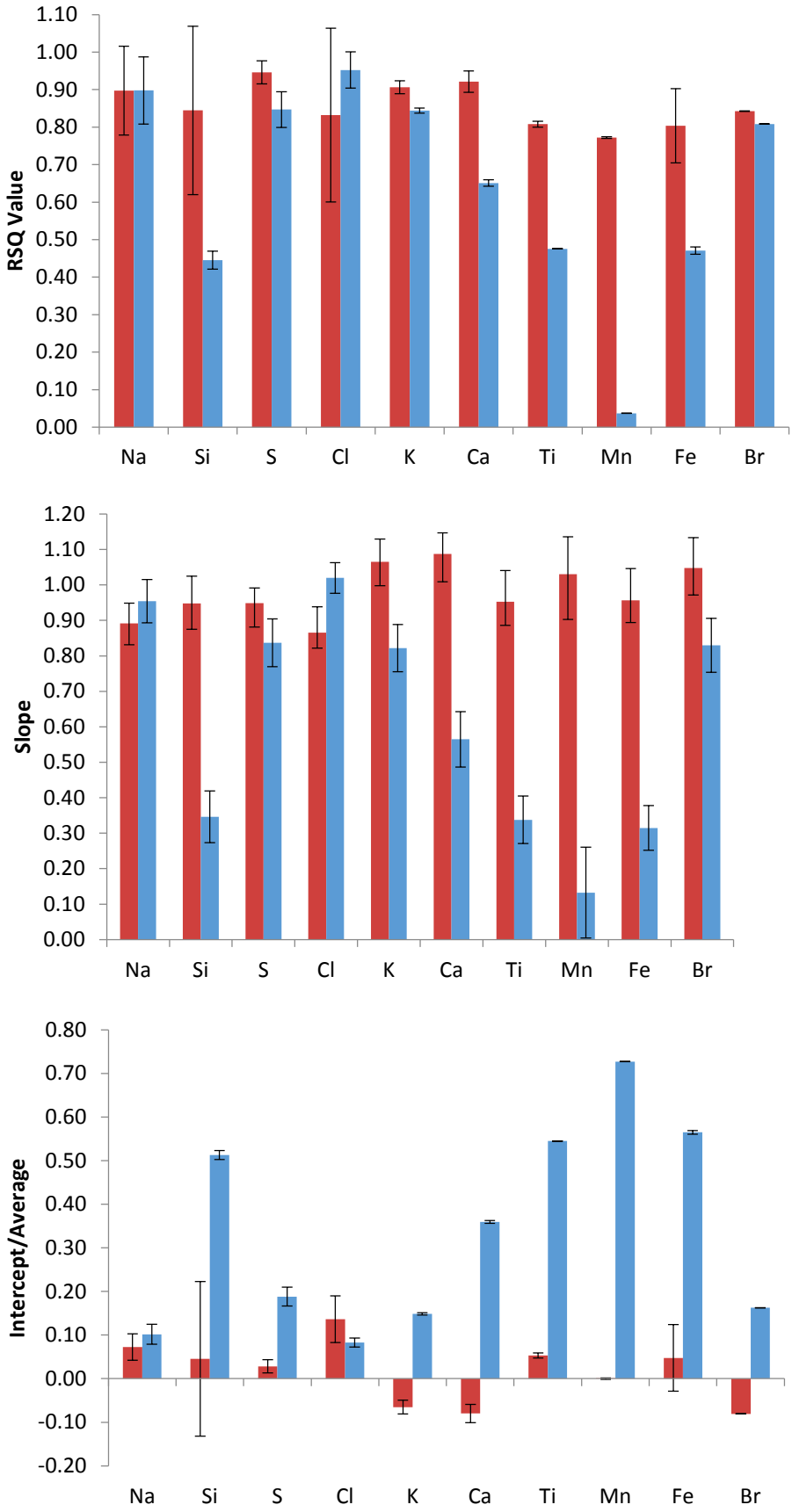

Figure 8a.2 Comparison between two IMPROVE samplers RONS and ROSN (ROSN = f(RONS)) for summer IMPROVE PM10 (red bars) and PM2.5 (blue bars) showing RSQ, slope, intercept/average and their uncertainties for each (error bars).

8b. RDI PM - RDI PM

Two forms of precision were tested with the RDI sampler. In the first form, the samples were analyzed twice by XRF at the LBL ALS, testing the precision of the XRF analysis on RDI samples. Tables 8b.1-4 and Figures 8b.1-2 show the precision of the XRF for PM10 and PM2.5 in the winter while Tables 8b.9-12 and Figures 8b.5-6 show the precision of the XRF for PM10 and PM2.5 in the summer. In the second form, the samples were compared between samplers, which tested the combined precision of the sampler and the XRF analysis. Tables 8b.5-8 and Figures 8b.3-4 show the combined precision of the samplers and the XRF analysis for PM10 and PM2.5 in the winter while Tables 8b.13-16 and Figures 8b.7-8 show the combined precision of the samplers and the XRF analysis for PM10 and PM2.5 in the summer.

In summary, the XRF is very precise for both PM10 and PM2.5 (comparisons of RDI-3a to RDI-3b and RDI-7a to RDI-7b below). Sampler-to-sampler comparisons are less precise (e.g., comparisons of RDI-3a to RDI-7a below).

Table 8b.1 Winter PM10 – RDI-3a vs RDI-3b.

(3b=f(3a))

Element	RSQ	RSQ SE	Slope	SLOPE SE	Intercept/Average	SE INTERCEPT /AVG
Na	0.995	0.011	1.017	0.019	0.012	0.022
Si	0.996	0.018	0.998	0.016	0.025	0.017
S	0.991	0.006	1.034	0.027	-0.007	0.028
Cl	1.000	0.006	1.023	0.005	0.013	0.013
K	0.998	0.002	1.016	0.012	0.014	0.011
Ca	0.998	0.004	0.989	0.989	0.023	0.022
Ti	0.993	0.001	1.011	0.022	0.011	0.033
Mn	0.996	0.000	1.001	0.016	-0.027	0.000
Fe	0.996	0.007	0.997	0.016	0.020	0.016
Br	0.936	0.000	1.081	0.075	-0.059	0.093

Table 8b.2 Winter PM2.5 – RDI-3a vs RDI-3b.

(3b=f(3a))

Element	RSQ	RSQ SE	Slope	SLOPE SE	Intercept/Average	SE INTERCEPT /AVG
Na	0.986	0.008	1.046	0.034	-0.005	0.035
Si	0.998	0.003	1.013	0.011	-0.007	0.012
S	0.981	0.006	1.022	0.038	0.007	0.044
Cl	0.998	0.005	1.081	0.012	-0.001	0.019
K	0.993	0.001	1.024	0.023	0.013	0.022
Ca	0.998	0.000	0.998	0.998	0.002	0.000
Ti	0.996	0.000	1.003	0.017	0.015	0.000
Mn	0.994	0.000	1.019	0.021	-0.051	0.000
Fe	0.998	0.002	1.004	0.011	0.015	0.011
Br	0.957	0.000	1.102	0.063	-0.074	0.123

Table 8b.3 Winter PM10 – RDI-7a vs RDI-7b.

(7b=f(7a))

Element	RSQ	RSQ SE	Slope	SLOPE SE	Intercept/Average	SE INTERCEPT /AVG
Na	0.994	0.012	0.941	0.019	0.029	0.020
Si	1.000	0.003	0.981	0.004	0.013	0.004
S	0.934	0.012	0.846	0.060	0.107	0.063
Cl	1.000	0.003	0.969	0.002	0.011	0.007
K	0.995	0.002	0.975	0.018	-0.008	0.024
Ca	0.999	0.001	0.985	0.985	0.007	0.006
Ti	0.999	0.000	0.983	0.009	-0.008	0.000
Mn	0.989	0.000	0.985	0.027	0.020	0.040
Fe	0.999	0.002	0.990	0.006	-0.001	0.005
Br	0.948	0.000	0.937	0.058	0.034	0.092

Table 8b.4 – Winter PM2.5 RDI-7a vs RDI-7b.

(7b=f(7a))

Element	RSQ	RSQ SE	Slope	SLOPE SE	Intercept/Average	SE INTERCEPT /AVG
Na	0.995	0.006	0.953	0.019	-0.020	0.021
Si	1.000	0.001	0.978	0.005	-0.011	0.007
S	0.903	0.011	0.787	0.069	0.152	0.074
Cl	0.999	0.003	0.948	0.006	0.017	0.017
K	0.993	0.002	0.973	0.022	-0.020	0.019
Ca	0.998	-0.001	0.986	0.986	-0.015	-0.019
Ti	0.999	0.000	0.984	0.009	-0.018	0.000
Mn	0.990	0.000	0.990	0.027	-0.012	0.000
Fe	0.999	0.001	0.988	0.007	-0.012	0.010
Br	0.946	0.000	0.901	0.057	0.061	0.117

Table 8b.5 – Winter PM10 RDI-3a vs RDI-7a.

(7a = f(3a))

Element	RSQ	RSQ SE	Slope	SLOPE SE	Intercept/Average	SE INTERCEPT /AVG
Na	0.994	0.012	0.918	0.019	-0.007	0.021
Si	0.640	0.182	1.110	0.222	-0.068	0.226
S	0.797	0.025	0.938	0.127	-0.080	0.144
Cl	0.999	0.008	0.933	0.006	0.036	0.013
K	0.721	0.018	0.890	0.148	0.163	0.148
Ca	0.681	-0.023	1.213	1.213	-0.132	-0.134
Ti	0.789	0.006	1.207	0.167	0.012	0.145
Mn	0.755	0.001	1.050	0.160	-0.539	0.201
Fe	0.779	0.053	1.089	0.155	0.038	0.158
Br	0.805	0.000	0.821	0.108	0.152	0.092

Table 8b.6 – Winter PM2.5 3a vs 7a.

(7a = f(3a))

Element	RSQ	RSQ SE	Slope	SLOPE SE	Intercept/Average	SE INTERCEPT /AVG
Na	0.984	0.007	0.733	0.025	0.177	0.026
Si	0.681	0.043	0.829	0.152	0.617	0.125
S	0.703	0.023	0.803	0.139	0.082	0.160
Cl	0.998	0.005	0.786	0.009	0.061	0.018
K	0.876	0.006	0.667	0.067	0.169	0.082
Ca	0.925	0.011	0.964	0.964	0.195	0.190
Ti	0.944	0.001	0.894	0.058	0.019	0.093
Mn	0.713	0.000	0.666	0.113	1.547	0.000
Fe	0.925	0.012	0.928	0.071	-0.037	0.086
Br	0.667	0.000	0.707	0.133	0.227	0.119

Table8b.7 – Winter PM10 3b vs 7b.

(7b = f(3b))

Element	RSQ	RSQ SE	Slope	SLOPE SE	Intercept/Average	SE INTERCEPT /AVG
Na	0.984	0.020	0.998	0.034	0.035	0.036
Si	0.666	0.124	0.578	0.109	0.368	0.122
S	0.740	0.024	0.690	0.109	0.368	0.111
Cl	0.999	0.013	1.015	0.010	-0.039	0.027
K	0.709	0.017	0.773	0.132	0.122	0.148
Ca	0.711	0.028	0.570	0.097	0.356	0.111
Ti	0.787	0.004	0.633	0.088	0.167	0.109
Mn	0.748	0.001	0.706	0.110	0.724	0.100
Fe	0.794	0.041	0.716	0.097	0.155	0.115
Br	0.822	0.000	0.853	0.106	0.127	0.092

Table 8b.8 – Winter PM2.5 3b vs 7b.

(7b = f(3b))

Element	RSQ	RSQ SE	Slope	SLOPE SE	Intercept/Average	SE INTERCEPT /AVG
Na	0.981	0.011	1.216	0.045	-0.220	0.047
Si	0.656	0.043	0.778	0.151	-0.243	0.195
S	0.604	0.023	0.651	0.141	0.377	0.143
Cl	0.994	0.010	1.111	0.022	-0.047	0.055
K	0.832	0.010	1.216	0.146	-0.090	0.143
Ca	0.918	0.006	0.946	0.075	-0.130	0.087
Ti	0.936	0.001	1.030	0.072	0.010	0.093
Mn	0.713	0.001	1.043	0.177	-1.560	0.281
Fe	0.921	0.013	0.978	0.077	0.090	0.086
Br	0.769	0.000	0.834	0.122	0.177	0.119

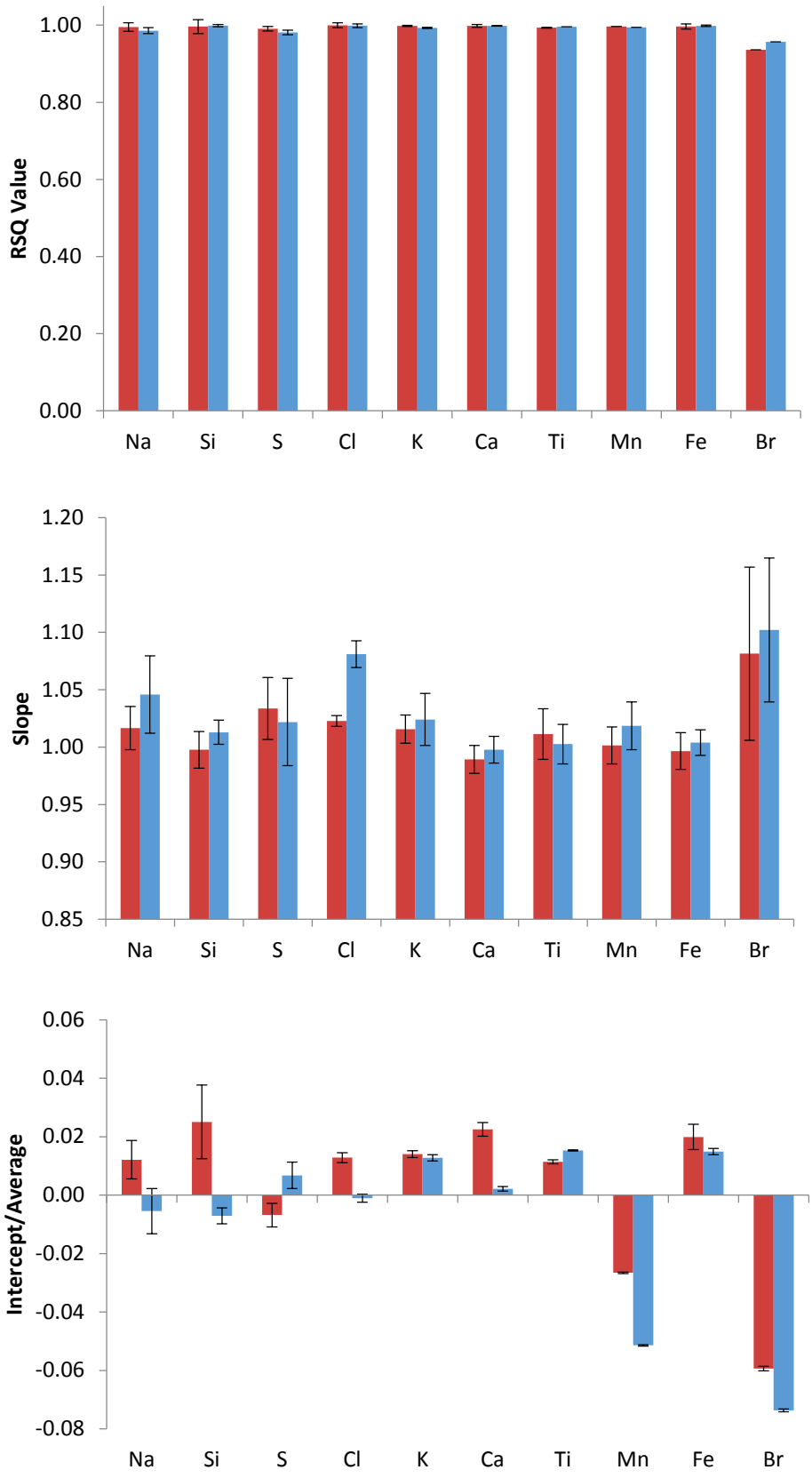

Figure 8b.1 Comparison between two XRF analyses 3a and 3b (3b = f(3a)) for Winter RDI PM10 (red bars) and PM2.5 (blue bars) showing RSQ, slope, intercept/average and their uncertainties for each (error bars).

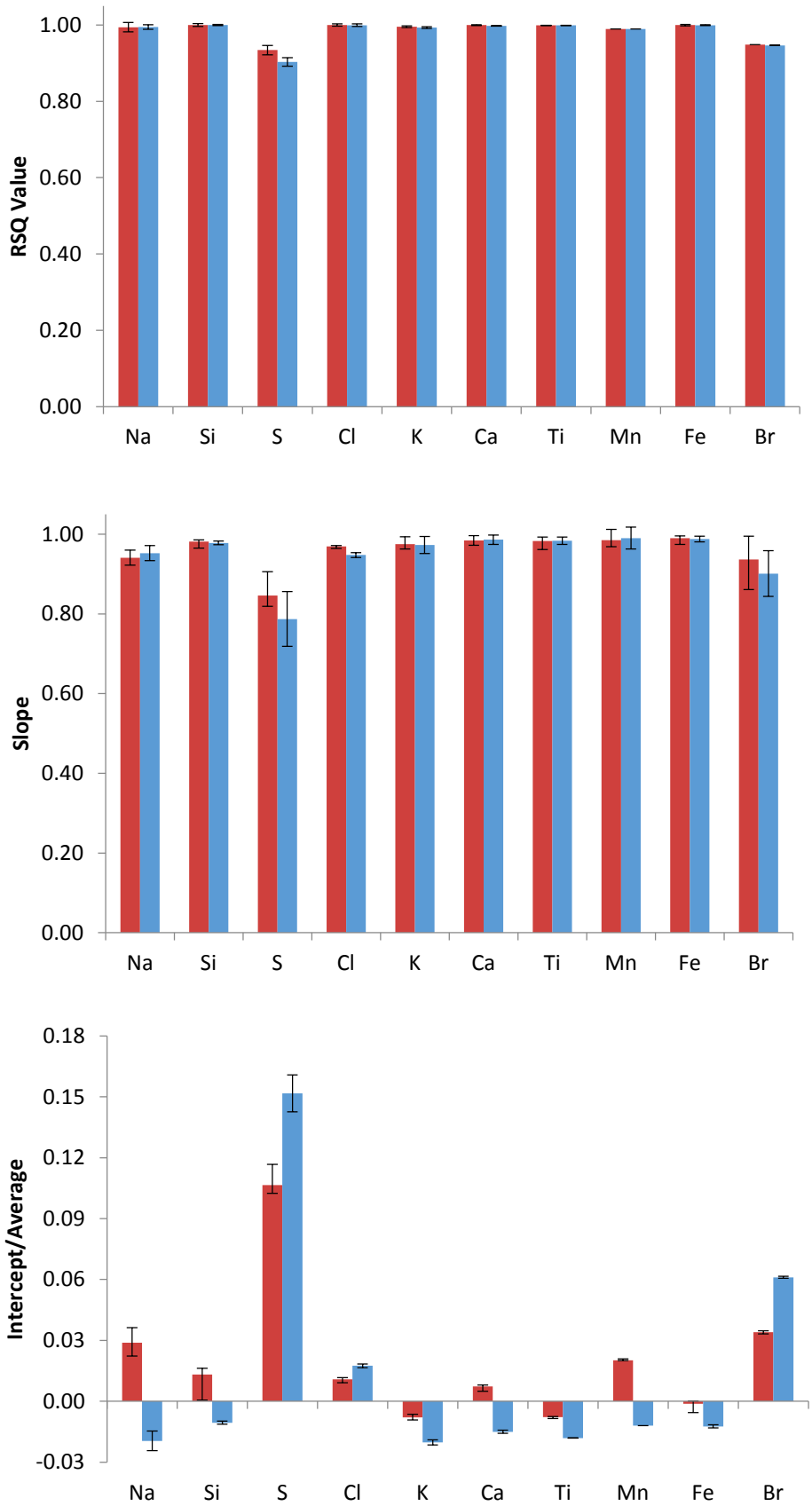

Figure 8b.2 Comparison between two XRF analyses 7a and 7b (7b = f(7a)) for Winter RDI PM10 (red bars) and PM2.5 (blue bars) showing RSQ, slope, intercept/average and their uncertainties for each (error bars).

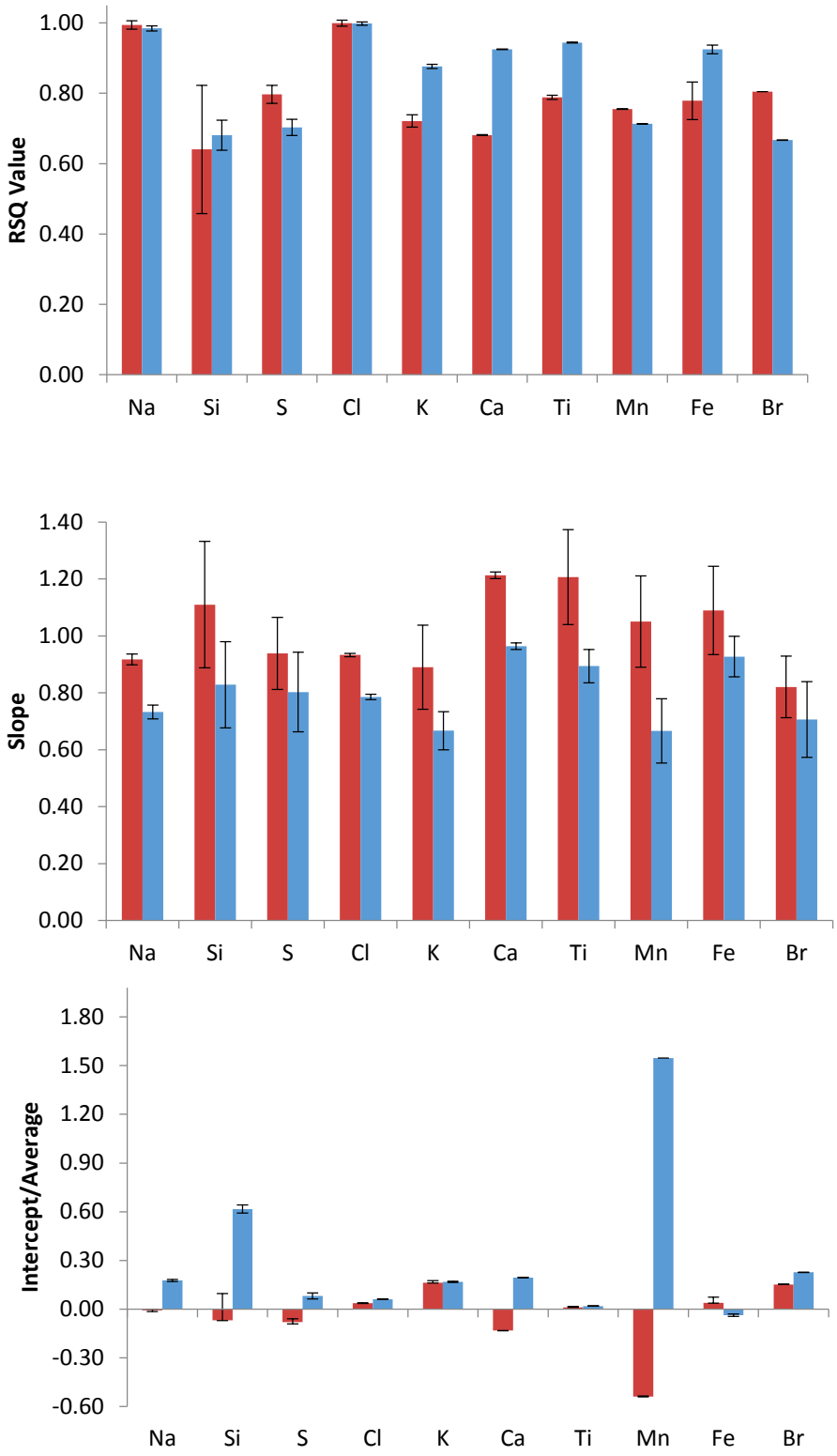

Figure 8b.3 Comparison between two samplers 3 and 7 (7a = f(3a)) for Winter RDI PM10 (red bars) and PM2.5 (blue bars) showing RSQ, slope, intercept/average and their uncertainties for each (error bars).

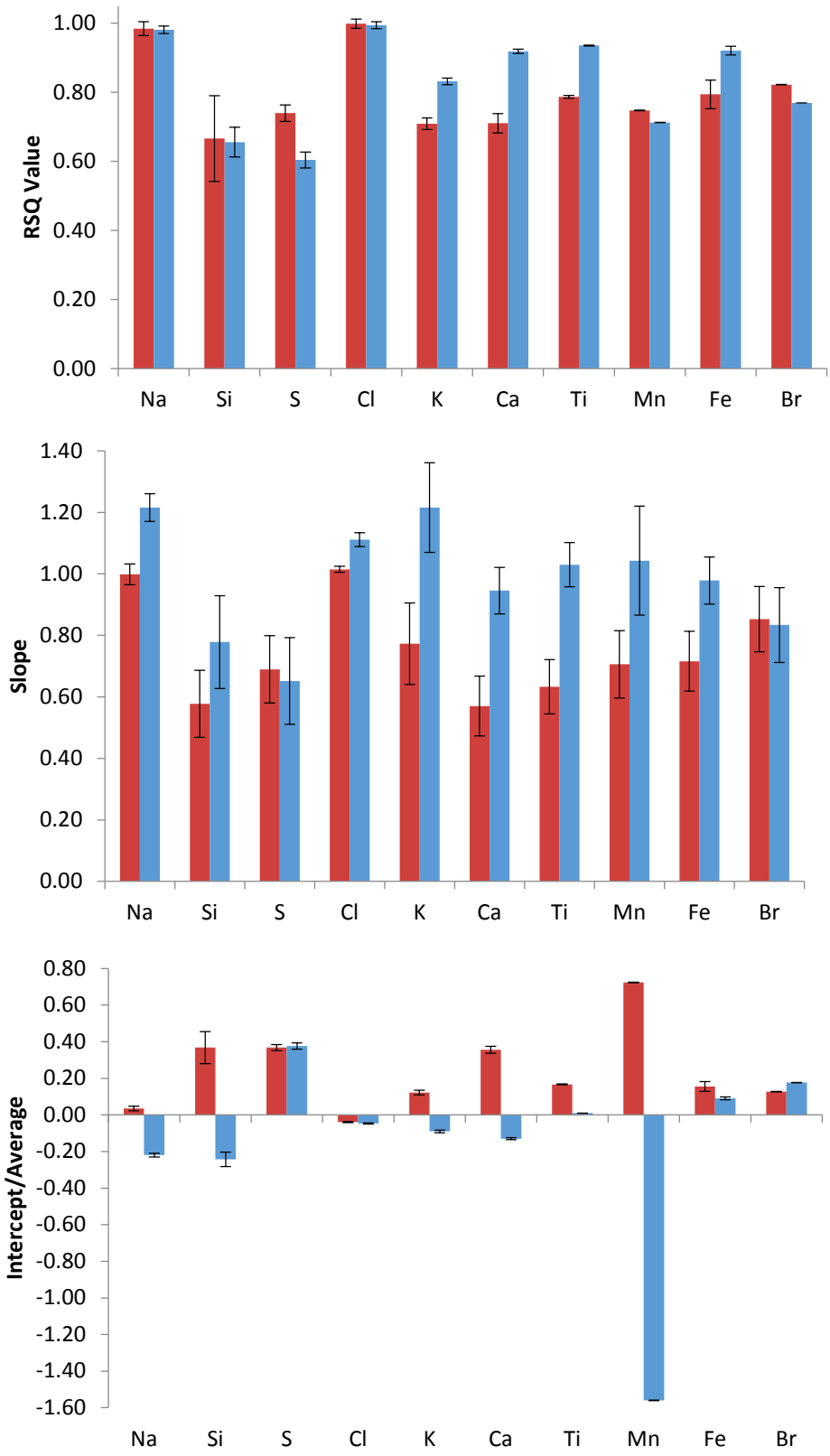

Figure 8b.4 Comparison between two samplers 3 and 7 (7b = f(3b)) for Winter RDI PM10 (red bars) and PM2.5 (blue bars) showing RSQ, slope, intercept/average and their uncertainties for each (error bars).

Table 8b.9 Summer PM10 – 3a vs 3b.

Element	RSQ	RSQ SE	SLOPE	SLOPE SE	INTERCEPT/AVG	SE INTERCEPT /AVG
Na	0.953	0.052	0.920	0.053	0.048	0.060
Si	0.870	0.066	0.777	0.078	0.204	0.079
S	0.977	0.031	1.012	0.040	0.000	0.044
Cl	0.970	0.103	0.949	0.043	-0.008	0.062
K	0.972	0.009	0.899	0.039	0.087	0.042
Ca	0.945	0.010	0.831	0.052	0.149	0.054
Ti	0.832	0.003	0.744	0.086	0.239	0.085
Mn	0.950	0.000	0.951	0.056	0.031	0.049
Fe	0.878	0.023	0.798	0.077	0.191	0.078
Br	0.984	0.000	1.005	0.034	0.007	0.000

Table 8b.10 Summer PM2.5 – 3a vs 3b.

Element	RSQ	RSQ SE	SLOPE	SLOPE SE	INTERCEPT/AVG	SE INTERCEPT /AVG
Na	0.935	0.047	0.877	0.060	0.089	0.070
Si	0.859	0.021	0.987	0.103	0.010	0.105
S	0.974	0.031	1.023	0.044	-0.006	0.046
Cl	0.903	0.095	0.879	0.074	0.037	0.112
K	0.982	0.005	0.979	0.034	0.031	0.042
Ca	0.953	0.005	0.914	0.052	0.075	0.053
Ti	0.815	0.001	0.859	0.106	0.147	0.124
Mn	0.898	0.000	0.931	0.081	0.049	0.073
Fe	0.799	0.008	0.861	0.112	0.147	0.114
Br	0.984	0.000	0.957	0.032	0.054	0.000

Table 8b.11 Summer PM10 – 7a vs 7b.

Element	RSQ	RSQ SE	SLOPE	SLOPE SE	INTERCEPT/AVG	SE INTERCEPT /AVG
Na	0.980	0.031	1.121	0.042	-0.086	0.044
Si	0.992	0.028	0.966	0.022	0.044	0.023
S	0.999	0.006	1.045	0.010	-0.002	0.009
Cl	0.996	0.035	1.042	0.016	-0.024	0.023
K	0.996	0.003	1.002	0.017	0.007	0.016
Ca	0.988	0.006	1.004	0.028	0.008	0.028
Ti	0.982	0.002	0.959	0.033	0.047	0.035
Mn	0.981	0.000	0.995	0.035	0.040	0.033
Fe	0.992	0.011	0.984	0.022	0.027	0.023
Br	0.971	0.000	1.054	0.047	-0.042	0.087

Table 8b.12 – Summer PM2.5 7a vs 7b.

(7b = f(7a))

Element	RSQ	RSQ SE	SLOPE	SLOPE SE	INTERCEPT/AVG	SE INTERCEPT /AVG
Na	0.976	0.029	1.148	0.046	-0.116	0.051
Si	0.992	0.009	1.054	0.024	-0.021	0.025
S	0.998	0.006	1.045	0.011	0.002	0.011
Cl	0.987	0.038	1.073	0.031	-0.054	0.046
K	0.996	0.002	1.030	0.017	-0.008	0.015
Ca	0.985	0.003	1.091	0.035	-0.059	0.033
Ti	0.990	0.000	1.074	0.028	-0.045	0.000
Mn	0.968	0.000	1.079	0.051	-0.009	0.079
Fe	0.994	0.003	1.048	0.021	-0.024	0.021
Br	0.975	0.000	1.029	0.043	-0.008	0.000

Table 8b.13 – Summer PM10 3a vs 7a.

(7a = f(3a))

Element	RSQ	RSQ SE	SLOPE	SLOPE SE	INTERCEPT/AVG	SE INTERCEPT /AVG
Na	0.635	0.118	0.607	0.119	0.323	0.154
Si	0.014	0.321	0.177	0.379	0.826	0.376
S	0.747	0.076	0.649	0.098	0.290	0.116
Cl	0.861	0.207	0.839	0.087	0.084	0.130
K	0.424	0.040	0.596	0.179	0.373	0.196
Ca	0.221	0.048	0.517	0.251	0.491	0.250
Ti	0.043	0.013	0.298	0.362	0.690	0.387
Mn	0.198	0.002	0.570	0.296	0.597	0.204
Fe	0.061	0.118	0.396	0.400	0.612	0.397
Br	0.814	0.000	0.747	0.092	0.231	0.087

Table 8b.14 – Summer PM2.5 3a vs 7a.

(7a = f(3a))

Element	RSQ	RSQ SE	SLOPE	SLOPE SE	INTERCEPT/AVG	SE INTERCEPT /AVG
Na	0.423	0.121	0.506	0.153	0.462	0.185
Si	0.005	0.094	0.125	0.467	0.864	0.510
S	0.704	0.073	0.613	0.103	0.319	0.125
Cl	0.628	0.191	0.754	0.150	0.200	0.227
K	0.542	0.018	0.538	0.128	0.427	0.150
Ca	0.128	0.023	0.386	0.260	0.589	0.289
Ti	0.001	0.004	0.050	0.527	0.948	0.591
Mn	0.049	0.001	0.328	0.372	0.629	0.409
Fe	0.005	0.042	0.150	0.564	0.850	0.571
Br	0.862	0.000	0.682	0.071	0.295	0.115

Table8b.15 – Summer PM10 3b vs 7b.

(7b = f(3b))

Element	RSQ	RSQ SE	SLOPE	SLOPE SE	INTERCEPT/AVG	SE INTERCEPT /AVG
Na	0.623	0.135	0.722	0.145	0.241	0.180
Si	0.007	0.313	0.143	0.443	0.886	0.429
S	0.692	0.087	0.638	0.110	0.312	0.133
Cl	0.899	0.184	0.929	0.080	0.062	0.115
K	0.480	0.038	0.699	0.188	0.278	0.202
Ca	0.247	0.047	0.645	0.291	0.396	0.282
Ti	0.026	0.012	0.272	0.433	0.720	0.440
Mn	0.273	0.002	0.688	0.290	0.645	0.204
Fe	0.069	0.117	0.488	0.462	0.544	0.451
Br	0.849	0.000	0.805	0.088	0.168	0.087

Table 8b.16 – Summer PM2.5 3b vs 7b.

(7b = f(3b))

Element	RSQ	RSQ SE	SLOPE	SLOPE SE	INTERCEPT/AVG	SE INTERCEPT /AVG
Na	0.416	0.142	0.643	0.197	0.362	0.228
Si	0.047	0.098	0.391	0.453	0.576	0.496
S	0.628	0.085	0.584	0.116	0.355	0.144
Cl	0.723	0.178	0.945	0.151	0.102	0.213
K	0.564	0.018	0.574	0.130	0.385	0.150
Ca	0.128	0.025	0.454	0.305	0.531	0.334
Ti	0.012	0.005	0.252	0.594	0.727	0.657
Mn	0.112	0.001	0.552	0.402	0.422	0.409
Fe	0.036	0.044	0.454	0.606	0.558	0.614
Br	0.841	0.000	0.728	0.082	0.251	0.115

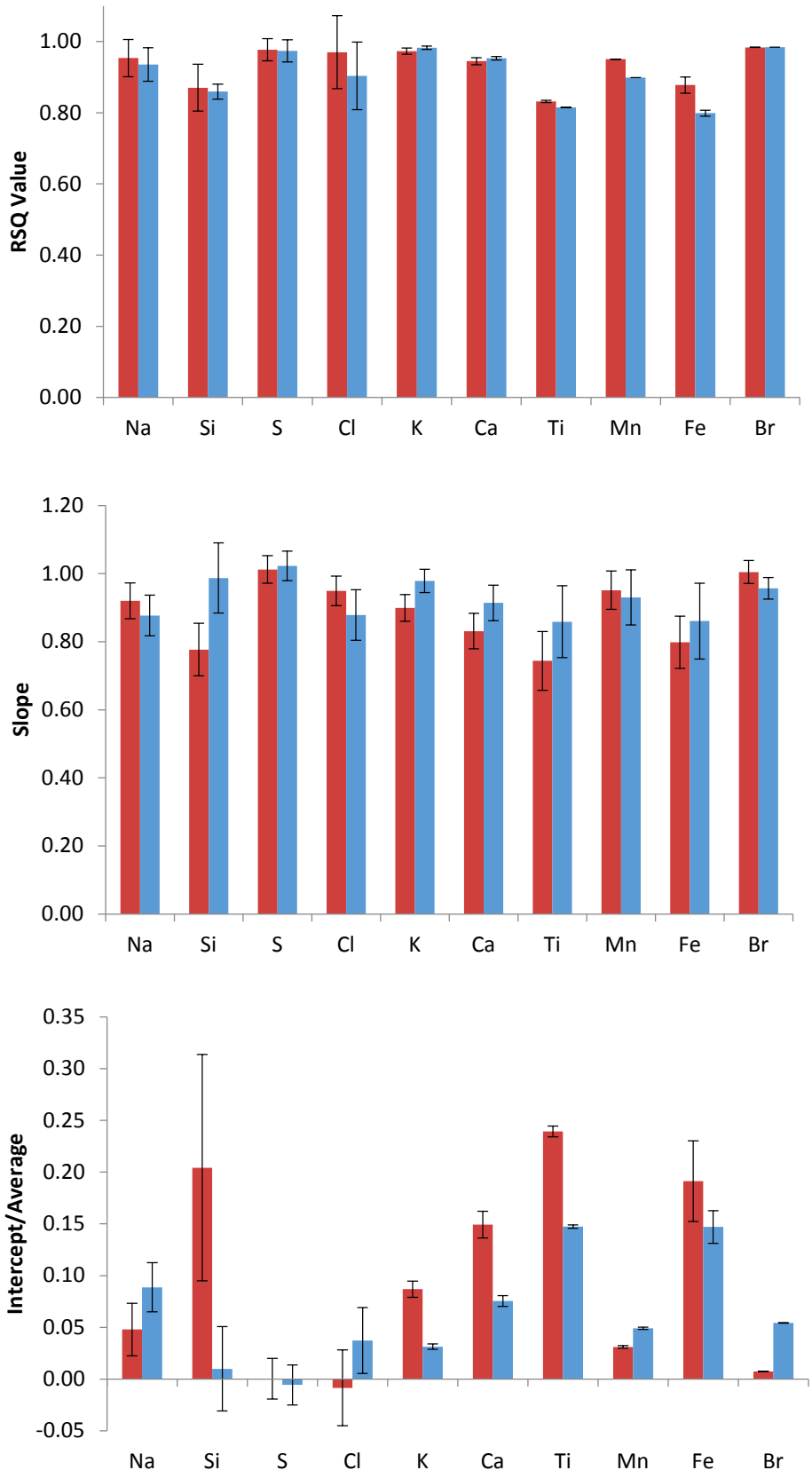

Figure 8b.5 Comparison between two XRF analyses 3a and 3b (3b = f(3a)) for Summer RDI PM10 (red bars) and PM2.5 (blue bars) showing RSQ, slope, intercept/average and their uncertainties for each (error bars).

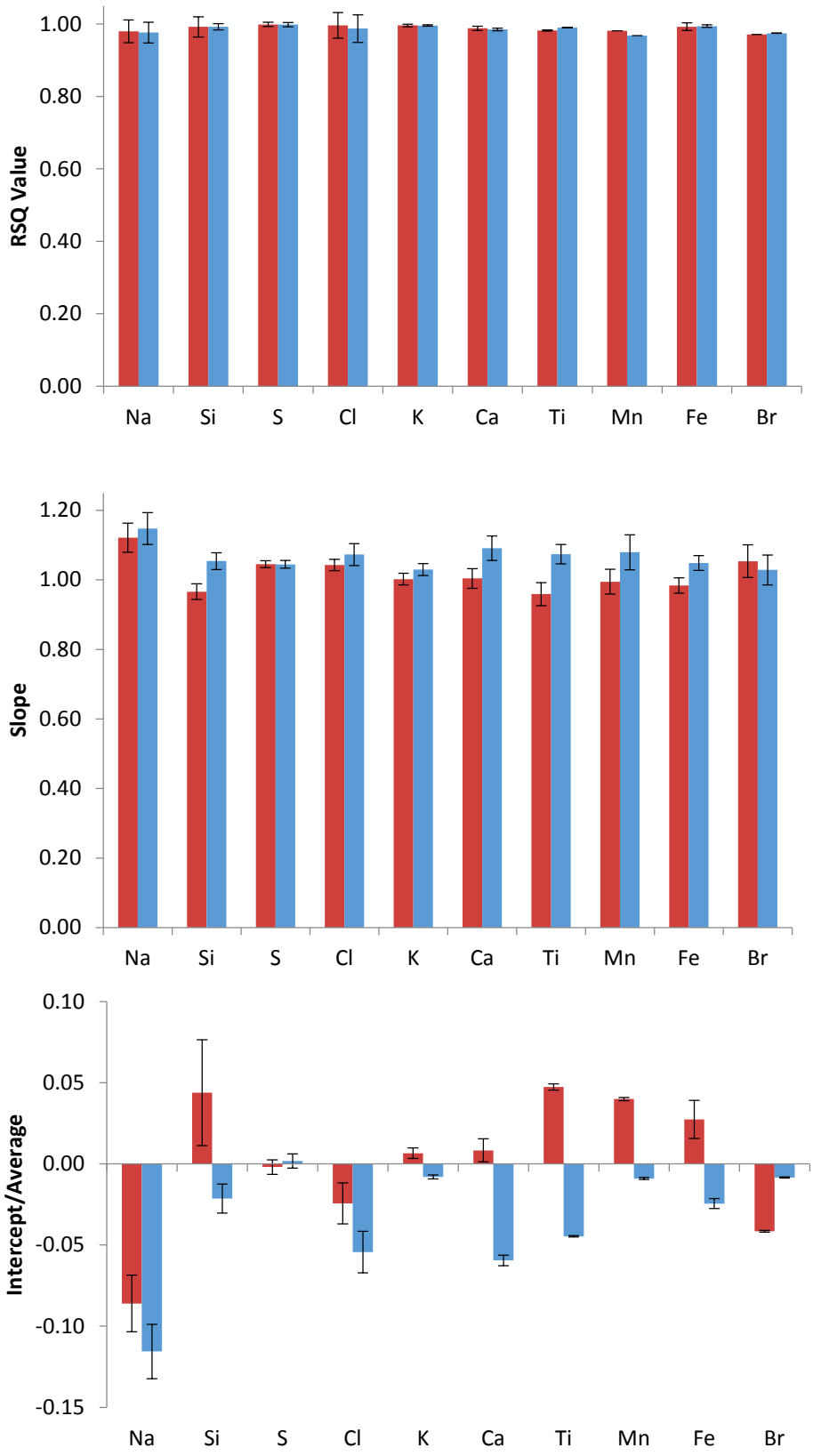

Figure 8b.6 Comparison between two XRF analyses 7a and 7b (7b = f(7a)) for Summer RDI PM10 (red bars) and PM2.5 (blue bars) showing RSQ, slope, intercept/average and their uncertainties for each (error bars).

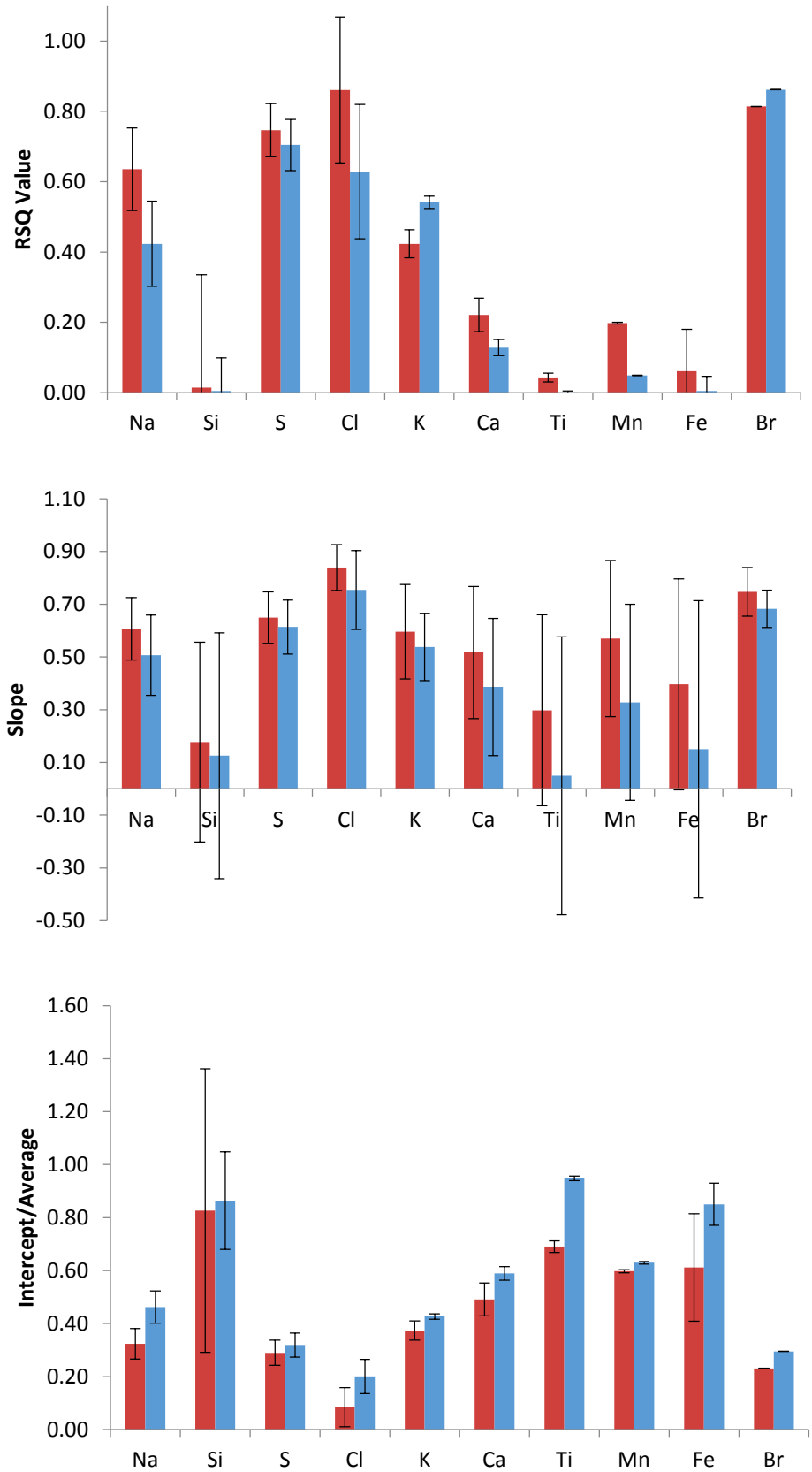

Figure 8b.7 Comparison between two samplers 3 and 7 (7a = f(3a)) for Summer RDI PM10 (red bars) and PM2.5 (blue bars) showing RSQ, slope, intercept/average and their uncertainties for each (error bars).

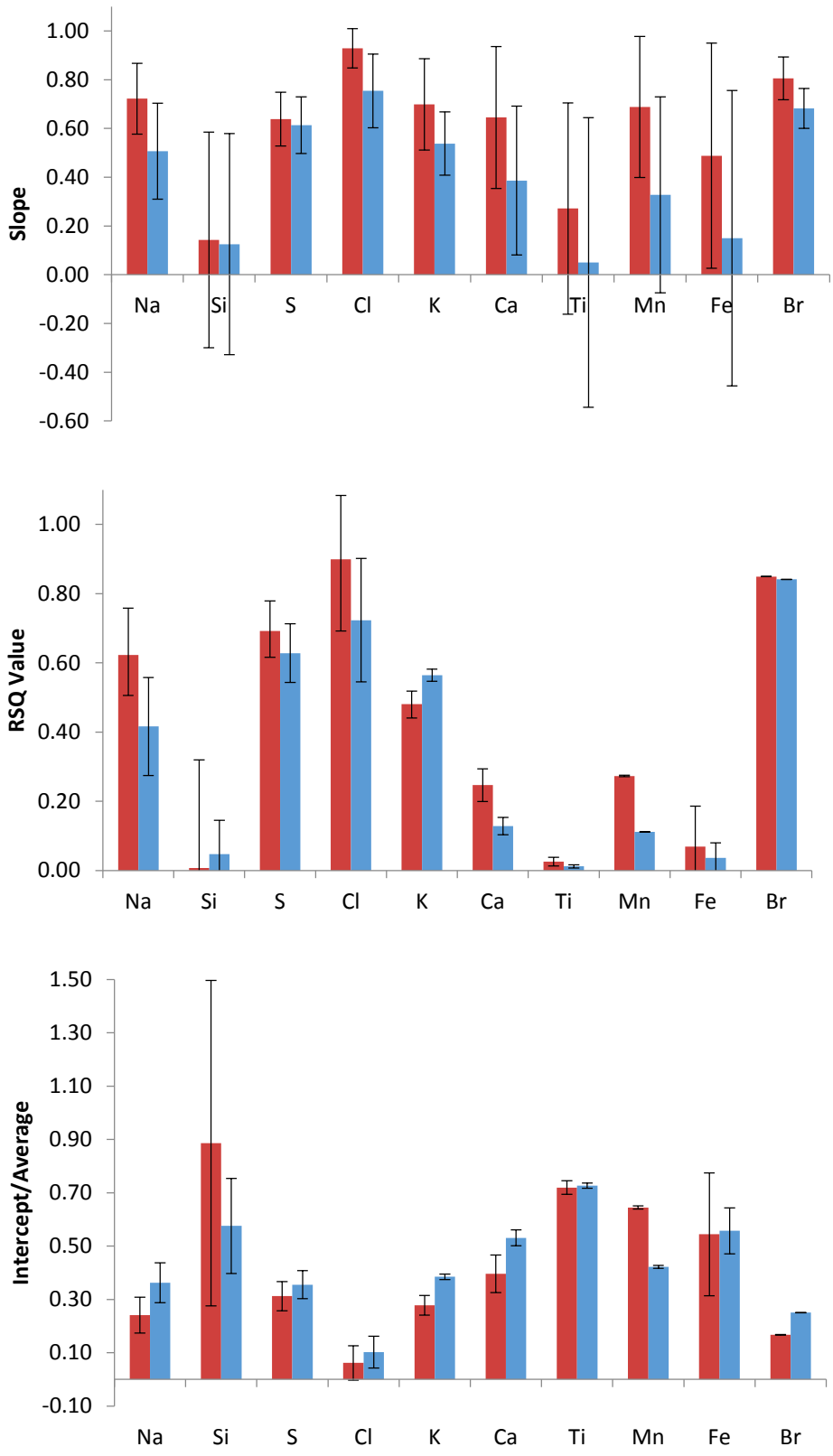

Figure 8b.8 Comparison between two samplers 3 and 7 (7b = f(3b)) for Summer RDI PM10 (red bars) and PM2.5 (blue bars) showing RSQ, slope, intercept/average and their uncertainties for each (error bars).

8c. MOUDI XRF PM1.8 – MOUDI XRF PM1.8

One set of precision was performed on the MOUDI substrates. The samples were analyzed twice by XRF using IMPROVE XRF instruments, testing the precision of the XRF analysis on MOUDI stage samples. Tables 8c.1-2 and Figure 8c.1 show the precision of the XRF for PM1.8 measured by the MOUDI for the winter and summer season.

Table 8c.1 Winter PM1.8 MOUDI (XRF test a) vs MOUDI (XRF test b).

(b = f(a))

Element	RSQ	SE RSQ	Slope	SE Slope	Intercept/Average	SE INTERCEPT /AVG
Na	0.660	0.003	0.649	0.269	0.100	0.179
Si	0.998	0.002	0.958	0.024	0.043	0.038
S	0.991	0.003	0.891	0.050	0.107	0.056
Cl	0.998	0.000	1.031	0.028	-0.038	0.028
K	0.996	0.001	1.065	0.037	-0.056	0.050
Ca	1.000	0.000	1.049	0.013	-0.020	0.000
Ti	0.960	0.000	0.878	0.103	0.079	0.000
Mn	0.972	0.000	0.978	0.096	0.059	0.000
Fe	0.997	0.002	0.981	0.031	0.028	0.041
Br	0.817	0.000	0.872	0.238	0.274	0.000

Table 8c.2 Summer PM1.8 MOUDI (XRF test a) vs MOUDI (XRF test b).

(b = f(a))

Element	RSQ	SE RSQ	Slope	SE Slope	Intercept/Average	SE INTERCEPT /AVG
Na	0.965	0.016	1.034	0.113	0.017	0.088
Si	0.999	0.001	1.077	0.023	-0.112	0.026
S	0.997	0.004	0.999	0.030	0.002	0.028
Cl	1.000	0.000	0.982	0.003	-0.004	0.000
K	0.996	0.001	1.021	0.039	-0.019	0.036
Ca	0.997	0.000	1.020	0.031	-0.011	0.049
Ti	0.838	0.000	0.949	0.241	-0.224	0.458
Mn	0.994	0.000	1.268	0.055	0.181	0.000
Fe	0.990	0.009	1.107	0.064	-0.115	0.061
Br	0.140	0.000	-0.146	0.208	1.114	0.000

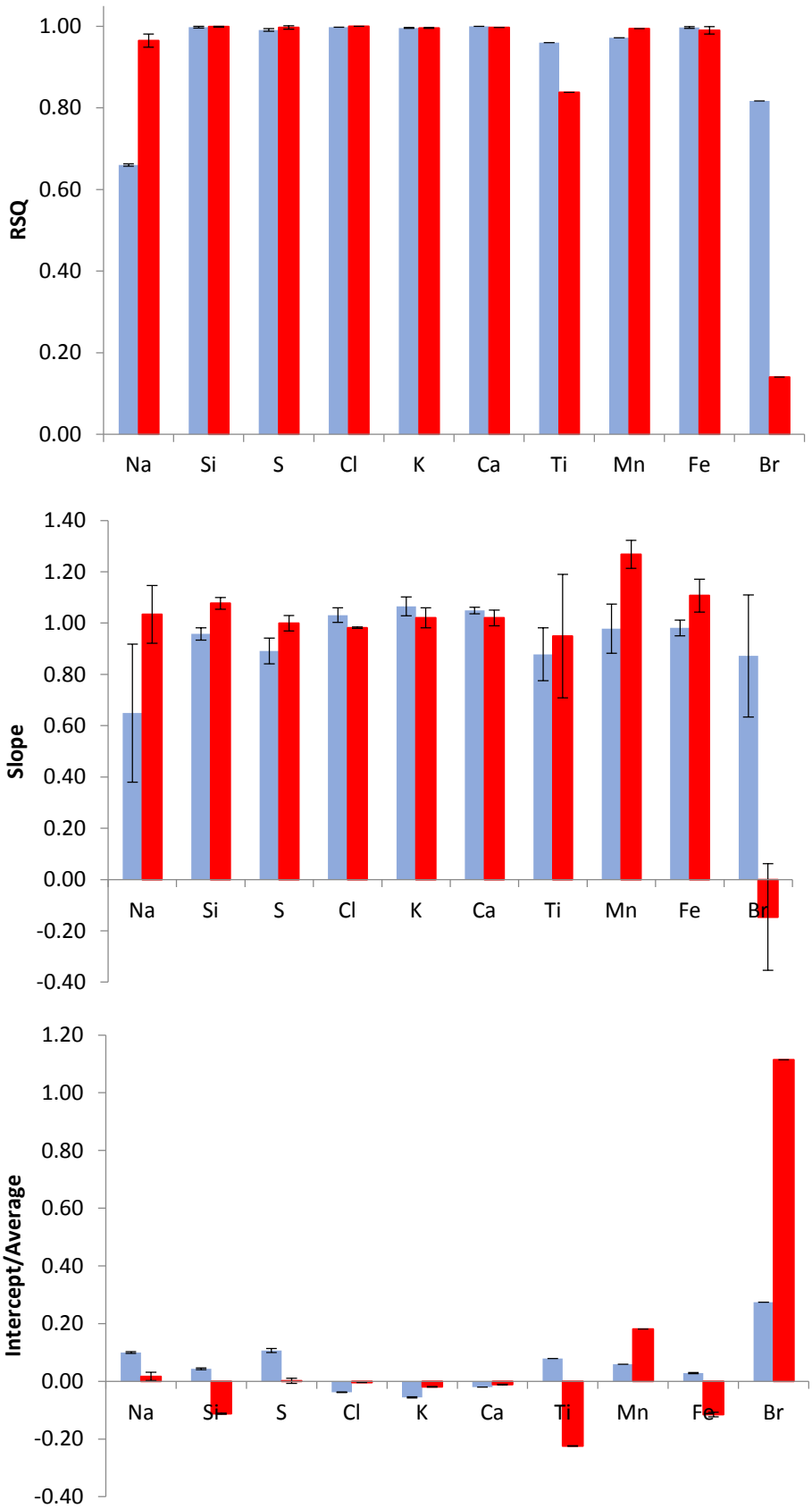

Figure 8c.1 Comparison between two XRF analyses MOUDI a and MOUDI b (MOUDI b = f(MOUDI a)) for Winter MOUDI PM1.8 (blue bars) and Summer PM1.8 (red bars) showing RSQ, slope, intercept/average and their uncertainties for each (error bars).

8d. MOUDI PM1.8 ICPMS – MOUDI PM1.8 ICPMS (repeat ICPMS analysis of the same substrate)

The following represents the precision of the ICPMS analysis technique from the winter and summer sampling events for MOUDI stages. Five 48-hr sets of 6 MOUDI Teflon filters from the 30-day collection period in the winter and summer were analyzed by the ICPMS twice on a single day. The two analyses were then compared to provide the precision of the ICPMS for both seasons.

Table 8d.1 Winter MOUDI ICPMS re-analysis precision (PM1.8).

Element	RSQ	RSQ SE	SLOPE	Slope SE	Intercept/Average	SE INTERCEPT /AVG
Li	<MDL	<MDL	<MDL	<MDL	<MDL	<MDL
S	0.993	0.019	0.980	0.023	-0.004	0.000
K	N/A	N/A	N/A	N/A	N/A	N/A
Ti	<MDL	<MDL	<MDL	<MDL	<MDL	<MDL
V	0.887	0.000	1.005	0.099	-0.056	0.000
Mn	0.845	0.000	1.034	0.123	-0.083	0.028
Fe	0.961	0.001	0.960	0.054	0.024	0.000
Ga[a]	0.987	0.000	0.986	0.031	-0.009	0.000
Ge	<MDL	<MDL	<MDL	<MDL	<MDL	<MDL
As	0.977	0.000	0.975	0.041	-0.018	0.000
Se	0.936	0.000	0.942	0.068	0.001	0.000
Br	0.982	0.000	0.944	0.035	0.030	0.000
Rb	<MDL	<MDL	<MDL	<MDL	<MDL	<MDL
Sr[a]	0.997	0.000	1.006	0.016	-0.024	0.000
Cd	<MDL	<MDL	<MDL	<MDL	<MDL	<MDL
Sn	0.999	0.000	0.991	0.009	-0.010	0.000
Sb	0.880	0.000	0.899	0.092	0.156	0.000
Ba	0.949	0.000	0.980	0.063	-0.026	0.000
Tl	<MDL	<MDL	<MDL	<MDL	<MDL	<MDL
Pb	0.996	0.000	0.971	0.018	0.020	0.000
Bi	N/A	N/A	N/A	N/A	N/A	N/A

N/A = element did not have an accurate set of external standards analyzed by the ICPMS to allow for calculation of mass.

<MDL = under MDL

[a] Element concentration was extremely close to MDL, however not under; could result in some noise/unreliability with measurement.

Table 8d.2 Summer MOUDI ICPMS re-analysis precision (PM1.8).

Element	RSQ	RSQ SE	Slope	Slope SE	Intercept/Average	SE INTERCEPT /AVG
Li	<MDL	<MDL	<MDL	<MDL	<MDL	<MDL
S	0.999	0.007	0.972	0.009	-0.001	0.153
K	N/A	N/A	N/A	N/A	N/A	N/A
Ti	<MDL	<MDL	<MDL	<MDL	<MDL	<MDL
V	0.859	0.000	1.003	0.113	0.049	0.000
Mn	0.939	0.000	0.920	0.065	0.010	0.000
Fe	0.995	0.001	0.981	0.018	0.003	0.000
Ga	0.989	0.000	0.984	0.028	-0.012	0.000
Ge[a]	<MDL	<MDL	<MDL	<MDL	<MDL	<MDL
As	0.962	0.000	1.000	0.055	-0.037	0.000
Se	0.999	0.000	1.009	0.009	-0.019	0.000
Br	0.984	0.000	1.008	0.035	-0.024	0.000
Rb	<MDL	<MDL	<MDL	<MDL	<MDL	<MDL
Sr[a]	0.878	0.000	0.844	0.087	0.040	0.000
Cd	<MDL	<MDL	<MDL	<MDL	<MDL	<MDL
Sn	<MDL	<MDL	<MDL	<MDL	<MDL	<MDL
Sb	<MDL	<MDL	<MDL	<MDL	<MDL	<MDL
Ba	0.986	0.000	0.966	0.031	0.017	0.000
Tl	<MDL	<MDL	<MDL	<MDL	<MDL	<MDL
Pb	0.972	0.000	0.992	0.047	-0.023	0.000
Bi	N/A	N/A	N/A	N/A	N/A	N/A

N/A = element did not have an accurate set of external standards analyzed by the ICPMS to allow for calculation of mass.

<MDL = under MDL

[a] Element concentration was extremely close to MDL, however not under; could result in some noise/unreliability with measurement.

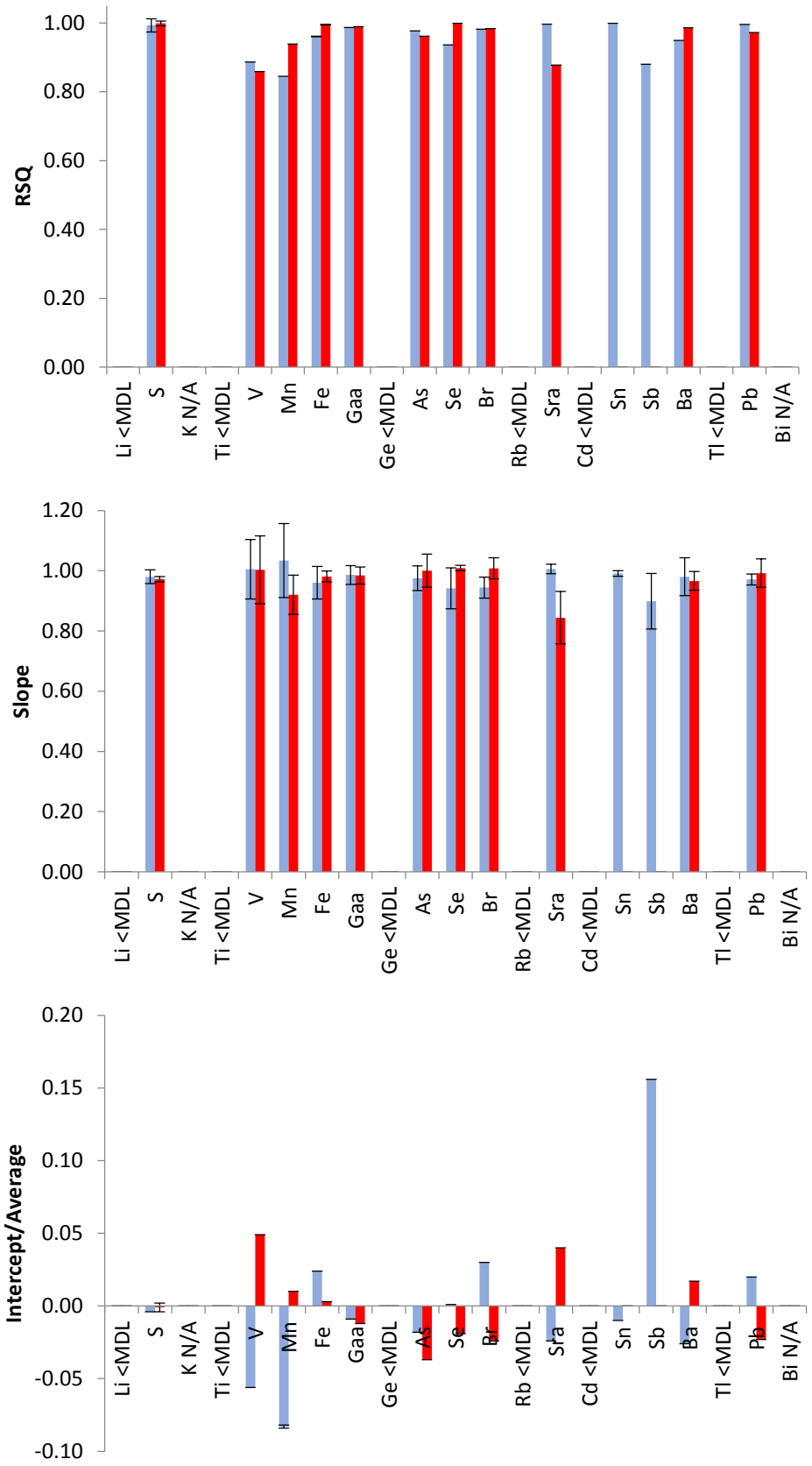

Figure 8d.1 Comparison between two ICPMS analyses MOUDI a and MOUDI b (MOUDI b = f(MOUDI a)) for Winter MOUDI PM1.8 (blue bars) and Summer PM1.8 (red bars) showing RSQ, slope, intercept/average and their uncertainties for each (error bars).

8e. MOUDI – MOUDI with ICPMS from Prior Observations

The two MOUDI samplers operated with different impaction substrates during the measurements performed during the current study so a direct sampler precision comparison was not possible. Nevertheless, prior research does provide an indication of MOUDI with ICPMS precision. The table below represents the average correlation between four MOUDIs during a single-day sampling event in 2006. The data was collected and analyzed with ICPMS (Herner et al., 2006).

Table 8e.1 Precision of two MOUDI samplers analyzed by ICPMS for 21 elements from Herner et al. (2006).

Element	RSQ	Slope	Intercept/ Average
Li	0.9	0.88	0.03
S	0.77	1.02	0.26
K	0.92	1.23	0
Ti	0.55	0.7	0.29
V	0.78	0.9	-0.28
Mn	0.95	1.07	-0.01
Fe	0.43	0.52	0.17
Ga	0.95	0.69	0
Ge	0.61	0.7	0.25
As	0.82	0.72	0.1
Se	0.78	0.74	0.09
Br	0.91	1.24	0
Rb	0.93	1.25	-0.01
Sr	0.82	0.74	0.13
Cd	0.74	0.74	0.16
Sn	0.57	0.9	0.14
Sb	0.88	1.08	0.03
Ba	0.66	0.73	0.24
Tl	0.96	0.73	-0.01
Pb	0.83	1.07	0.06
Bi	0.96	0.87	0.05

8f. MOUDI PM1.8 XRF – MOUDI PM1.8 ICPMS

We analyzed MOUDI stages with XRF and ICPMS. As is known from prior investigations, XRF and ICPMS work well for different sets of elements with nearly no overlap relevant to the atmosphere. The tables below compare the elements that had concentration above MDL for XRF analysis and ICP-MS analysis, however they did not always coincide with the core 21 ICPMS elements referenced above.

Table 8f.1 MOUDI PM1.8 analyzed by XRF vs MOUDI PM1.8 analyzed by ICPMS for Summer 2013.

Element	RSQ	RSQ SE	Slope	Slope SE	Intercept/Average	SE INTERCEPT /AVG
S	0.282	0.192	-2.423	1.072	2.551	0.461
V	0.000	0.000	0.002	0.084	0.605	0.000
Mn	0.047	0.001	0.061	0.076	0.782	0.000
Fe	0.027	0.007	0.062	0.104	0.454	0.052
Se	0.138	0.000	-0.166	0.115	1.227	0.000
Br	0.064	0.001	0.220	0.232	0.747	0.000

Table 8f.2 MOUDI PM1.8 analyzed by XRF vs MOUDI PM1.8 analyzed by ICPMS for Summer 2013.

Elements	RSQ	RSQ SE	SLOPE	Slope SE	Intercept/Average	SE INTERCEPT /AVG
S	0.555	0.147	1.354	0.336	-0.806	0.456
V	0.272	0.000	0.130	0.059	0.269	0.000
Mn	0.001	0.001	0.010	0.085	0.676	0.000
Fe	0.017	0.011	-0.014	0.029	0.231	0.038
Se	0.143	0.000	0.308	0.209	0.836	0.000
Br	0.783	0.001	0.989	0.144	0.115	0.000

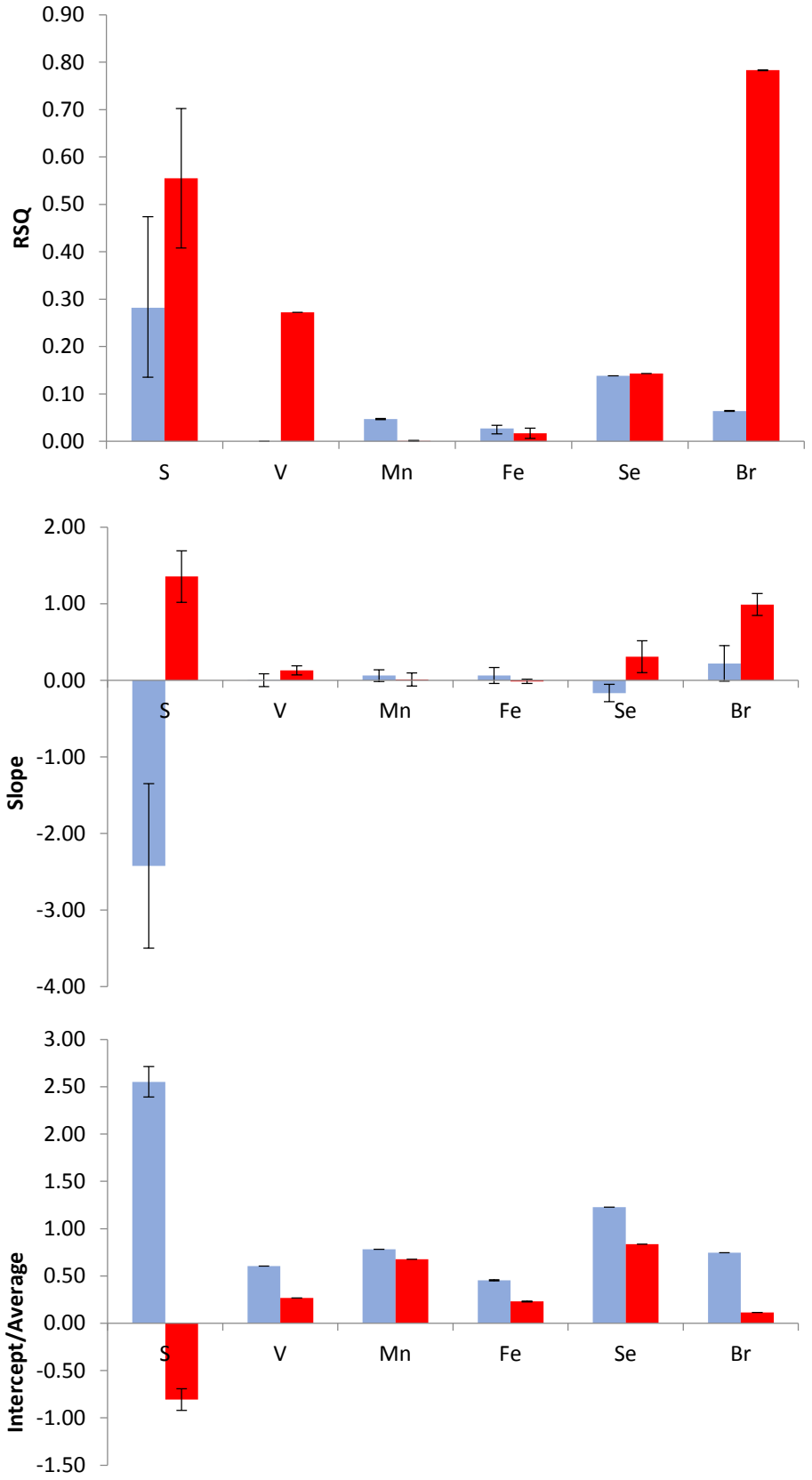

Figure 8f.1 Comparison between MOUDI PM1.8 analyzed by XRF vs MOUDI PM1.8 analyzed by ICPMS (MOUDI ICP-MS = f(MOUDI XRF)) for Winter (blue bars) and Summer (red bars) showing RSQ, slope, intercept/average and their uncertainties for each (error bars).

8g. RDI Stage Precision

We compared stage results to each other for the two samplers and the two seasons. Tables 8g.1-8 show stage precision for the elements that passed RDI PM2.5 precision as discussed in sections 9 and 10; results appear at the end of section 10b. Some of the elements compare quite well, others quite poorly. We hypothesized that this is due to difficulty with time synchronizing the RDI Mylar strips to each other. In Tables 8g.9-16, we show the same comparisons as in Tables 8g.1-8, but instead of the 90 minute time average we show the precision statistics for a 6 hour comparison by averaging 4 adjacent time steps. The comparisons are substantially improved suggesting that the RDI can be useful for diurnal cycle measurements. Despite this improvement, some elements have very poor sampler-to-sampler correlation suggesting another problem may exist in the sample collection or analysis.

Note that XRF was performed on each strip twice for the XRF precision evaluation. The strips were XRF analyzed in order of strip 1 through 8, then run again strip 1 through 8, but they were not repositioned between XRF measurements.

8g.a. RDI Stage Precision – 90-minute samples

Table 8g.1. RDI Stage 1 precision RDI-7a = f(RDI-3a) with 90 minute resolution.

Summer Element	RSQ	RSQ SE	Slope	Slope SE	Intercept/ Average	SE INTERCEPT /AVG
Na	0.004	20.190	0.071	0.046	0.929	0.089
S	0.193	6.106	0.475	0.042	0.508	0.048
Cl	0.663	41.450	0.788	0.024	0.186	0.033
Br	0.020	0.296	0.140	0.043	0.862	0.043

Winter Element	RSQ	RSQ SE	Slope	Slope SE	Intercept/ Average	SE INTERCEPT /AVG
Na	0.194	37.452	0.508	0.045	0.563	0.052
S	0.355	6.015	0.439	0.026	0.668	0.025
K	0.034	8.345	0.117	0.027	0.809	0.051
Fe	0.066	32.360	0.172	0.028	0.745	0.049
Cu	0.008	1.289	0.052	0.025	0.959	0.030
Zn	0.032	1.582	0.132	0.031	0.828	0.051
Br	0.015	0.393	0.171	0.061	0.809	0.069

Table 8g.2. RDI Stage 2 precision RDI-7a = f(RDI-3a) with 90 minute resolution.

Summer Element	RSQ	RSQ SE	Slope	Slope SE	Intercept/ Average	SE INTERCEPT /AVG
Na	0.510	45.646	0.606	0.026	0.030	0.068
S	0.830	7.186	0.701	0.014	0.352	0.016
Cl	0.848	86.685	0.773	0.014	0.100	0.025
Br	0.099	0.440	0.460	0.060	0.518	0.065

Winter Element	RSQ	RSQ SE	Slope	Slope SE	Intercept/ Average	SE INTERCEPT /AVG
Na	0.790	31.576	0.880	0.020	0.111	0.033
S	0.654	7.943	0.668	0.021	0.443	0.024
K	0.176	9.627	0.314	0.029	0.599	0.044
Fe	0.195	39.347	0.384	0.034	0.558	0.045
Cu	0.090	1.191	0.251	0.035	0.818	0.029
Zn	0.022	1.301	0.129	0.037	0.864	0.045
Br	0.101	0.402	0.457	0.059	0.474	0.069

Table 8g.3. RDI Stage 3 precision RDI-7a = f(RDI-3a) with 90 minute resolution.

Summer Element	RSQ	RSQ SE	Slope	Slope SE	Intercept/ Average	SE INTERCEPT /AVG
Na	0.081	183.926	0.278	0.041	0.721	0.081
S	0.261	47.398	0.483	0.035	0.535	0.051
Cl	0.254	381.712	0.456	0.034	0.541	0.079
Br	0.390	0.448	0.570	0.031	0.409	0.034

Winter Element	RSQ	RSQ SE	Slope	Slope SE	Intercept/ Average	SE INTERCEPT /AVG
Na	0.727	28.621	1.015	0.027	0.093	0.036
S	0.706	7.806	0.916	0.026	0.202	0.029
K	0.710	4.696	0.877	0.024	0.226	0.025
Fe	0.787	20.356	0.942	0.021	0.142	0.024
Cu	0.723	1.136	0.888	0.024	0.162	0.027
Zn	0.673	0.796	0.826	0.025	0.246	0.026
Br	0.006	0.239	0.074	0.041	0.929	0.040

Table 8g.4. RDI Stage 4 precision RDI-7a = f(RDI-3a) with 90 minute resolution.

Summer Element	RSQ	RSQ SE	Slope	Slope SE	Intercept/ Average	SE INTERCEPT /AVG
Na	0.609	29.614	0.353	0.012	0.454	0.029
S	0.621	10.179	0.317	0.011	0.602	0.020
Cl	0.737	34.369	0.435	0.011	0.285	0.044
Br	0.090	0.414	0.409	0.056	0.474	0.074

Winter Element	RSQ	RSQ SE	Slope	Slope SE	Intercept/ Average	SE INTERCEPT /AVG
Na	0.609	29.614	0.353	0.012	0.454	0.029
S	0.621	10.179	0.317	0.011	0.602	0.020
K	0.737	34.369	0.435	0.011	0.285	0.044
Fe	0.090	0.414	0.409	0.056	0.474	0.074
Cu	0.609	29.614	0.353	0.012	0.454	0.029
Zn	0.621	10.179	0.317	0.011	0.602	0.020
Br	0.737	34.369	0.435	0.011	0.285	0.044

Table 8g.5. RDI Stage 5 precision RDI-7a = f(RDI-3a) with 90 minute resolution.

Summer Element	RSQ	RSQ SE	Slope	Slope SE	Intercept/ Average	SE INTERCEPT /AVG
Na	0.304	21.988	0.474	0.031	0.530	0.037
S	0.175	117.304	0.298	0.028	0.675	0.044
Cl	0.438	0.402	0.342	0.017	0.546	0.052
Br	0.332	0.350	0.312	0.019	0.627	0.025

Winter Element	RSQ	RSQ SE	Slope	Slope SE	Intercept/ Average	SE INTERCEPT /AVG
Na	0.125	13.354	0.430	0.049	0.611	0.047
S	0.012	54.904	0.098	0.038	0.902	0.073
K	0.045	13.508	0.216	0.043	0.781	0.077
Fe	0.423	6.243	0.621	0.031	0.384	0.045
Cu	0.186	1.130	0.580	0.052	0.475	0.061
Zn	0.199	2.571	0.542	0.047	0.450	0.067
Br	0.084	0.653	0.244	0.035	0.742	0.041

Table 8g.6. RDI Stage 6 precision RDI-7a = f(RDI-3a) with 90 minute resolution.

Summer Element	RSQ	RSQ SE	Slope	Slope SE	Intercept/ Average	SE INTERCEPT /AVG
Na	0.018	10.897	0.078	0.025	0.938	0.024
S	0.785	4.271	1.570	0.036	-1.427	0.058
Cl	0.088	1.032	0.194	0.027	0.390	0.104
Br	0.005	0.237	0.054	0.034	0.966	0.023

Winter Element	RSQ	RSQ SE	Slope	Slope SE	Intercept/ Average	SE INTERCEPT /AVG
Na	0.005	10.495	0.070	0.042	0.933	0.042
S	0.087	2.495	0.382	0.054	0.712	0.050
K	0.277	0.839	0.868	0.061	0.443	0.050
Fe	0.141	1.097	0.241	0.026	0.665	0.045
Cu	0.011	0.145	0.159	0.065	0.850	0.062
Zn	0.008	0.379	0.207	0.097	0.842	0.076
Br	0.002	0.230	0.039	0.039	0.961	0.040

Table 8g.7. RDI Stage 7 precision RDI-7a = f(RDI-3a) with 90 minute resolution.

Summer Element	RSQ	RSQ SE	Slope	Slope SE	Intercept/ Average	SE INTERCEPT /AVG
Na	0.008	9.266	0.079	0.039	0.915	0.044
S	0.688	26.074	0.659	0.019	0.087	0.032
Cl	0.006	1.270	0.252	0.137	0.832	0.199
Br	0.076	0.276	0.231	0.035	0.734	0.041

Winter Element	RSQ	RSQ SE	Slope	Slope SE	Intercept/ Average	SE INTERCEPT /AVG
Na	0.000	9.271	0.001	0.046	0.999	0.042
S	0.125	36.012	0.789	0.090	0.462	0.076
K	0.143	16.414	0.926	0.098	0.372	0.087
Fe	0.327	0.952	0.299	0.019	0.568	0.037
Cu	0.039	0.246	0.267	0.057	0.765	0.052
Zn	0.308	1.412	0.908	0.059	0.346	0.052
Br	0.089	0.585	0.521	0.072	0.559	0.063

Table 8g.8. RDI Stage 8 precision RDI-7a = f(RDI-3a) with 90 minute resolution.

Summer Element	RSQ	RSQ SE	Slope	Slope SE	Intercept/ Average	SE INTERCEPT /AVG
Na	0.002	9.878	-0.051	0.049	1.045	0.045
S	0.152	23.708	0.526	0.054	0.649	0.043
Cl	0.001	0.555	-0.034	0.061	1.023	0.118
Br	0.009	0.313	0.119	0.053	0.894	0.047

Winter Element	RSQ	RSQ SE	Slope	Slope SE	Intercept/ Average	SE INTERCEPT /AVG
Na	0.000	8.676	0.005	0.042	0.995	0.044
S	0.500	6.253	0.892	0.039	0.279	0.037
K	0.579	4.985	0.962	0.036	0.220	0.037
Fe	0.733	0.346	0.589	0.015	0.246	0.027
Cu	0.328	0.072	0.515	0.032	0.504	0.031
Zn	0.837	0.334	1.139	0.022	-0.017	0.022
Br	0.069	0.293	0.290	0.046	0.717	0.046

8g.b. RDI Stage Precision – Average of four 90-minute samples

Table 8g.9. RDI Stage 1 precision RDI-7a = f(RDI-3a) with a 6 hour average.

Summer Element	RSQ	RSQ SE	Slope	Slope SE	Intercept/ Average	SE INTERCEPT /AVG
Na	0.001	12.130	0.026	0.047	0.974	0.065
S	0.255	5.411	0.549	0.041	0.432	0.046
Cl	0.688	39.355	0.800	0.023	0.174	0.032
Br	0.094	0.163	0.327	0.044	0.678	0.044

Winter Element	RSQ	RSQ SE	Slope	Slope SE	Intercept/ Average	SE INTERCEPT /AVG
Na	0.498	22.079	0.736	0.032	0.365	0.035
S	0.444	5.306	0.506	0.025	0.617	0.023
K	0.037	8.006	0.122	0.027	0.802	0.050
Fe	0.074	31.112	0.182	0.028	0.731	0.048
Cu	0.047	0.856	0.127	0.025	0.899	0.025
Zn	0.067	1.321	0.197	0.032	0.743	0.048
Br	0.025	0.256	0.236	0.064	0.737	0.072

Table 8g.10. RDI Stage 2 precision RDI-7a = f(RDI-3a) with a 6 hour average.

Summer Element	RSQ	RSQ SE	Slope	Slope SE	Intercept/ Average	SE INTERCEPT /AVG
Na	0.698	32.411	0.694	0.020	-0.113	0.050
S	0.893	5.581	0.724	0.011	0.330	0.013
Cl	0.898	69.591	0.795	0.012	0.075	0.020
Br	0.423	0.245	0.995	0.050	-0.045	0.053

Winter Element	RSQ	RSQ SE	Slope	Slope SE	Intercept/ Average	SE INTERCEPT /AVG
Na	0.910	19.646	0.928	0.013	0.063	0.021
S	0.689	7.388	0.684	0.020	0.430	0.023
K	0.186	9.293	0.321	0.029	0.590	0.043
Fe	0.209	37.850	0.392	0.033	0.549	0.044
Cu	0.132	1.007	0.287	0.032	0.793	0.026
Zn	0.033	1.106	0.148	0.035	0.844	0.041
Br	0.343	0.238	0.837	0.050	0.038	0.058

Table 8g.11. RDI Stage 3 precision RDI-7a = f(RDI-3a) with a 6 hour average.

Summer Element	RSQ	RSQ SE	Slope	Slope SE	Intercept/ Average	SE INTERCEPT /AVG
Na	0.155	144.119	0.380	0.038	0.618	0.067
S	0.319	40.549	0.528	0.033	0.492	0.046
Cl	0.421	277.414	0.587	0.030	0.409	0.060
Br	0.553	0.326	0.658	0.026	0.318	0.028

Winter Element	RSQ	RSQ SE	Slope	Slope SE	Intercept/ Average	SE INTERCEPT /AVG
Na	0.926	14.216	1.191	0.015	-0.057	0.019
S	0.824	5.755	1.041	0.021	0.099	0.023
K	0.769	3.855	0.907	0.022	0.201	0.022
Fe	0.828	16.945	0.952	0.019	0.136	0.020
Cu	0.803	0.868	0.928	0.020	0.126	0.022
Zn	0.781	0.586	0.874	0.020	0.205	0.021
Br	0.025	0.142	0.162	0.044	0.843	0.043

Table 8g.12. RDI Stage 4 precision RDI-7a = f(RDI-3a) with a 6 hour average.

Summer Element	RSQ	RSQ SE	Slope	Slope SE	Intercept/ Average	SE INTERCEPT /AVG
Na	0.700	23.889	0.361	0.010	0.442	0.024
S	0.658	9.232	0.321	0.010	0.596	0.018
Cl	0.769	30.624	0.441	0.010	0.275	0.040
Br	0.341	0.254	0.777	0.047	0.000	0.061

Winter Element	RSQ	RSQ SE	Slope	Slope SE	Intercept/ Average	SE INTERCEPT /AVG
Na	0.539	16.759	1.033	0.041	0.169	0.038
S	0.017	36.605	0.218	0.073	0.770	0.110
K	0.066	5.292	0.351	0.057	0.747	0.056
Fe	0.382	12.368	0.656	0.036	0.466	0.038
Cu	0.076	1.333	0.363	0.055	0.425	0.092
Zn	0.031	1.552	0.189	0.046	0.830	0.054
Br	0.005	0.184	0.057	0.035	0.961	0.025

Table 8g.13. RDI Stage 5 precision RDI-7a = f(RDI-3a) with a 6 hour average.

Summer Element	RSQ	RSQ SE	Slope	Slope SE	Intercept/ Average	SE INTERCEPT /AVG
Na	0.453	16.568	0.557	0.027	0.448	0.031
S	0.286	90.533	0.368	0.025	0.598	0.037
Cl	0.625	0.289	0.395	0.013	0.475	0.038
Br	0.563	0.238	0.383	0.015	0.542	0.019

Winter Element	RSQ	RSQ SE	Slope	Slope SE	Intercept/ Average	SE INTERCEPT /AVG
Na	0.396	8.215	0.817	0.044	0.261	0.041
S	0.029	37.500	0.156	0.039	0.843	0.057
K	0.115	8.797	0.338	0.041	0.657	0.058
Fe	0.635	4.055	0.755	0.025	0.252	0.032
Cu	0.511	0.682	0.969	0.041	0.123	0.044
Zn	0.443	1.574	0.753	0.037	0.235	0.047
Br	0.193	0.431	0.336	0.030	0.644	0.034

Table 8g.14. RDI Stage 6 precision RDI-7a = f(RDI-3a) with a 6 hour average.

Summer Element	RSQ	RSQ SE	Slope	Slope SE	Intercept/ Average	SE INTERCEPT /AVG
Na	0.110	6.911	0.216	0.027	0.828	0.023
S	0.845	3.477	1.660	0.031	-1.568	0.050
Cl	0.205	0.752	0.282	0.024	0.117	0.087
Br	0.015	0.134	0.103	0.037	0.934	0.024

Winter Element	RSQ	RSQ SE	Slope	Slope SE	Intercept/ Average	SE INTERCEPT /AVG
Na	0.059	5.970	0.251	0.043	0.757	0.042
S	0.135	2.277	0.498	0.054	0.624	0.049
K	0.382	0.723	1.045	0.058	0.329	0.045
Fe	0.190	0.981	0.276	0.025	0.619	0.042
Cu	0.024	0.119	0.261	0.073	0.754	0.069
Zn	0.010	0.357	0.253	0.106	0.807	0.083
Br	0.000	0.115	0.009	0.036	0.991	0.037

Table 8g.15. RDI Stage 7 precision RDI-7a = f(RDI-3a) with a 6 hour average.

Summer Element	RSQ	RSQ SE	Slope	Slope SE	Intercept/ Average	SE INTERCEPT /AVG
Na	0.015	4.663	0.101	0.036	0.891	0.039
S	0.792	19.273	0.752	0.017	-0.044	0.027
Cl	0.018	0.897	0.440	0.139	0.707	0.156
Br	0.292	0.164	0.449	0.030	0.483	0.035

Winter Element	RSQ	RSQ SE	Slope	Slope SE	Intercept/ Average	SE INTERCEPT /AVG
Na	0.001	4.878	0.037	0.049	0.967	0.044
S	0.288	23.567	1.037	0.071	0.293	0.056
K	0.351	10.510	1.234	0.073	0.161	0.061
Fe	0.439	0.763	0.337	0.016	0.509	0.032
Cu	0.205	0.179	0.635	0.054	0.442	0.048
Zn	0.425	1.171	1.076	0.054	0.225	0.046
Br	0.272	0.415	0.977	0.069	0.172	0.060

Table 8g.16. RDI Stage 8 precision RDI-7a = f(RDI-3a) with a 6 hour average.

Summer Element	RSQ	RSQ SE	Slope	Slope SE	Intercept/ Average	SE INTERCEPT /AVG
Na	0.018	5.197	0.164	0.052	0.854	0.047
S	0.151	20.569	0.501	0.052	0.664	0.040
Cl	0.002	0.356	-0.068	0.064	1.046	0.083
Br	0.031	0.200	0.272	0.066	0.760	0.059

Winter Element	RSQ	RSQ SE	Slope	Slope SE	Intercept/ Average	SE INTERCEPT /AVG
Na	0.016	4.405	0.122	0.041	0.875	0.042
S	0.752	3.852	1.055	0.026	0.145	0.024
K	0.814	2.965	1.149	0.024	0.066	0.024
Fe	0.827	0.234	0.618	0.012	0.212	0.020
Cu	0.530	0.044	0.615	0.025	0.408	0.024
Zn	0.883	0.248	1.191	0.019	-0.066	0.019
Br	0.309	0.175	0.679	0.044	0.339	0.043

9. Regression Analysis

In this section, we compare each pair of samplers to each other for the 10 XRF elements that are typically well above MDL for all three samplers.

9a. MOUDI (PM1.8) XRF vs IMPROVE (PM2.5) XRF

The following correlations are for IMPROVE = f(MOUDI). For the IMPROVE, the cut is at 2.5 um while for MOUDI, the sum less than 1.8 um was used because there is no 2.5 um cut point. As a result, the slopes should be greater than 1 because there is more mass counted in the IMPROVE sum than in the MOUDI sum. Tables 9a.1-2 and Figure 9a.1 show the precision between the MOUDI PM1.8 and IMPROVE PM2.5 analyzed by XRF for the winter and summer season.

Table 9a.1 Winter IMPROVE (PM2.5) vs MOUDI (PM1.8) XRF.

(IMPROVE = f(MOUDI))

Element	RSQ	SE RSQ	SLOPE	SE SLOPE	INTERCEPT/AVG	SE INTERCEPT /AVG
Na	0.970	0.017	1.582	0.076	0.206	0.127
Si	0.008	0.030	-0.078	0.240	0.810	0.328
S	0.870	0.020	1.062	0.114	-0.261	0.130
Cl	0.963	0.017	1.770	0.097	-0.588	0.153
K	0.936	0.005	1.070	0.078	-0.068	0.084
Ca	0.137	0.010	0.533	0.371	0.797	0.320
Ti	0.015	0.001	-0.128	0.287	1.004	0.384
Mn	0.060	0.001	-0.050	0.055	0.355	0.000
Fe	0.051	0.023	0.302	0.361	0.589	0.401
Br	0.761	0.001	0.951	0.148	0.521	0.000

Table 9a.2 Summer IMPROVE (PM2.5) vs MOUDI (PM1.8) XRF.

(IMPROVE = f(MOUDI))

Element	RSQ	SE RSQ	SLOPE	SE SLOPE	INTERCEPT/AVG	SE INTERCEPT /AVG
Na	0.939	0.052	1.404	0.099	0.001	0.101
Si	0.445	0.018	0.495	0.153	0.562	0.119
S	0.850	0.035	0.686	0.080	0.076	0.104
Cl	0.962	0.032	1.722	0.095	-0.176	0.124
K	0.756	0.006	1.252	0.197	-0.268	0.095
Ca	0.713	0.006	1.095	0.193	0.157	0.116
Ti	0.411	0.001	0.452	0.150	0.689	0.000
Mn	0.002	0.000	0.005	0.049	0.555	0.000
Fe	0.081	0.010	-0.028	0.026	0.528	0.092
Br	0.635	0.000	0.590	0.124	0.308	0.000

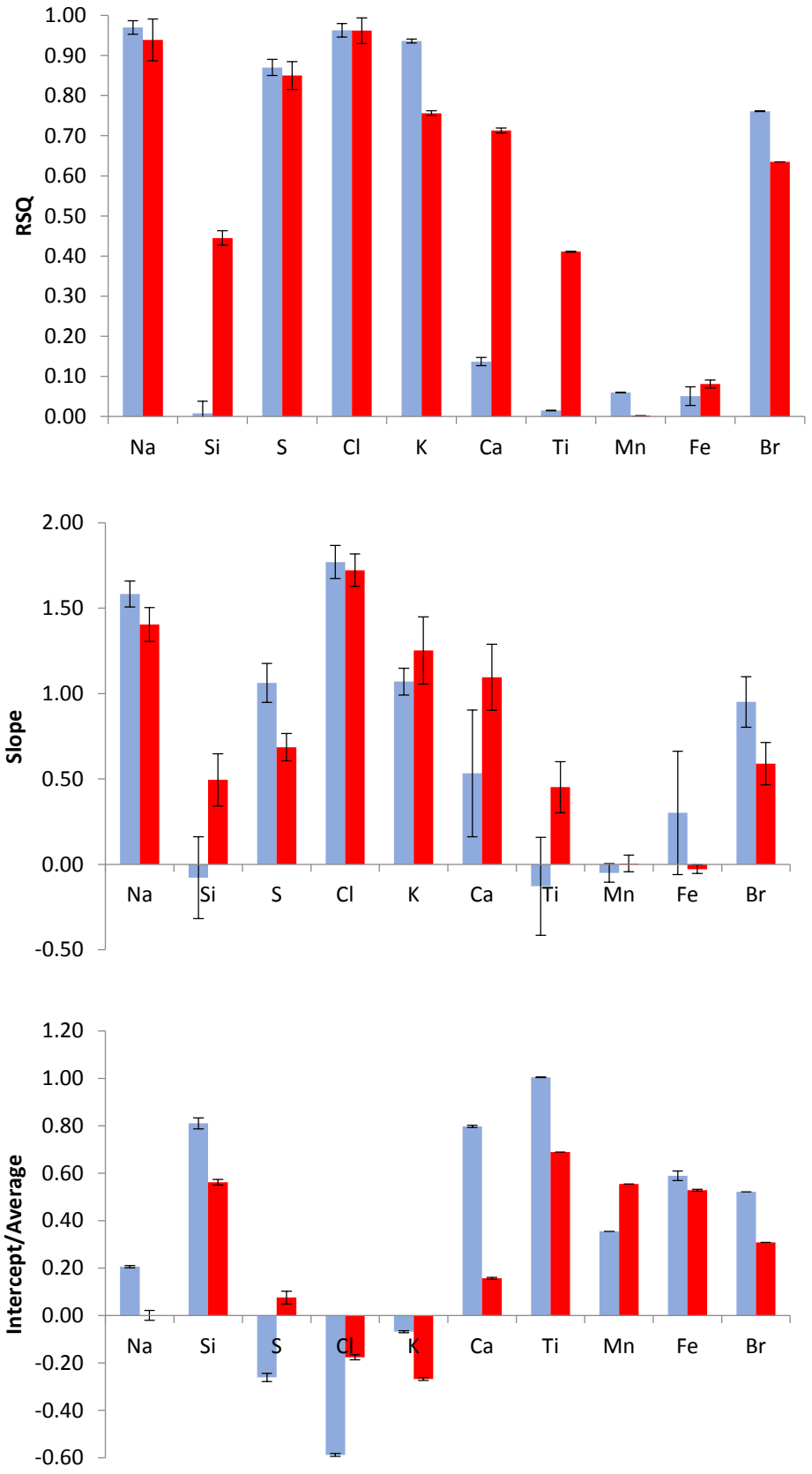

Figure 9a.1 Comparison between IMPROVE PM2.5 and MOUDI PM1.8 (IMPROVE= f(MOUDI)) analyzed by XRF for Winter (blue bars) and Summer PM1.8 (red bars) showing RSQ, slope, intercept/average and their uncertainties for each (error bars).

9b. RDI vs IMPROVE

The following correlations are for IMPROVE = f(RDI). IMPROVE sampler RONS was used to compare to RDI 3a and 7a, as the comparison between RONS and ROSN (IMPROVE samplers) was quite good. Tables 9b.1-4 and Figures 9b.1-2 show the precision between the RDI and IMPROVE winter PM10 and PM2.5 while Tables 9b.5-8 and Figures 9b.3-5 show the precision between the RDI and IMPROVE summer PM10 and PM2.5. Figures 9b.6-9 show the precision between the RDI and IMPROVE PM10 and PM2.5 for the summer and winter seasons.

Table 9b.1. Winter IMPROVE PM10 vs RDI 3a PM10 XRF.

Element	RSQ	SE RSQ	SLOPE	SE SLOPE	INTERCEPT/AVG	SE INTERCEPT /AVG
Na	0.958	0.046	1.344	0.078	-1.318	0.123
Si	0.935	0.087	1.123	0.082	-0.251	0.432
S	0.726	0.033	0.944	0.161	0.090	1.912
Cl	0.991	0.034	1.022	0.027	-0.055	0.232
K	0.928	0.010	1.076	0.083	0.033	0.052
Ca	0.886	0.033	1.188	0.118	-0.259	0.236
Ti	0.930	0.003	0.766	0.058	-0.137	0.012
Mn	0.874	0.001	1.190	0.125	-1.348	2.140
Fe	0.947	0.030	1.122	0.074	-0.023	1.925
Br	0.702	0.001	1.152	0.208	-1.525	0.306

Table 9b.2. Winter IMPROVE PM2.5 vs RDI 3a PM2.5 XRF.

Element	RSQ	SE RSQ	SLOPE	SE SLOPE	INTERCEPT/AVG	SE INTERCEPT /AVG
Na	0.940	0.024	1.525	0.107	-2.111	0.181
Si	0.659	0.018	0.320	0.064	-0.194	0.622
S	0.690	0.032	1.120	0.208	-0.087	3.287
Cl	0.978	0.013	0.768	0.032	0.028	0.112
K	0.909	0.006	1.099	0.096	0.001	0.085
Ca	0.868	0.004	0.440	0.047	-0.204	0.066
Ti	0.950	0.000	0.262	0.017	-0.065	0.000
Mn	0.687	0.000	0.639	0.120	-1.129	4.085
Fe	0.927	0.006	0.509	0.040	0.029	0.620
Br	0.810	0.000	1.393	0.187	-1.805	0.395

Table 9b.3. Winter IMPROVE PM10 vs RDI 7a PM10 XRF.

Element	RSQ	SE RSQ	SLOPE	SE SLOPE	INTERCEPT/AVG	SE INTERCEPT /AVG
Na	0.946	0.052	1.235	0.082	-1.129	0.118
Si	0.442	0.254	1.136	0.354	-0.217	0.379
S	0.649	0.038	0.930	0.190	-0.031	0.245
Cl	0.989	0.039	0.952	0.028	-0.014	0.250
K	0.725	0.020	1.068	0.183	0.116	0.177
Ca	0.466	0.073	1.320	0.392	-0.297	0.396
Ti	0.625	0.006	0.923	0.198	-0.114	0.207
Mn	0.636	0.002	1.267	0.266	-1.792	0.000
Fe	0.627	0.080	1.196	0.256	0.053	3.905
Br	0.691	0.001	1.046	0.194	-1.137	1.731

Table 9b.4. Winter IMPROVE PM2.5 vs RDI 7a PM2.5 XRF.

Element	RSQ	SE RSQ	SLOPE	SE SLOPE	INTERCEPT/AVG	SE INTERCEPT /AVG
Na	0.955	0.020	1.134	0.068	-1.323	0.102
Si	0.899	0.010	0.378	0.035	-0.039	0.066
S	0.585	0.036	0.972	0.227	-0.060	0.303
Cl	0.975	0.014	0.602	0.027	0.077	0.270
K	0.897	0.006	0.802	0.075	0.126	0.089
Ca	0.800	0.005	0.422	0.058	-0.074	0.075
Ti	0.946	0.000	0.239	0.016	-0.052	0.025
Mn	0.659	0.000	0.497	0.099	-0.074	0.000
Fe	0.955	0.005	0.496	0.030	-0.031	0.643
Br	0.643	0.001	1.087	0.224	-1.172	2.001

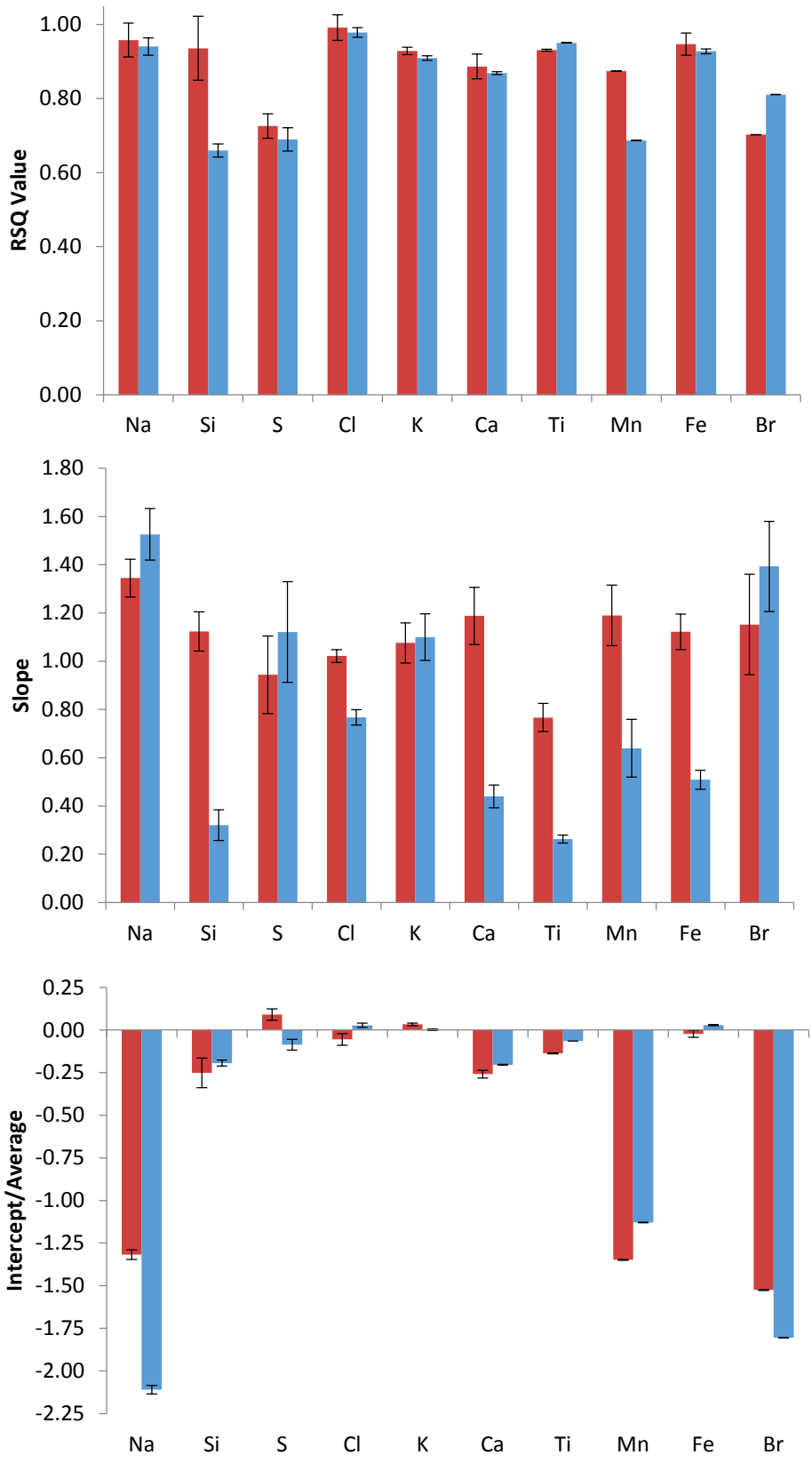

Figure 9b.1 Comparison between IMPROVE and RDI3a (IMPROVE = f(RDI3a) for Winter PM10 (red bars) and PM2.5 (blue bars) showing RSQ, slope, intercept/average and their uncertainties for each (error bars).

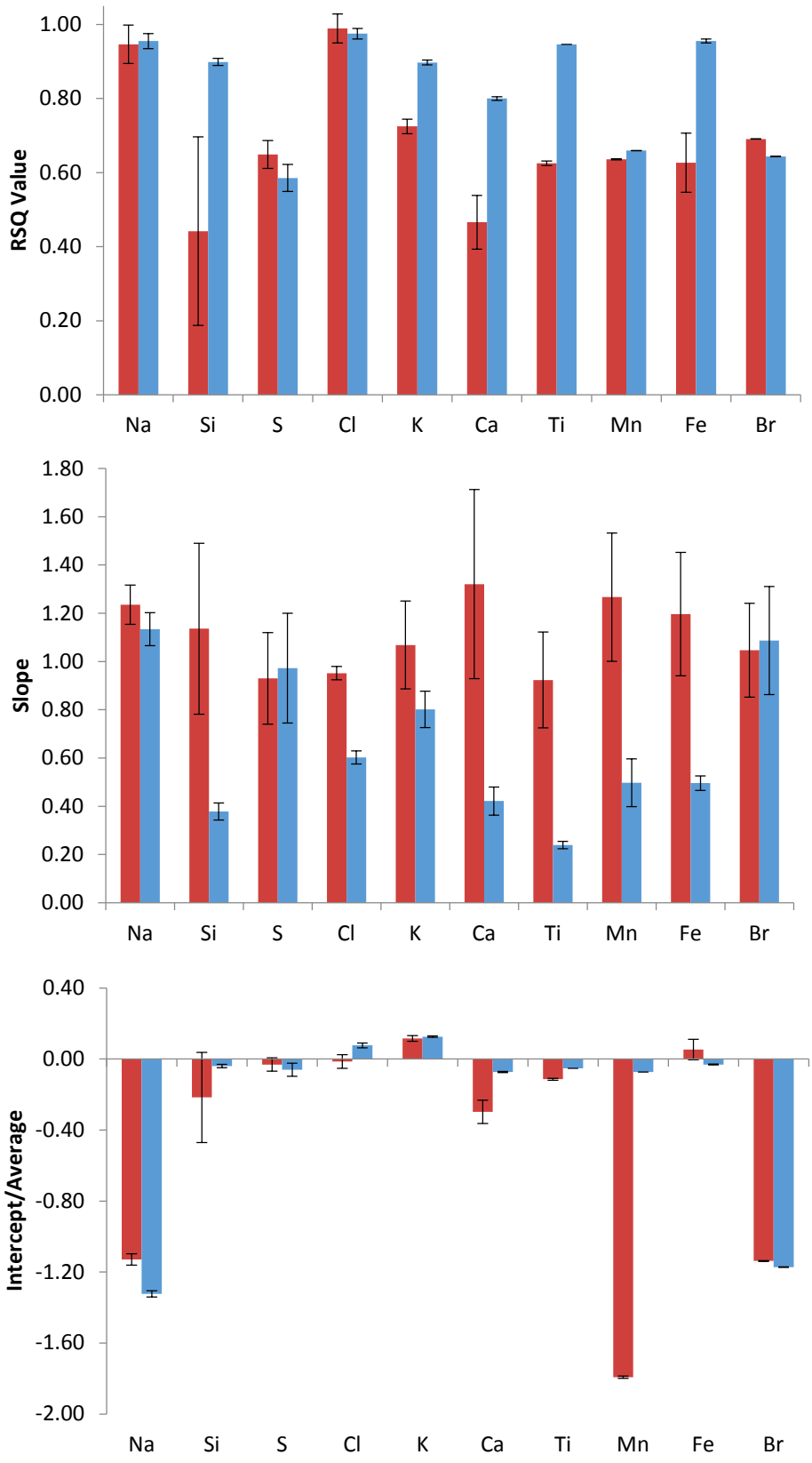

Figure 9b.2 Comparison between IMPROVE and RDI7a (IMPROVE = f(RDI7a) for Winter PM10 (red bars) and PM2.5 (blue bars) showing RSQ, slope, intercept/average and their uncertainties for each (error bars).

Table 9b.5. Summer IMPROVE PM10 vs RDI 3a PM10 XRF.

Element	RSQ	SE RSQ	SLOPE	SE SLOPE	INTERCEPT/AVG	SE INTERCEPT /AVG
Na	0.617	0.223	1.075	0.235	-0.254	0.292
Si	0.277	0.419	1.165	0.522	0.348	0.403
S	0.344	0.099	0.336	0.129	0.456	0.162
Cl	0.716	0.280	0.709	0.124	-0.071	0.196
K	0.244	0.042	0.389	0.190	0.756	0.179
Ca	0.341	0.063	0.879	0.339	0.409	0.292
Ti	0.330	0.013	0.928	0.367	0.200	0.350
Mn	0.273	0.003	0.992	0.449	-0.154	0.470
Fe	0.334	0.155	1.373	0.538	0.222	0.408
Br	0.042	0.000	-0.034	0.045	0.090	1.203

Table 9b.6. Summer IMPROVE PM2.5 vs RDI 3a PM2.5 XRF.

Element	RSQ	SE RSQ	SLOPE	SE SLOPE	INTERCEPT/AVG	SE INTERCEPT /AVG
Na	0.917	0.072	1.298	0.109	-0.569	0.135
Si	0.417	0.043	0.663	0.217	-0.515	0.330
S	0.556	0.078	0.604	0.150	0.192	0.179
Cl	0.817	0.081	0.524	0.069	-0.158	0.143
K	0.720	0.008	0.648	0.112	-0.136	0.161
Ca	0.499	0.013	0.573	0.159	-0.286	0.230
Ti	0.182	0.002	0.339	0.199	-0.151	0.303
Mn	0.041	0.000	0.186	0.251	-0.137	0.392
Fe	0.297	0.022	0.732	0.312	-0.382	0.437
Br	0.577	0.001	1.065	0.253	-1.285	0.361

Table 9b.7. Summer IMPROVE PM10 vs RDI 7a PM10 XRF.

Element	RSQ	SE RSQ	SLOPE	SE SLOPE	INTERCEPT/AVG	SE INTERCEPT /AVG
Na	0.657	0.211	1.429	0.287	-0.421	0.304
Si	0.689	0.275	1.275	0.238	0.254	0.205
S	0.888	0.041	0.812	0.080	0.021	0.085
Cl	0.735	0.270	0.786	0.131	-0.005	0.180
K	0.691	0.027	0.911	0.169	0.376	0.151
Ca	0.636	0.047	1.240	0.260	0.101	0.239
Ti	0.677	0.009	0.970	0.186	0.189	0.181
Mn	0.632	0.002	1.444	0.306	-1.096	0.400
Fe	0.738	0.097	1.325	0.219	0.246	0.187
Br	0.031	0.000	0.193	0.069	-0.030	0.128

Table 9b.8. Summer IMPROVE PM2.5 vs RDI 7a PM2.5 XRF.

Element	RSQ	SE RSQ	SLOPE	SE SLOPE	INTERCEPT/AVG	SE INTERCEPT /AVG
Na	0.375	0.197	0.920	0.329	-0.144	0.393
Si	0.017	0.056	0.079	0.165	0.326	0.213
S	0.638	0.071	0.745	0.155	0.094	0.167
Cl	0.483	0.137	0.403	0.116	0.005	0.211
K	0.230	0.014	0.340	0.172	0.239	0.220
Ca	0.066	0.018	0.189	0.198	0.244	0.256
Ti	0.021	0.002	0.055	0.104	0.257	0.169
Mn	0.008	0.000	-0.051	0.156	0.233	0.217
Fe	0.041	0.026	0.121	0.164	0.394	0.217
Br	0.367	0.001	3.593	0.274	-0.504	0.305

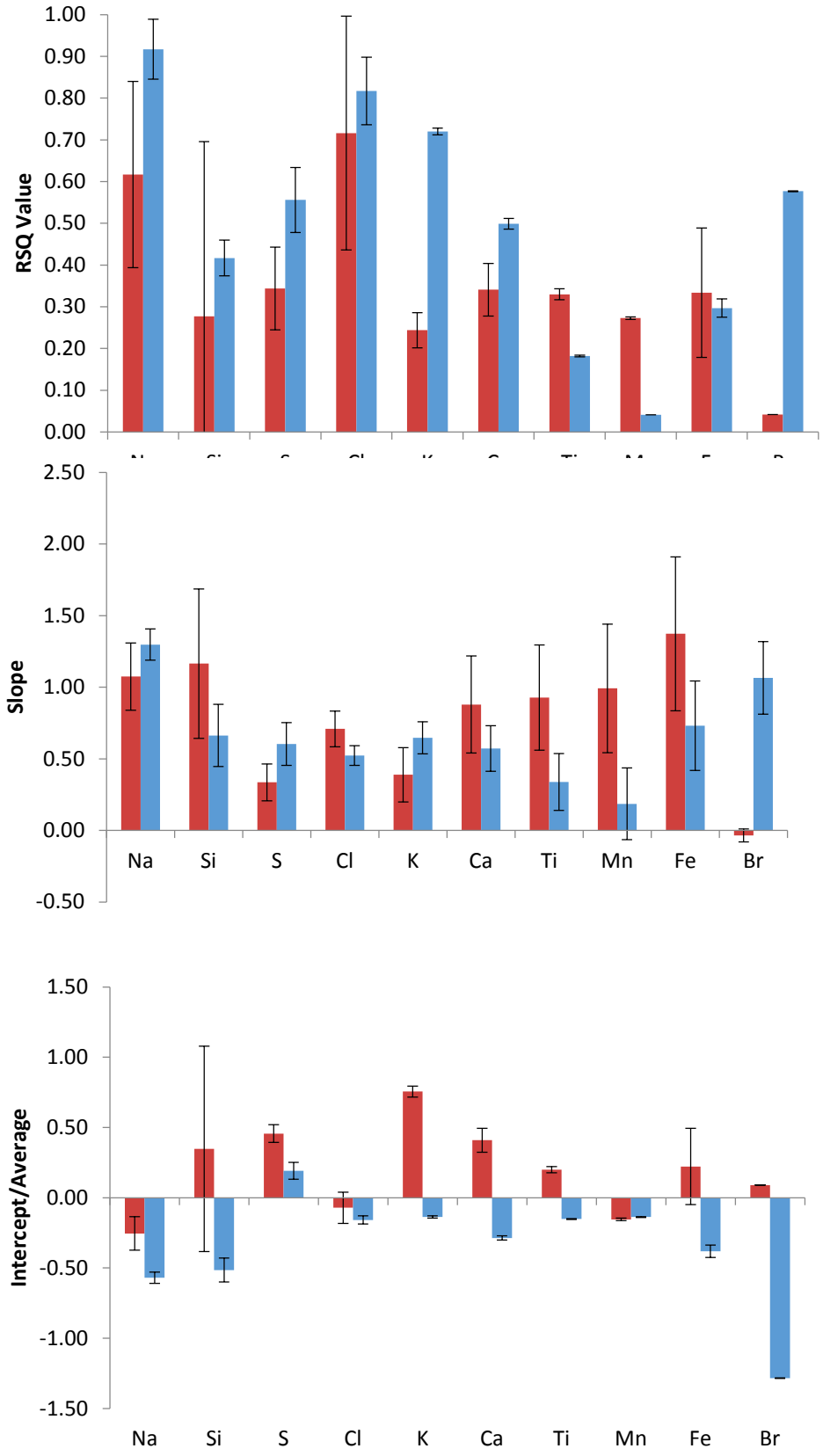

Figure 9b.3 Comparison between IMPROVE and RDI3a (IMPROVE = f(RDI3a) for Summer PM10 (red bars) and PM2.5 (blue bars) showing RSQ, slope, intercept/average and their uncertainties for each (error bars).

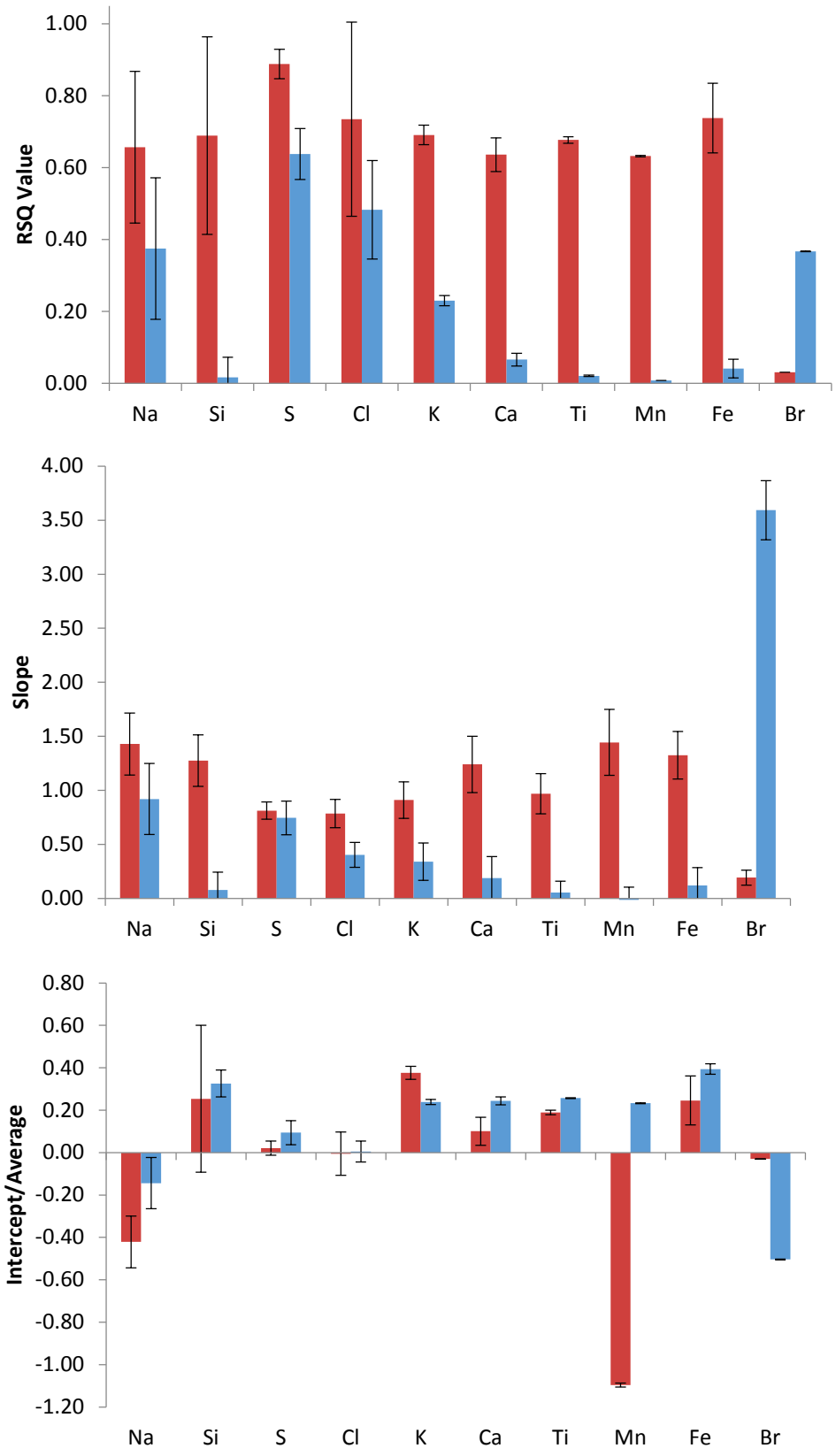

Figure 9b.4 Comparison between IMPROVE and RDI7a (IMPROVE = f(RDI7a) for Summer PM10 (red bars) and PM2.5 (blue bars) showing RSQ, slope, intercept/average and their uncertainties for each (error bars).

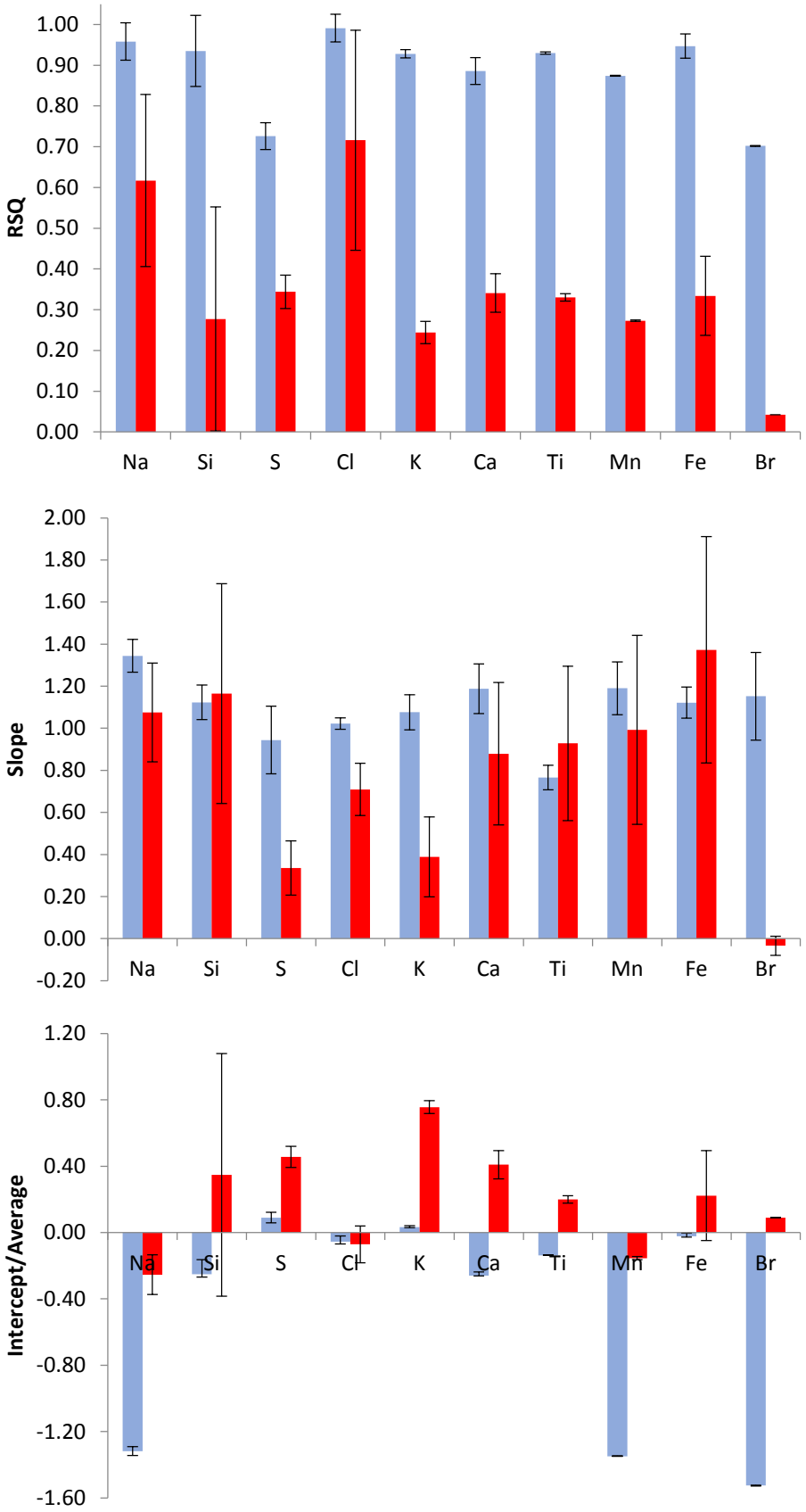

Figure 9b.5 Comparison between IMPROVE PM10 and RDI3a PM10 (IMPROVE= f(RDI3a)) analyzed by XRF for Winter (blue bars) and Summer (red bars) showing RSQ, slope, intercept/average and their uncertainties for each (error bars).

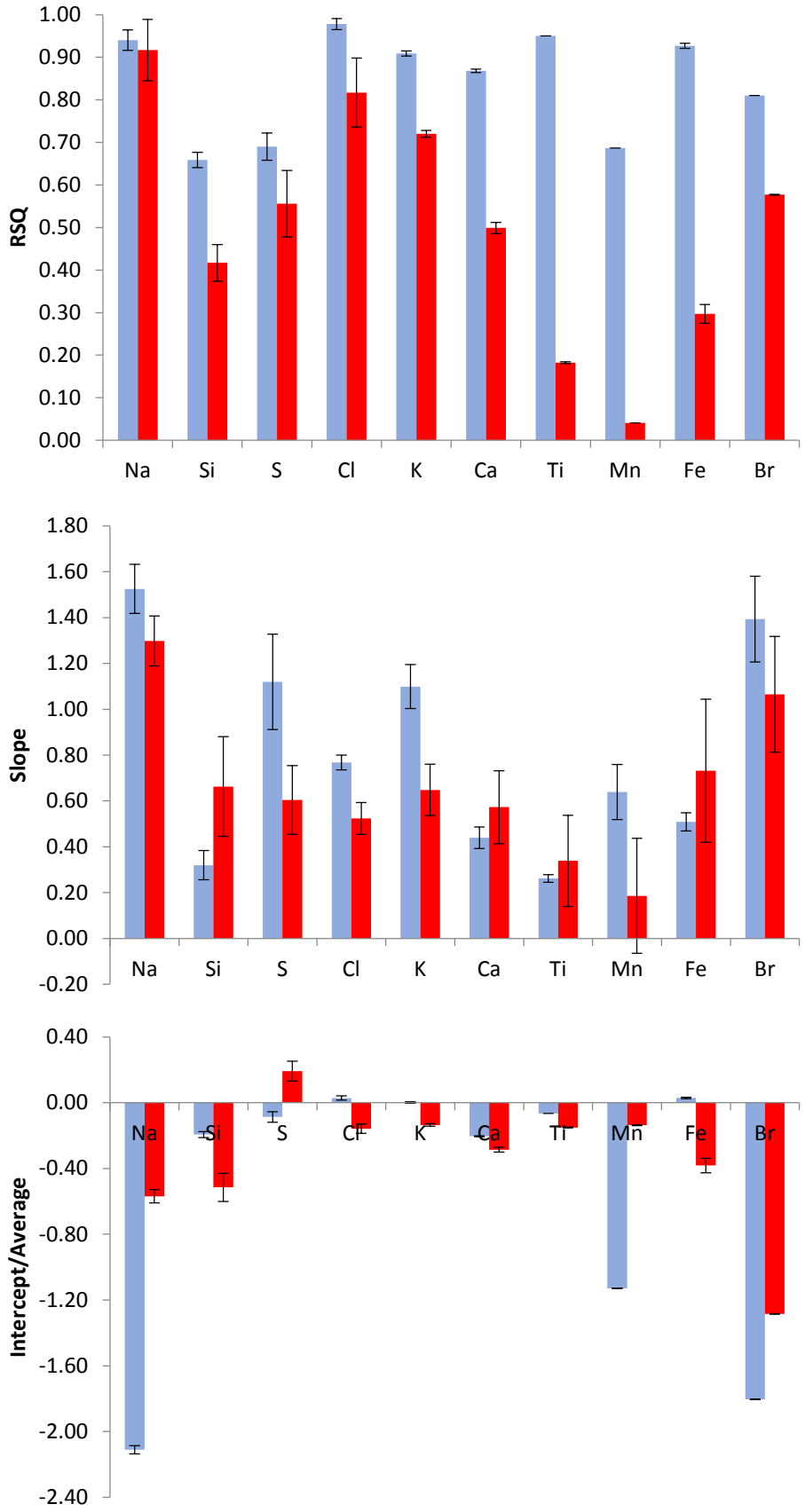

Figure 9b.6 Comparison between IMPROVE PM2.5 and RDI3a PM2.5 (IMPROVE= f(RDI3a)) analyzed by XRF for Winter (blue bars) and Summer (red bars) showing RSQ, slope, intercept/average and their uncertainties for each (error bars).

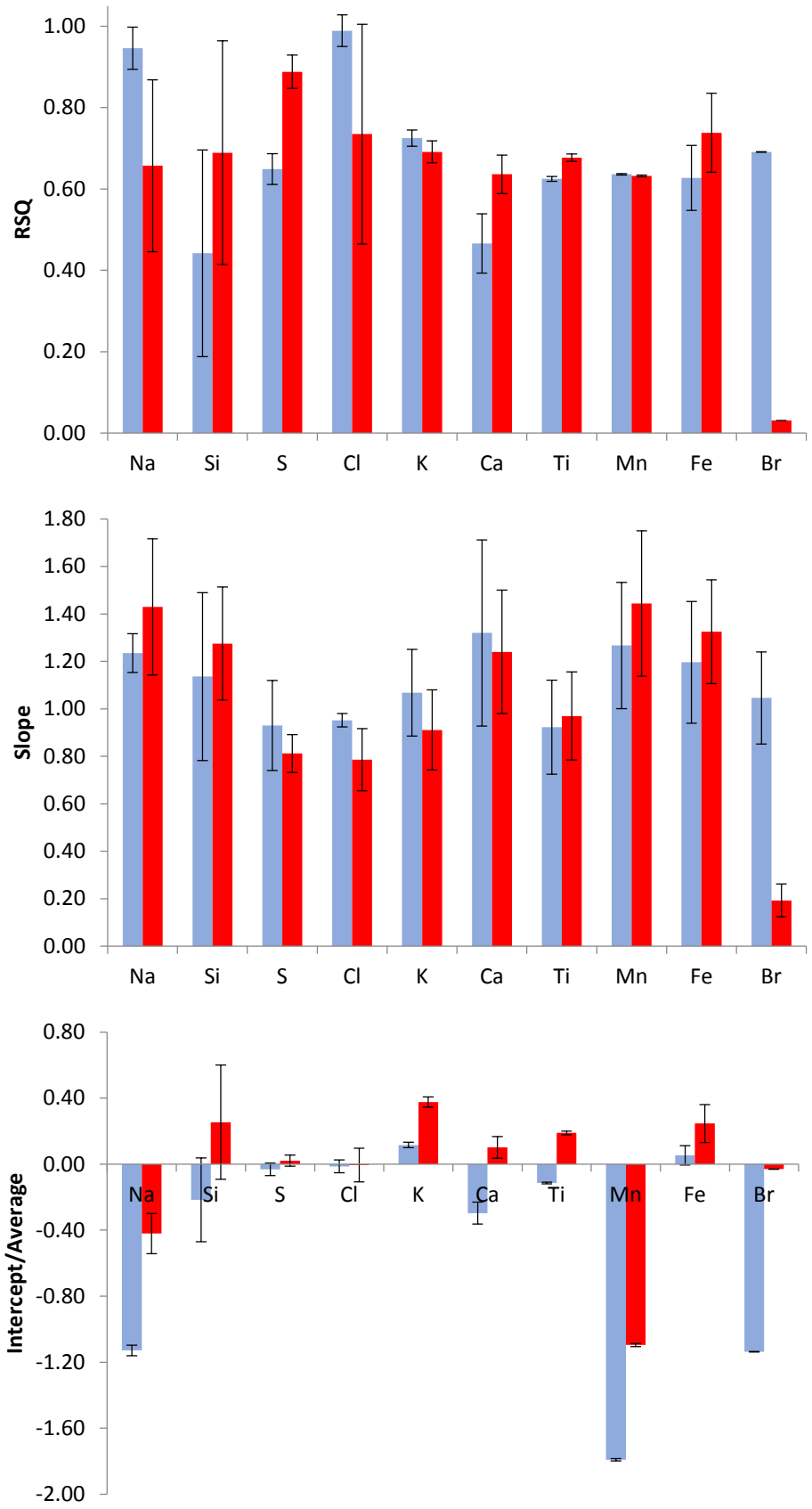

Figure 9b.7 Comparison between IMPROVE PM10 and RDI7a PM10 (IMPROVE= f(RDI7a)) analyzed by XRF for Winter (blue bars) and Summer (red bars) showing RSQ, slope, intercept/average and their uncertainties for each (error bars).

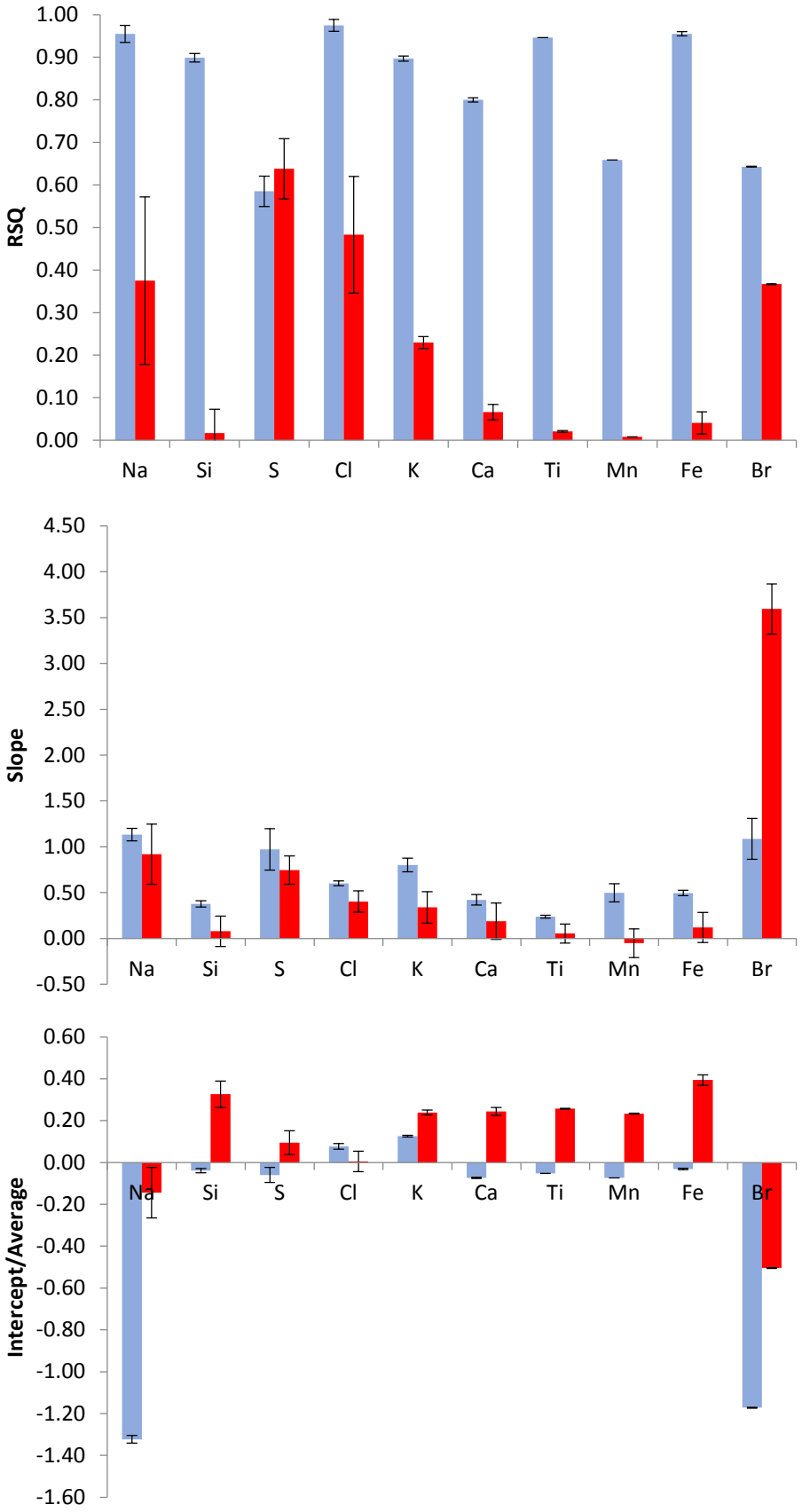

Figure 9b.8 Comparison between IMPROVE PM2.5 and RDI7a PM2.5 (IMPROVE= f(RDI7a)) analyzed by XRF for Winter (blue bars) and Summer (red bars) showing RSQ, slope, intercept/average and their uncertainties for each (error bars).

9c. RDI (PM2.5) XRF vs MOUDI (PM1.8) XRF

The following correlations are for RDI = f(MOUDI). For the RDI, the mass was the sum of all stages smaller than 2.5 um while for MOUDI, the sum less than 1.8 um was used because there is no 2.5 um cut point. As a result, the slopes should be greater than 1 because there is more mass counted in the RDI sum than in the MOUDI sum. Tables 9c.1-4 and Figures 9c.1-2 show the precision of the RDI PM2.5 compared to MOUDI PM1.8 analyzed by XRF for both the winter and summer season.

Table 9c.1 Winter RDI 3a PM2.5 vs MOUDI PM1.8 XRF.

Element	RSQ	SE RSQ	SLOPE	SE SLOPE	INTERCEPT/AVG	SE INTERCEPT /AVG
Na	0.894	0.020	0.926	0.089	-1.434	0.167
Si	0.014	0.001	-0.054	0.070	0.619	0.104
S	0.688	0.011	0.982	0.028	0.240	0.246
Cl	0.947	0.008	0.418	0.129	0.326	0.176
K	0.800	0.006	0.932	0.076	0.158	0.135
Ca	0.293	0.001	0.177	0.072	0.035	0.154
Ti	0.003	0.000	-0.015	0.555	0.481	0.000
Mn	0.040	0.017	-0.759	0.106	1.631	0.143
Fe	0.063	0.004	0.099	0.156	0.650	3.611
Br	0.612	0.001	1.110	0.245	-1.646	0.000

Table 9c.2 Winter RDI 7a PM2.5 vs MOUDI PM1.8 XRF.

Element	RSQ	SE RSQ	SLOPE	SE SLOPE	INTERCEPT/AVG	SE INTERCEPT /AVG
Na	0.908	0.018	0.689	0.061	-0.865	0.395
Si	0.007	0.001	0.039	0.064	0.528	0.266
S	0.533	0.011	0.815	0.020	0.296	0.631
Cl	0.955	0.009	0.330	0.101	0.314	1.051
K	0.773	0.007	0.673	0.081	0.264	2.574
Ca	0.203	0.001	0.147	0.065	0.106	2.122
Ti	0.000	0.000	-0.002	0.442	0.374	0.000
Mn	0.116	0.017	-1.021	0.099	0.954	18.157
Fe	0.115	0.004	0.129	1.550	0.526	13.144
Br	0.591	0.001	0.955	0.220	-1.169	0.000

Table 9c.3 Summer RDI 3a PM2.5 vs MOUDI PM1.8 XRF.

Element	RSQ	SE RSQ	SLOPE	SE SLOPE	INTERCEPT/AVG	SE INTERCEPT /AVG
Na	0.855	0.055	0.727	0.083	-0.340	0.127
Si	0.001	0.033	-0.019	0.165	0.356	0.280
S	0.354	0.097	0.498	0.187	0.376	0.215
Cl	0.904	0.029	0.271	0.024	-0.045	0.056
K	0.508	0.006	0.291	0.079	0.189	0.109
Ca	0.411	0.007	0.244	0.081	-0.049	0.139
Ti	0.015	0.001	0.057	0.128	0.137	0.222
Mn	0.142	0.002	-1.719	1.170	3.292	2.085
Fe	0.137	0.101	-2.082	1.447	3.113	1.500
Br	0.313	0.001	0.786	0.323	-0.900	0.553

Table 9c.4 Summer RDI 7a PM2.5 vs MOUDI PM1.8 XRF.

Element	RSQ	SE RSQ	SLOPE	SE SLOPE	INTERCEPT/AVG	SE INTERCEPT /AVG
Na	0.555	0.097	0.649	0.161	-0.212	0.216
Si	0.125	0.031	0.123	0.090	0.106	0.125
S	0.659	0.071	0.782	0.156	0.130	0.166
Cl	0.675	0.053	0.234	0.045	0.008	0.088
K	0.265	0.007	0.195	0.090	0.285	0.115
Ca	0.250	0.008	0.173	0.083	0.063	0.116
Ti	0.164	0.001	0.090	0.056	0.066	0.089
Mn	0.033	0.002	-0.508	0.759	0.848	0.975
Fe	0.085	0.104	-0.735	0.668	1.718	0.725
Br	0.332	0.001	3.431	0.277	-0.505	0.308

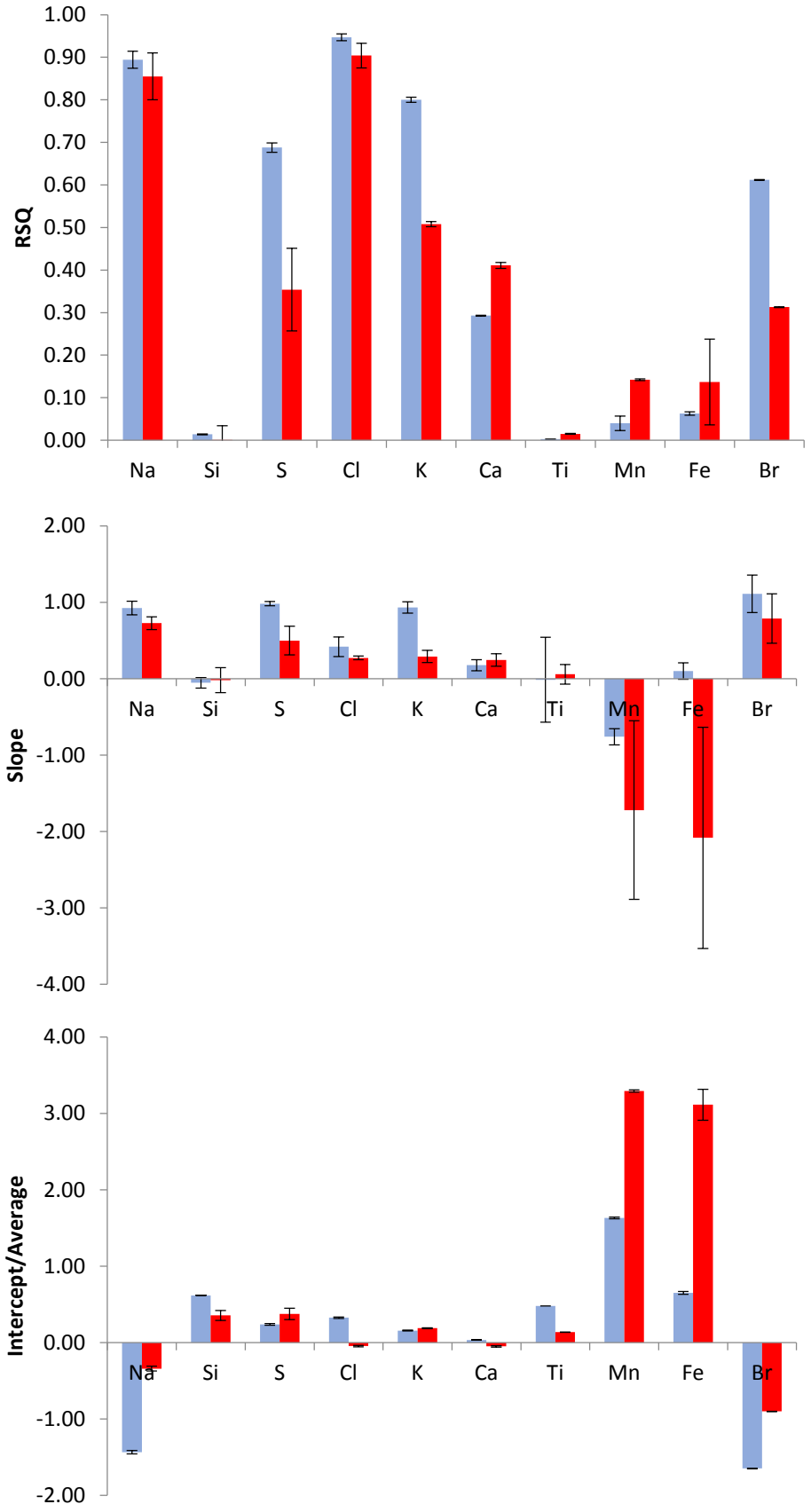

Figure 9c.1 Comparison between RDI3a PM2.5 and MOUDI PM1.8 (RDI3a = f(MOUDI)) analyzed by XRF for Winter (blue bars) and Summer (red bars) showing RSQ, slope, intercept/average and their uncertainties for each (error bars).

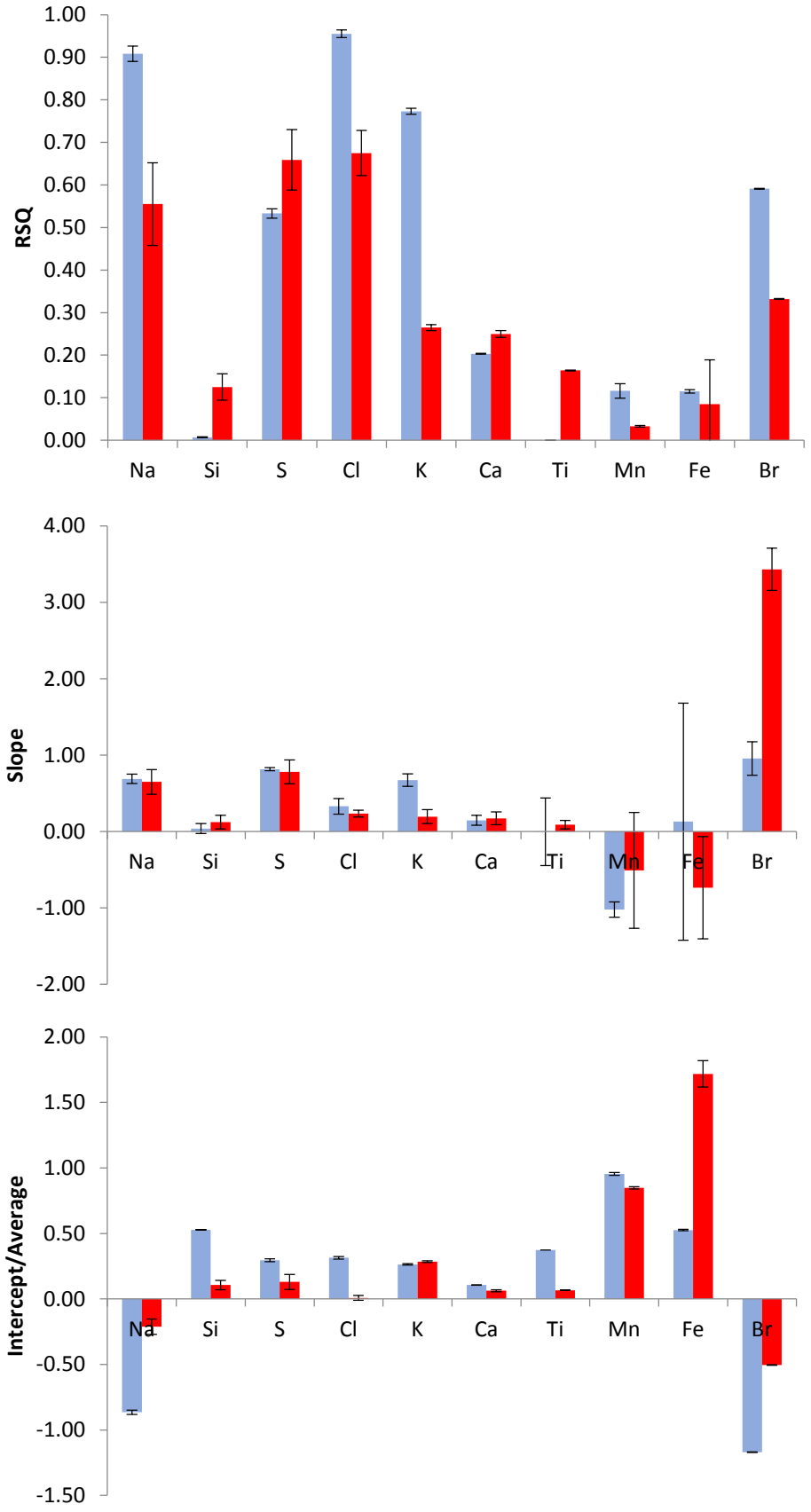

Figure 9c.2 Comparison between RDI7a PM2.5 and MOUDI PM1.8 (RDI7a = f(MOUDI)) analyzed by XRF for Winter (blue bars) and Summer (red bars) showing RSQ, slope, intercept/average and their uncertainties for each (error bars).

9d. IMPROVE (PM2.5) XRF, RDI (PM2.5) XRF and MOUDI (PM1.8) XRF Time Series

The following plots show time series plots for both winter and summer PM2.5 (RDI and IMPROVE) and PM1.8 (MOUDI) for the 10 elements of interest. Figures 9d.1-10 show the winter data, while Figures 9d.11-20 show the summer data. Orange squares represent the IMPROVE concentration, grey triangles represent the RDI 3a concentration and blue diamonds represent the MOUDI concentration. Since RDI-3 and RDI-7 are highly correlated with each other and XRF analyses a and b are also highly correlated, only the results for RDI-3a are presented. The MOUDI and IMPROVE samplers generally agree quite well. For the RDI, three categories of behavior are observed: (1) the results agree well with the MOUDI and IMPROVE (e.g., Figure 9d.3), (2) the temporal patterns of the RDI agree well with those of the IMPROVE and MOUDI, but are shifted up but a substantial amount (e.g., Figure 9d.1), and (3) there is little correlation between the RDI and the other two samplers (e.g., Figure 9d.13).

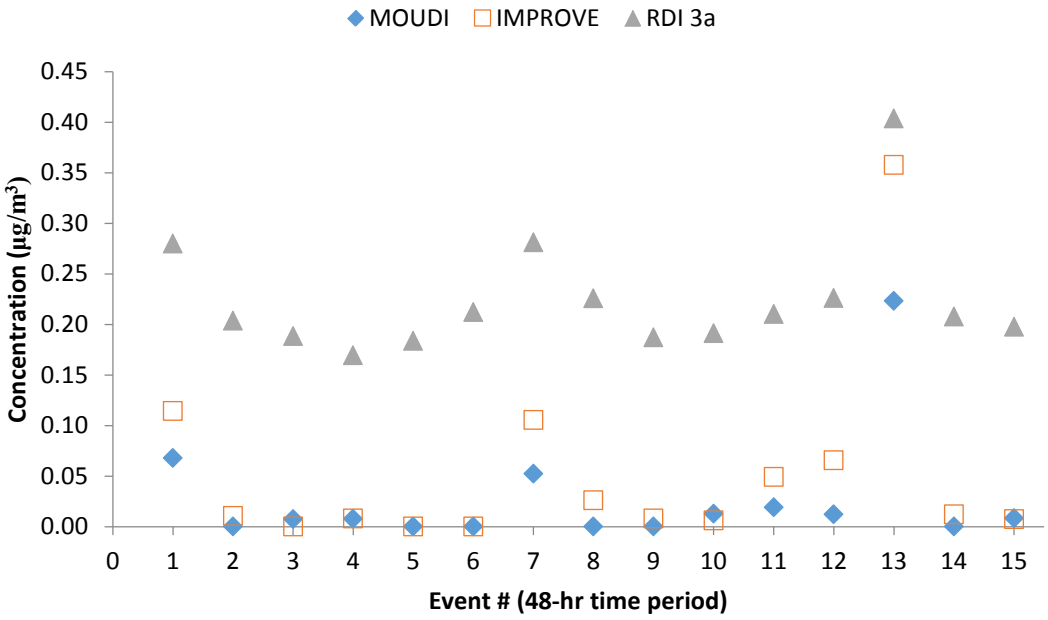

Figure 9d.1 Sodium time series over 15, 48hr events in winter 2013.

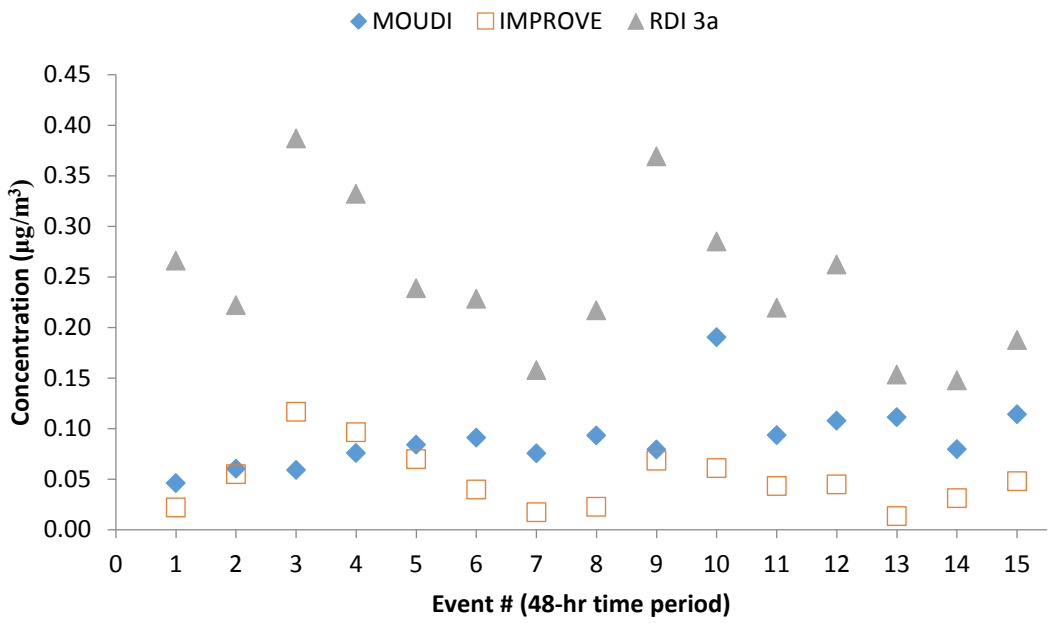

Figure 9d.2 Silicon time series over 15, 48-hr events in winter 2013.

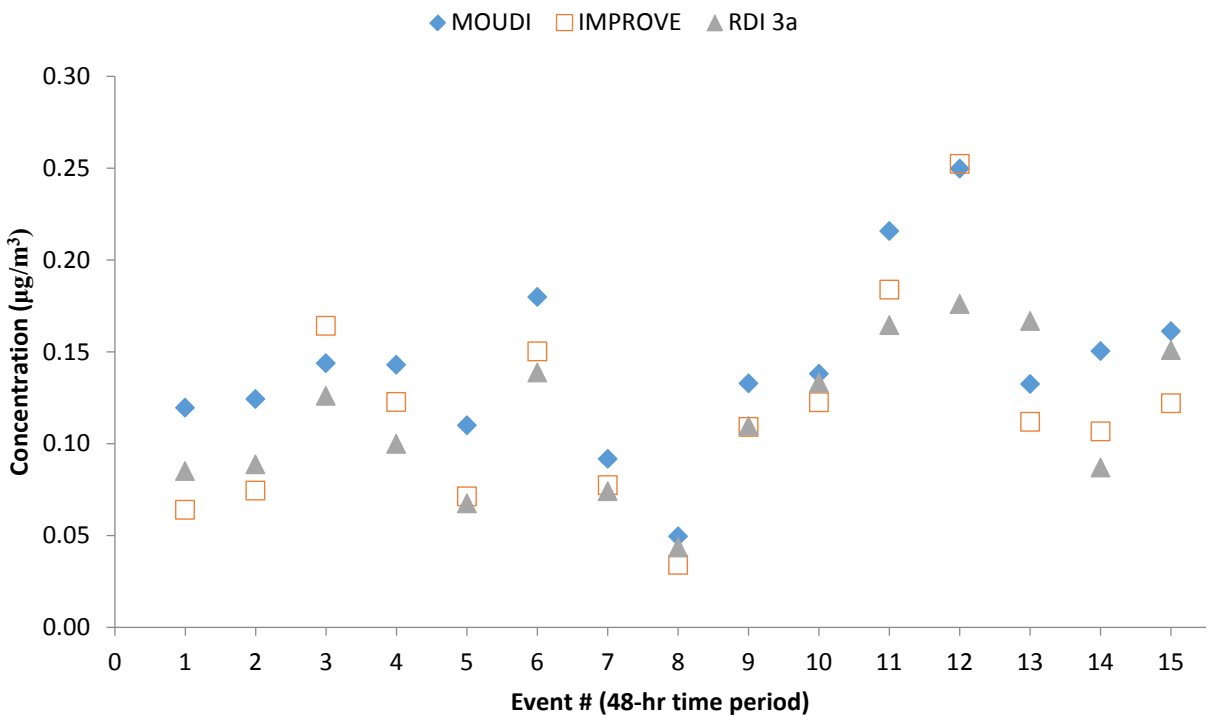

Figure 9d.3 Sulfur time series over 15, 48-hr events in winter 2013.

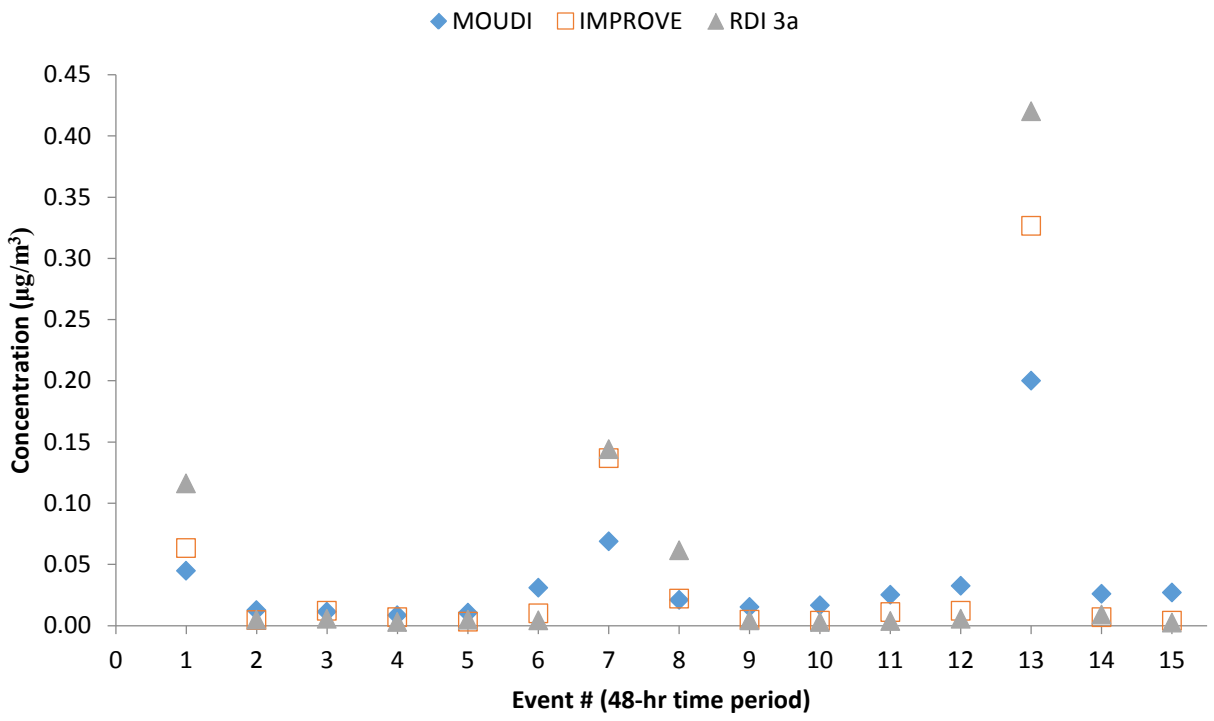

Figure 9d.4 Chlorine time series over 15, 48-hr events in winter 2013.

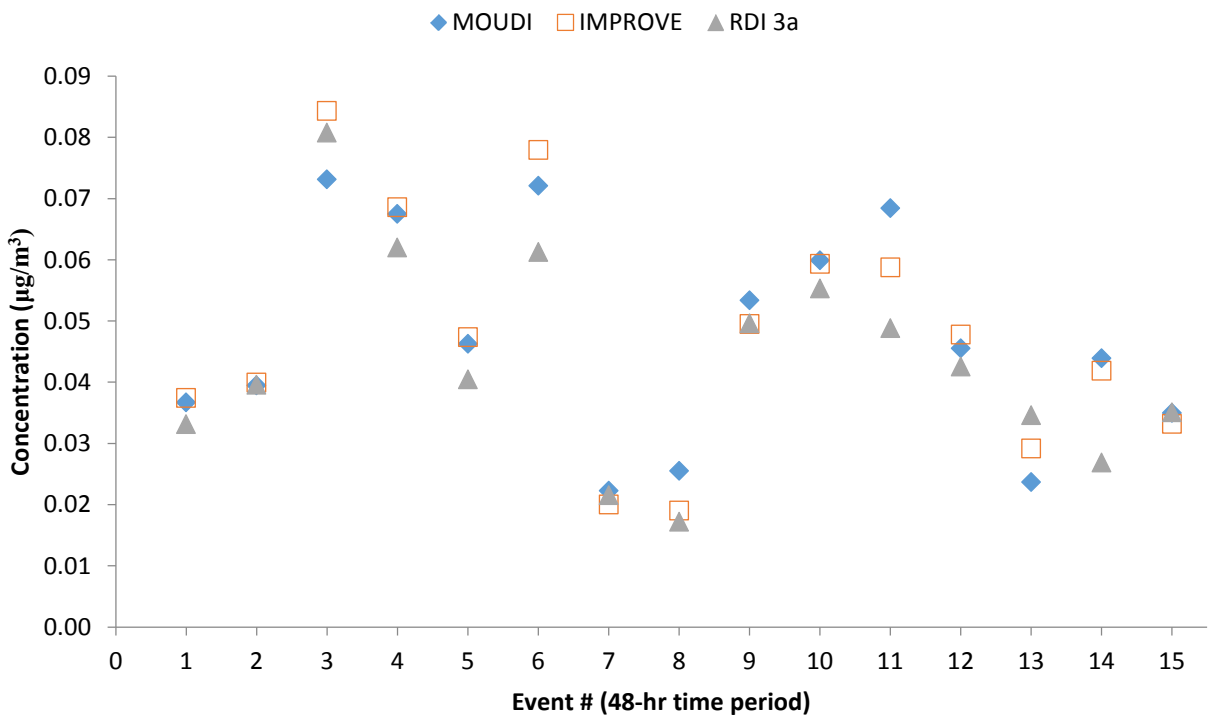

Figure 9d.5 Potassium time series over 15, 48-hr events in winter 2013.

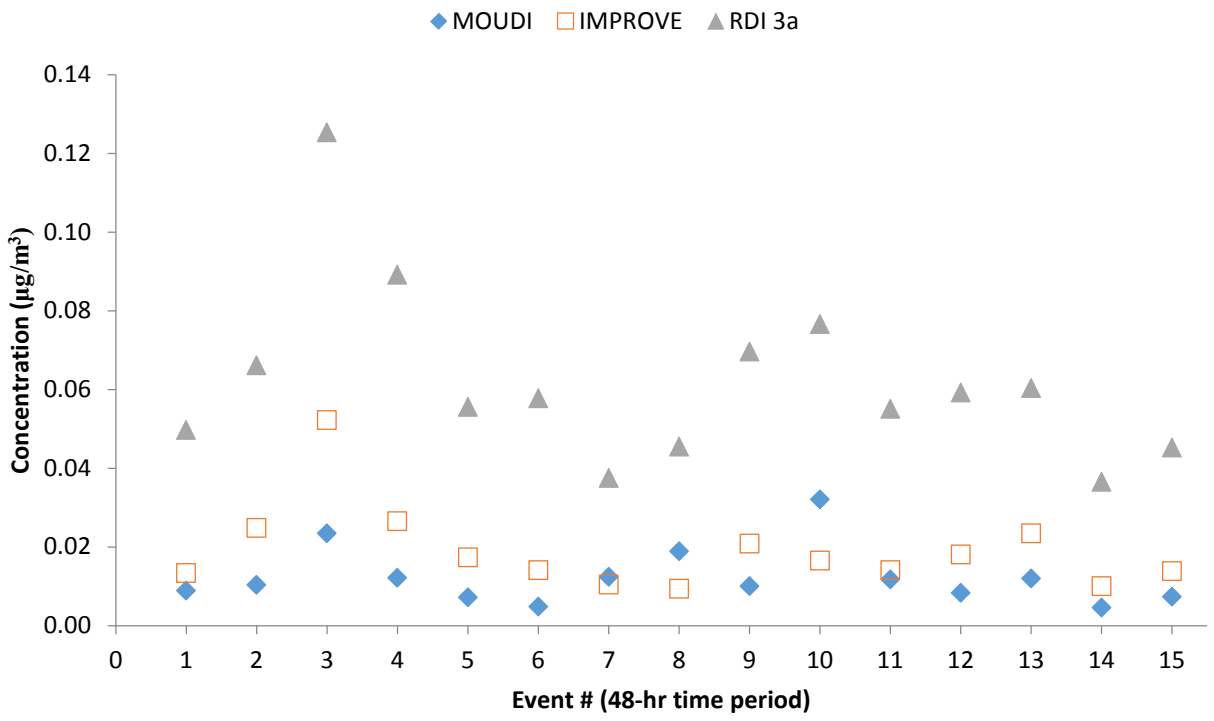

Figure 9d.6 Calcium time series over 15, 48-hr events in winter 2013.

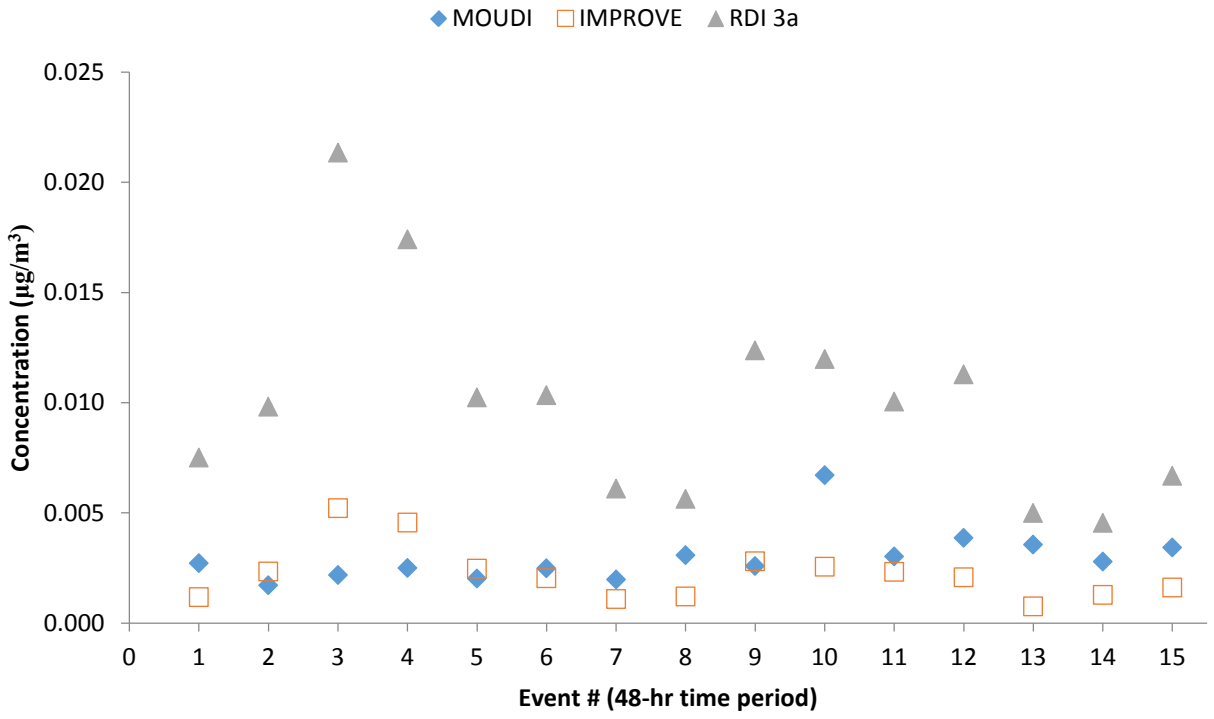

Figure 9d.7 Titanium time series over 15, 48-hr events in winter 2013.

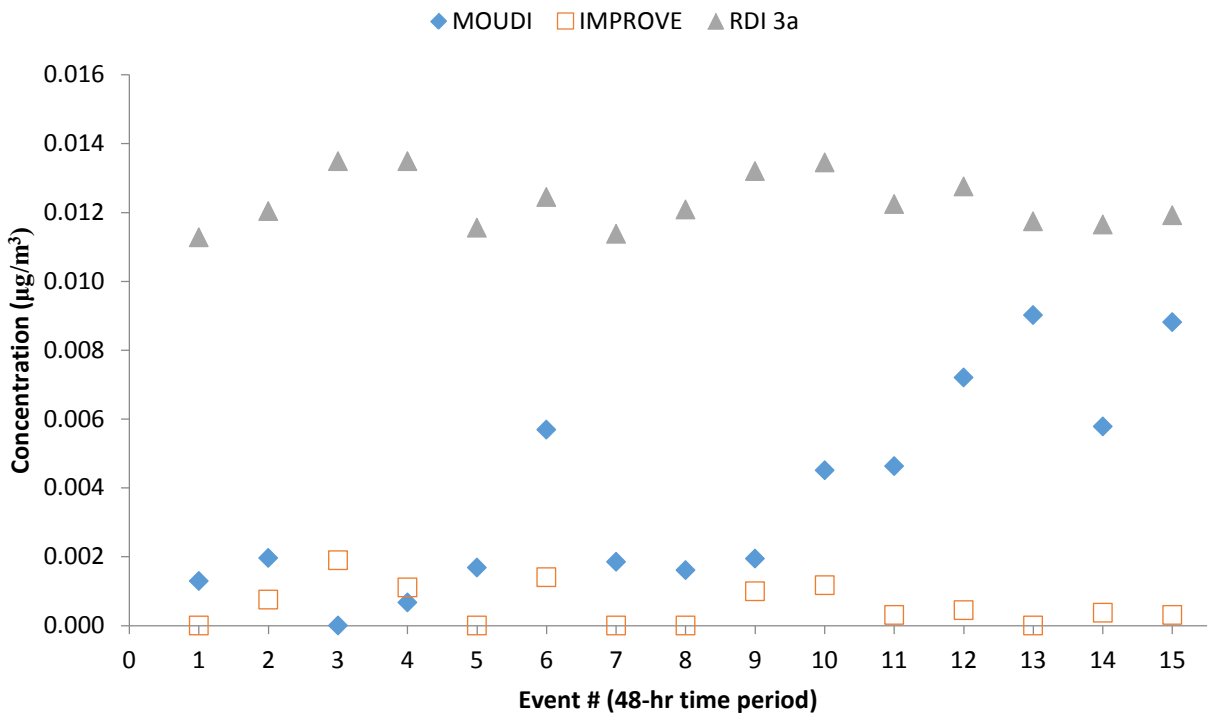

Figure 9d.8 Manganese time series over 15, 48-hr events in winter 2013.

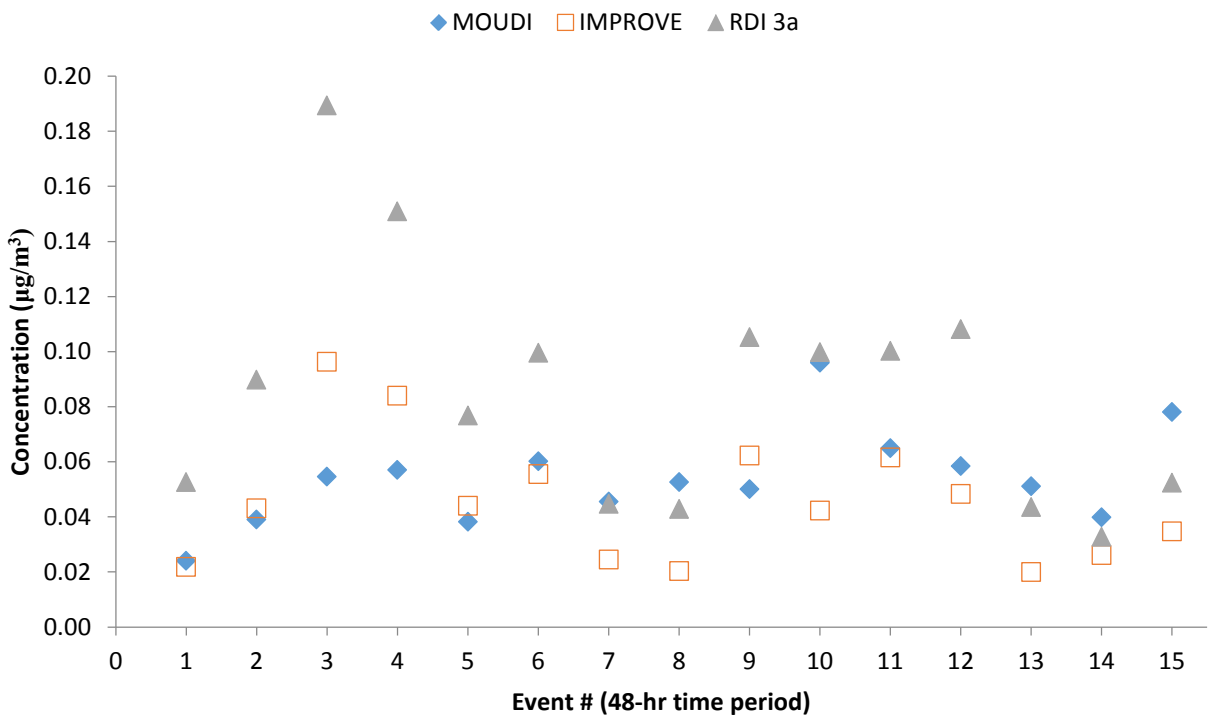

Figure 9d.9 Iron time series over 15, 48-hr events in winter 2013.

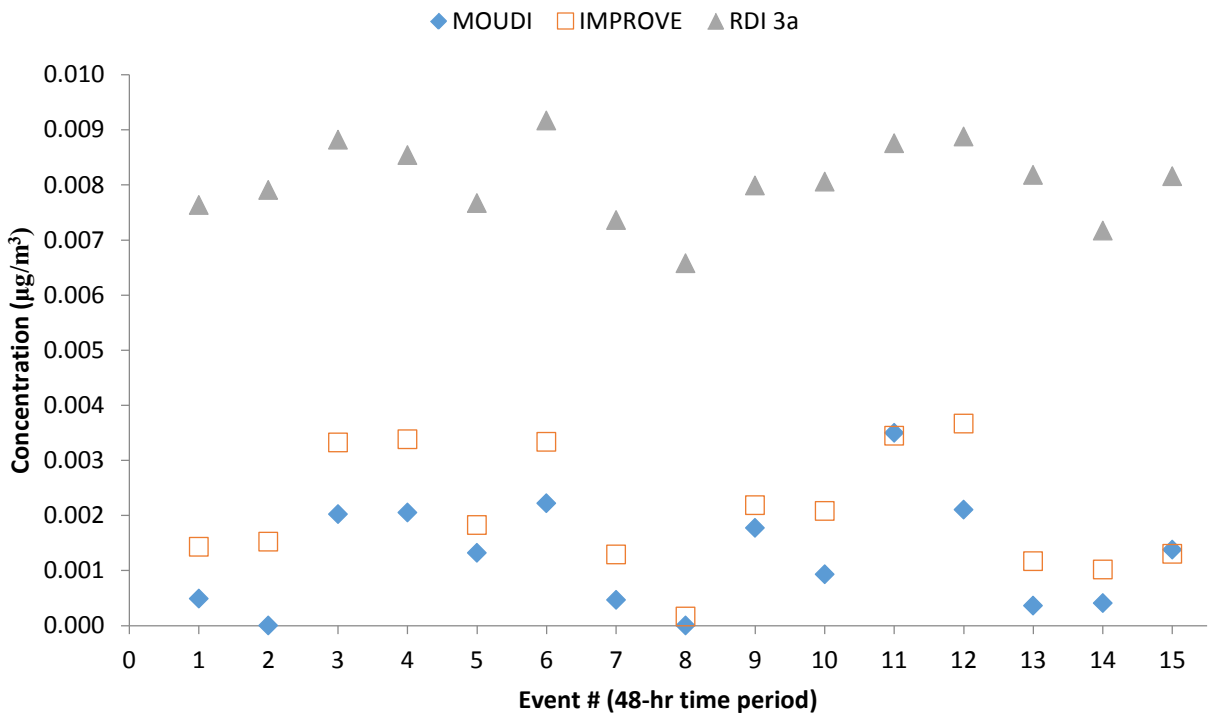

Figure 9d.10 Bromine time series over 15, 48-hr events in winter 2013.

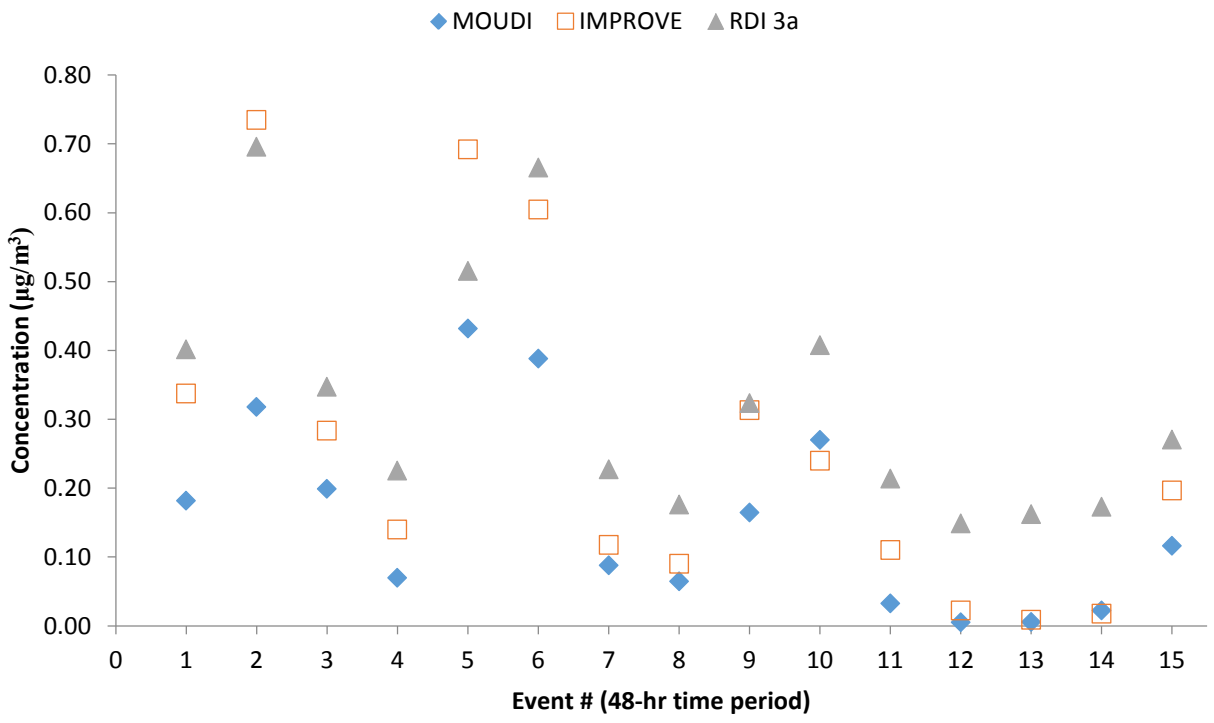

Figure 9d.11 Sodium time series over 15, 48-hr events in summer 2013.

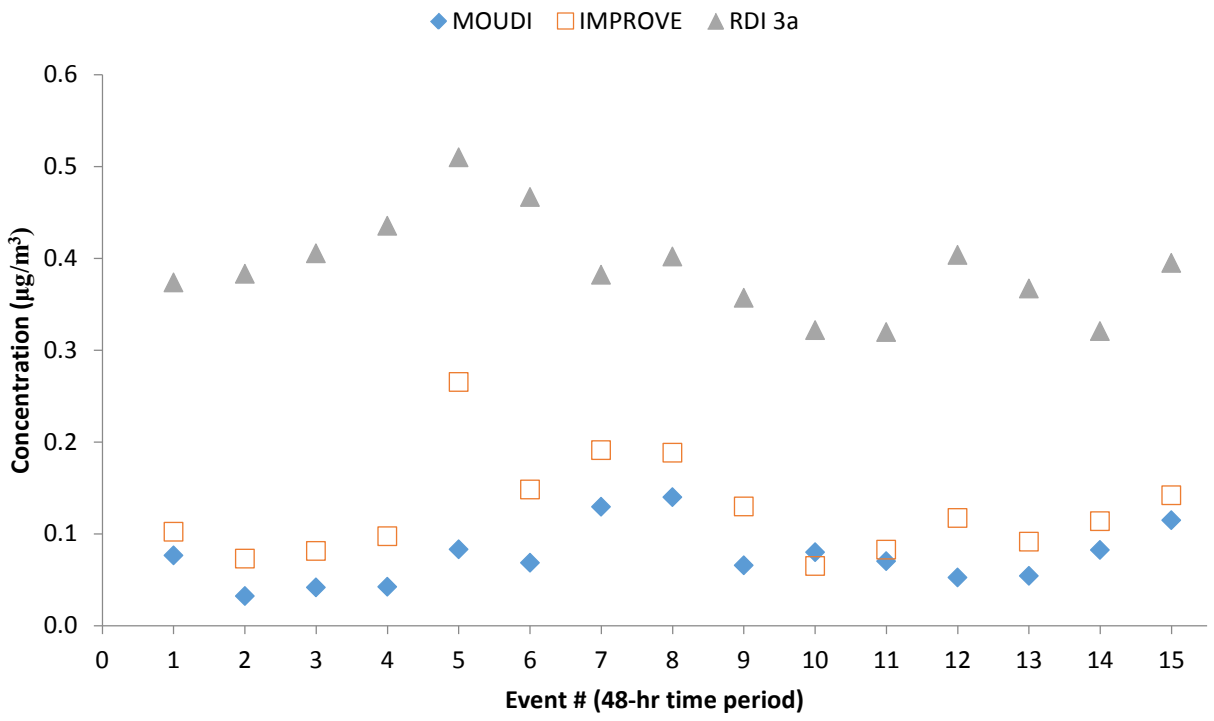

Figure 9d.12 Silicon time series over 15, 48-hr events in summer 2013.

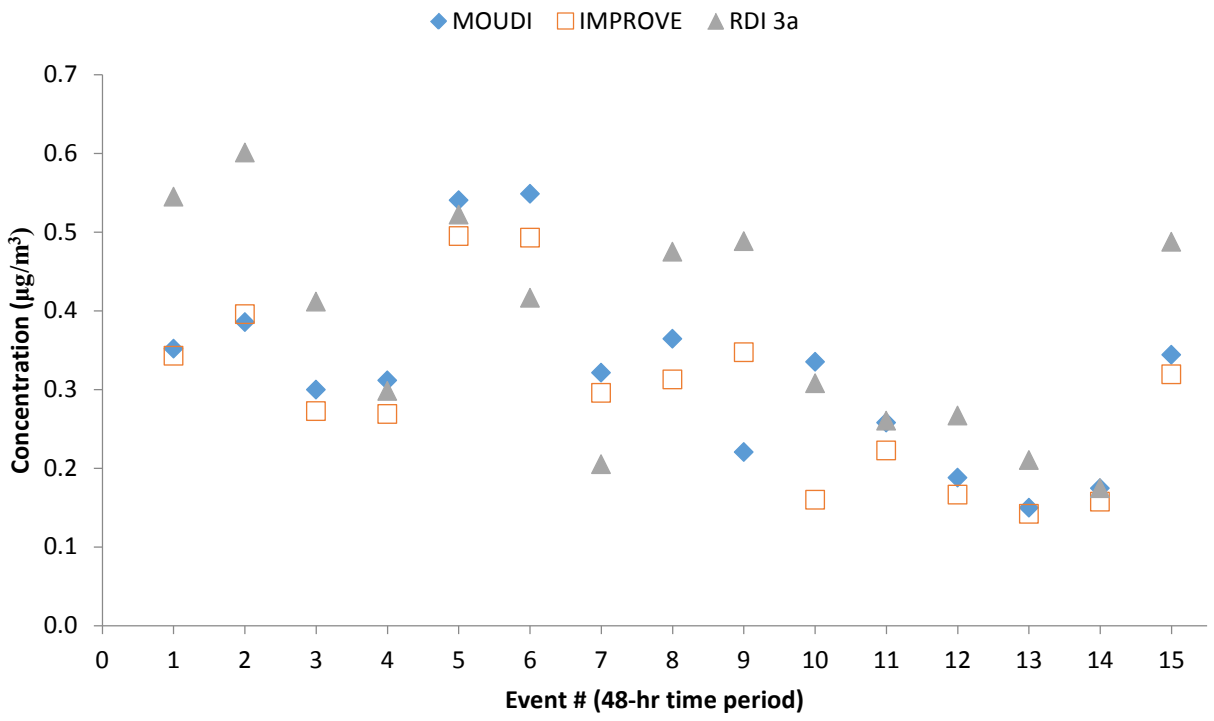

Figure 9d.13 Sulfur time series over 15, 48-hr events in summer 2013.

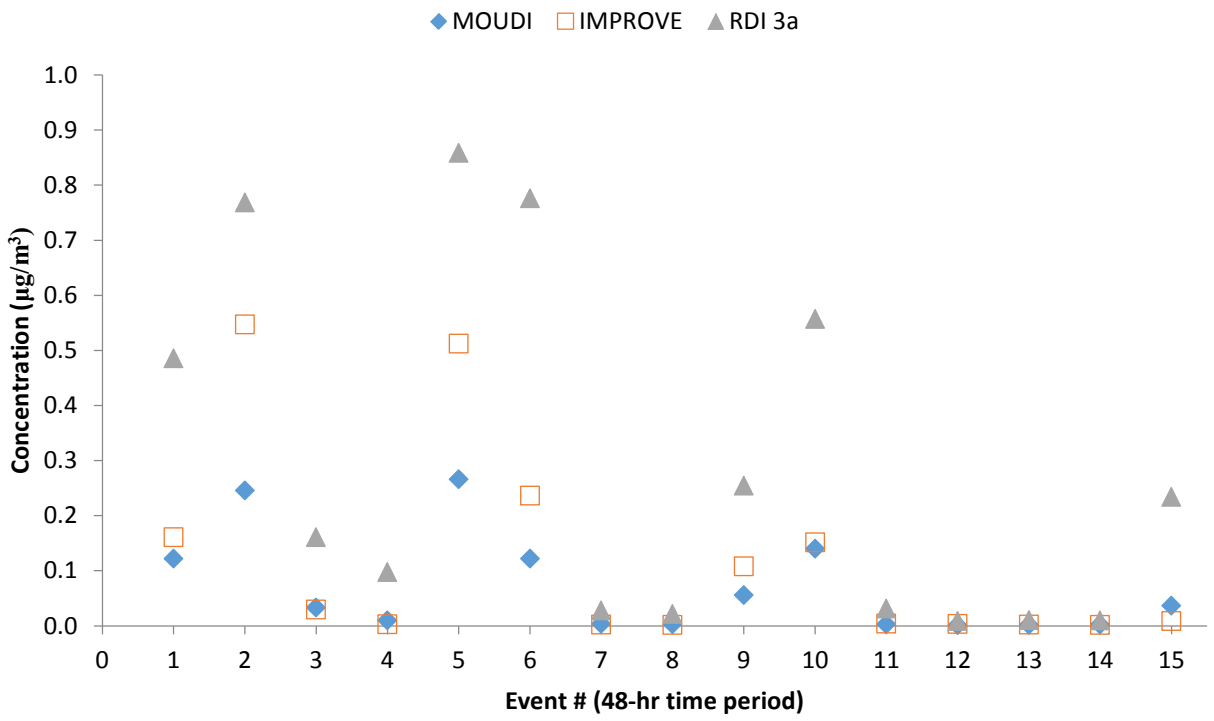

Figure 9d.14 Chlorine time series over 15, 48-hr events in summer 2013.

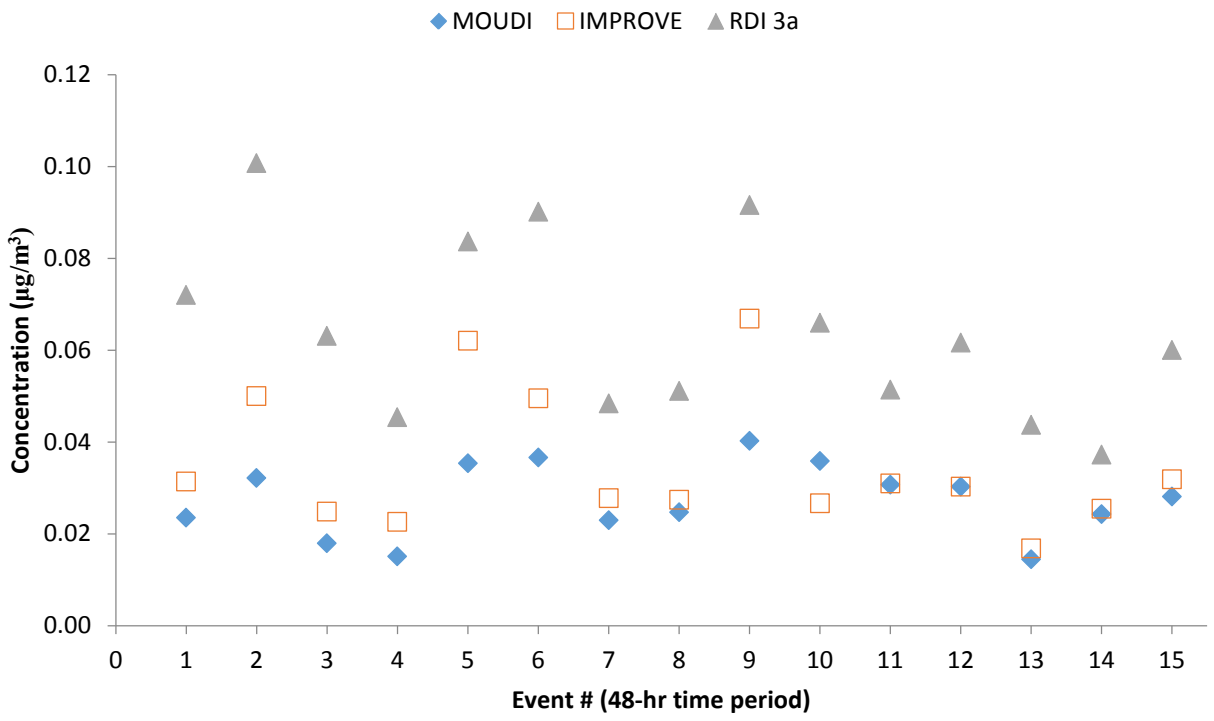

Figure 9d.15 Potassium time series over 15, 48-hr events in summer 2013.

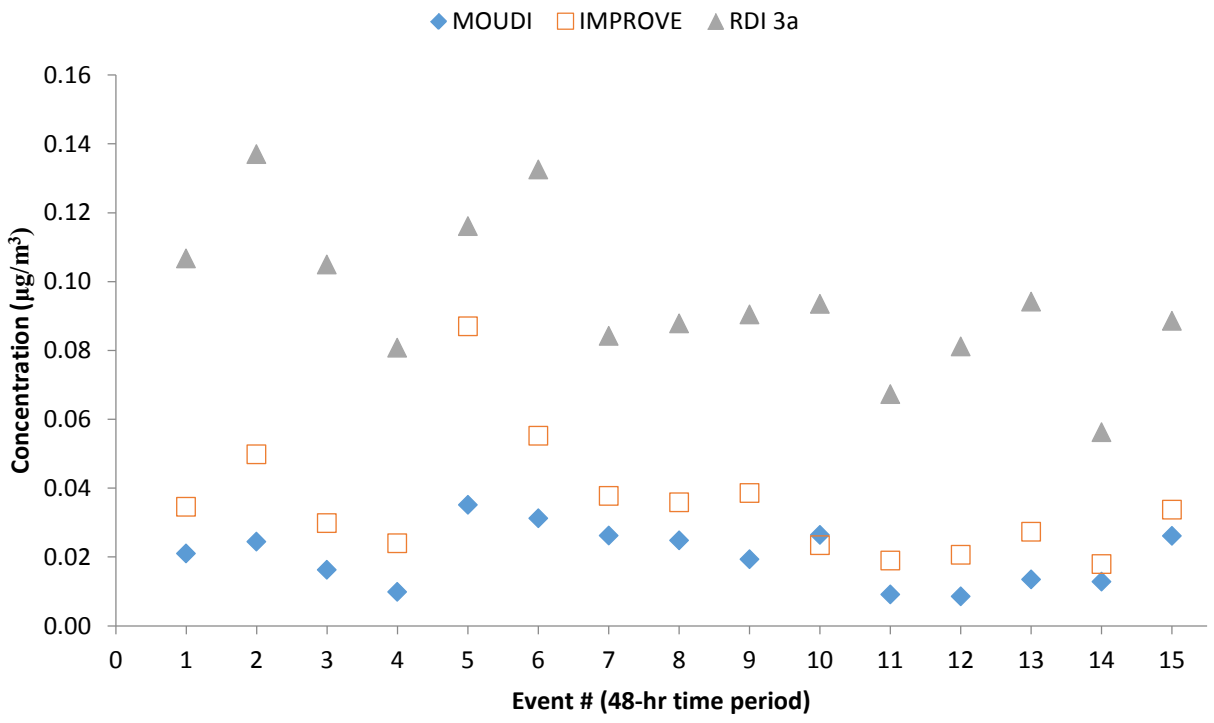

Figure 9d.16 Calcium time series over 15, 48-hr events in summer 2013.

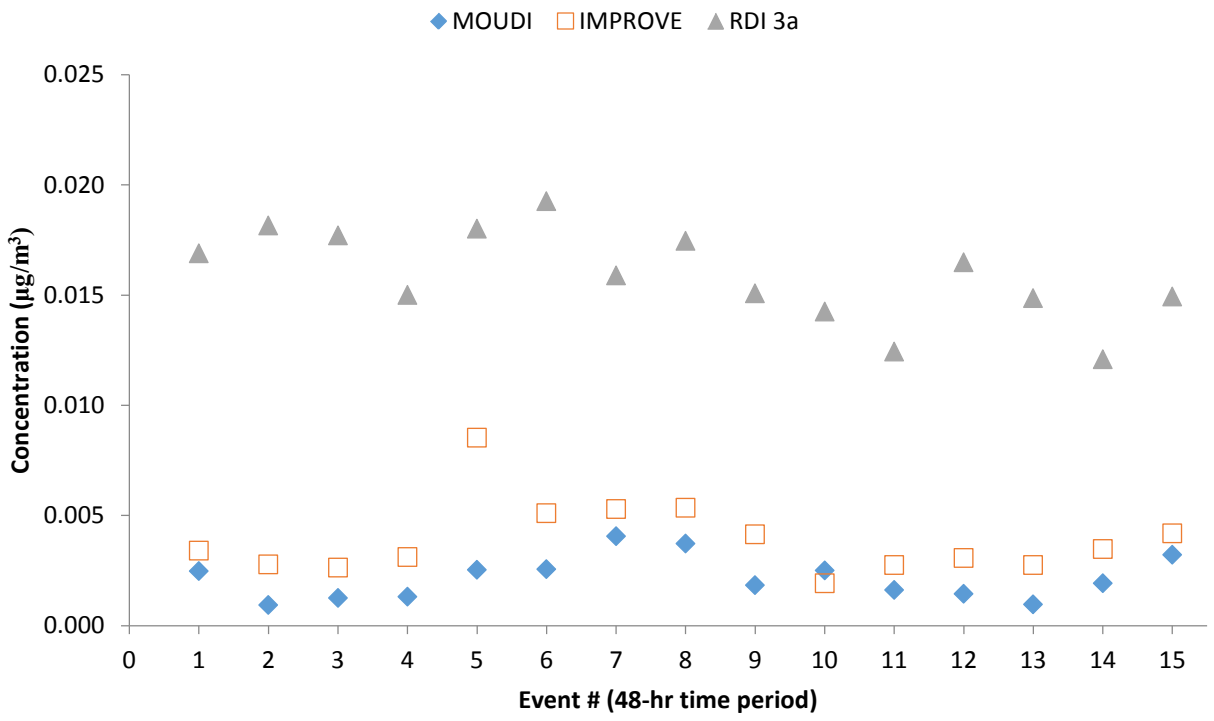

Figure 9d.17 Titanium time series over 15, 48-hr events in summer 2013.

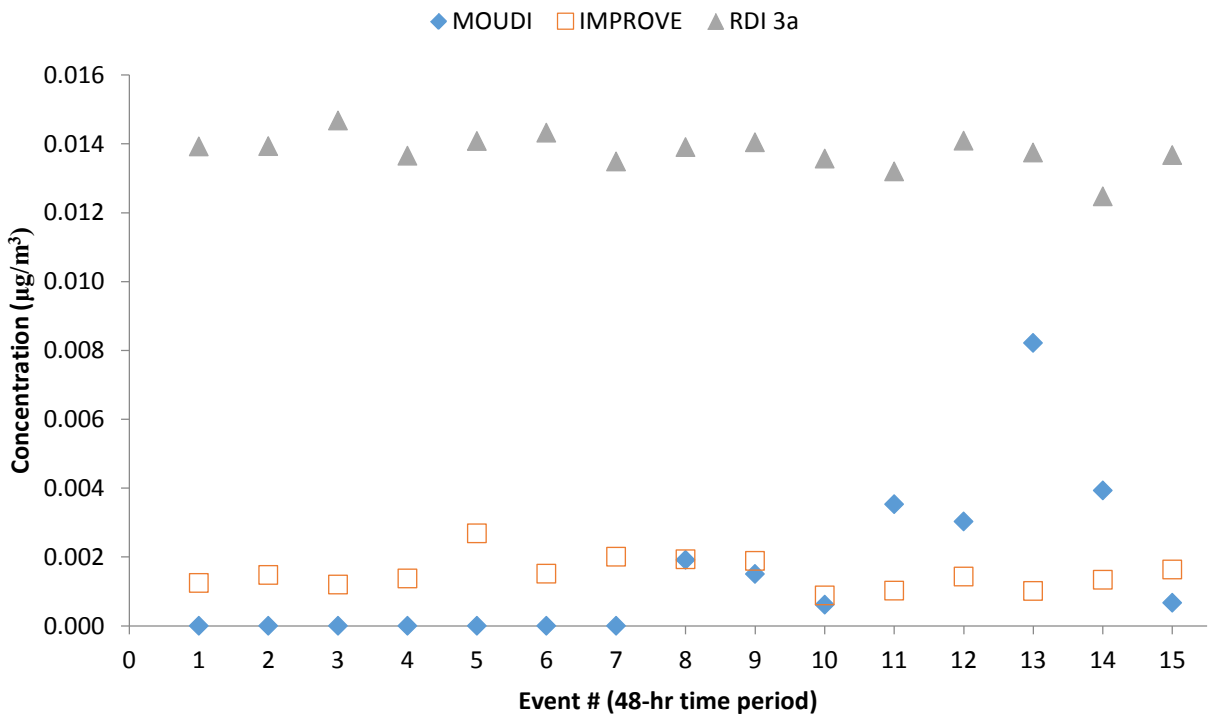

Figure 9d.18 Manganese time series over 15, 48-hr events in summer 2013.

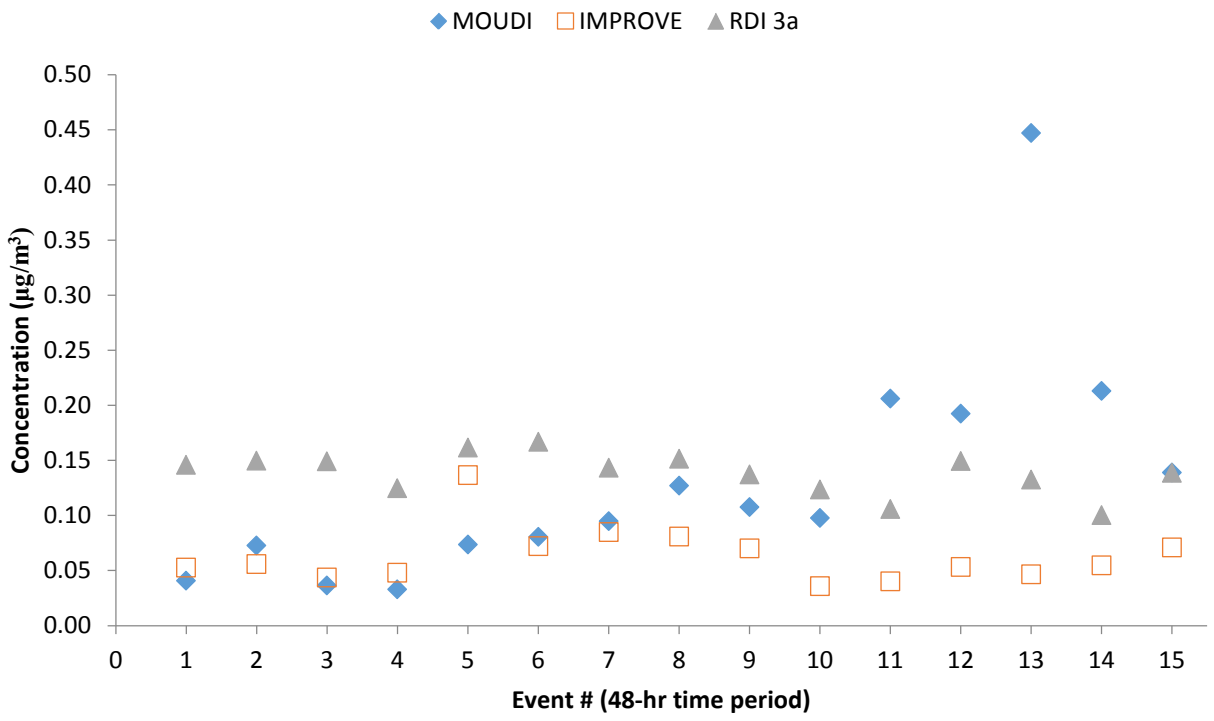

Figure 9d.19 Iron time series over 15, 48-hr events in summer 2013.

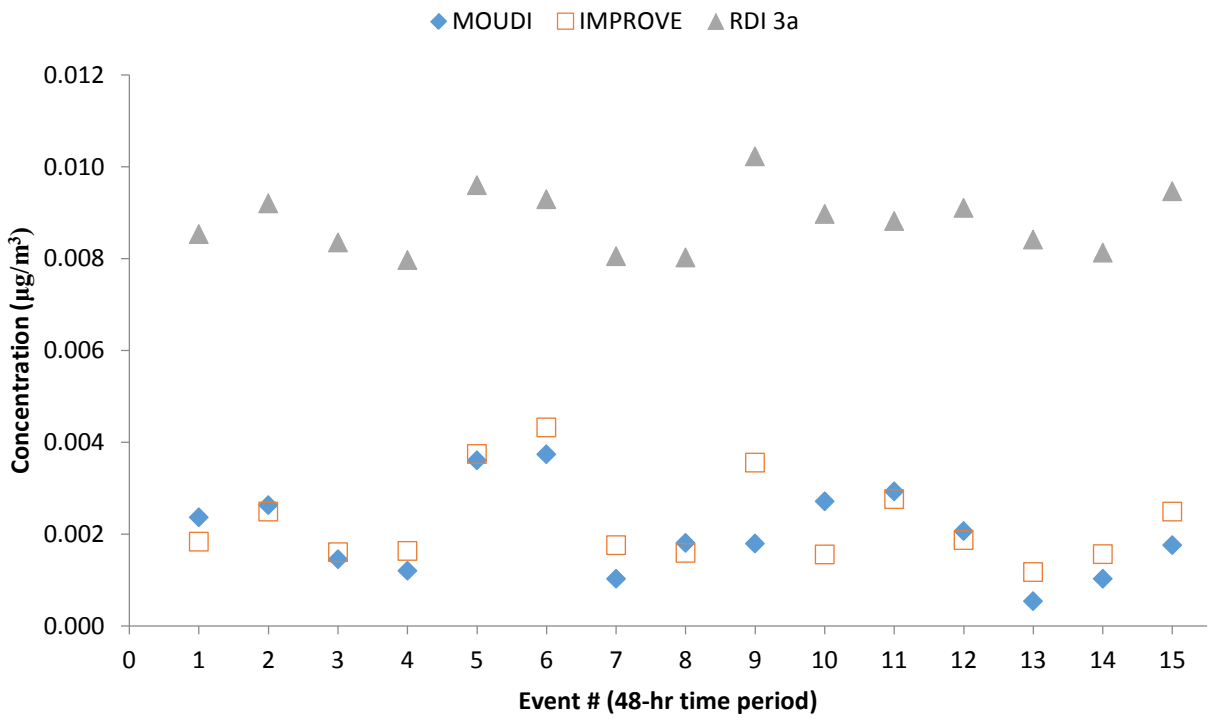

Figure 9d.20 Bromine time series over 15, 48-hr events in summer 2013.

9e. IMPROVE (PM2.5) ICPMS vs MOUDI (PM1.8) ICPMS

Here we the compare the IMPROVE and MOUDI samplers using the ICPMS analysis. The correlations used the functional relationship IMPROVE RONSa (PM2.5) = f(MOUDI) (PM1.8) for the 21 elements presented in Section 7b. Since the IMPROVE size cut is at 2.5 um while the closest MOUDI size cut is at 1.8 um, the slopes should be greater than 1 because there is more mass counted in the IMPROVE sum than in the MOUDI sum. ICPMS analysis on the IMPROVE and MOUDI Teflon filters was conducted after XRF analysis had already been performed, so contamination between analyses although unlikely could have occurred. Tables 9e.1-2 and Figure 9e.1 show the precision of the IMPROVE PM2.5 versus the MOUDI PM1.8 analyzed by ICPMS for both the winter and summer season.

Table 9e.1 Winter ICPMS comparison for IMPROVE PM2.5 vs MOUDI PM1.8. (IMPROVE = f(MOUDI))

Element	RSQ	RSQ SE	Slope	Slope SE	Intercept/ Average	SE INTERCEPT /AVG
Li	<MDL	<MDL	<MDL	<MDL	<MDL	<MDL
S	0.237	0.304	0.675	0.373	0.403	0.339
K	N/A	N/A	N/A	N/A	N/A	N/A
Ti	<MDL	<MDL	<MDL	<MDL	<MDL	<MDL
V	**0.783**	**0.000**	**2.027**	**0.538**	**-0.437**	0.000
Mn	**0.536**	**0.002**	**1.043**	**0.506**	**0.036**	0.369
Fe	**0.480**	**0.013**	**1.813**	**0.524**	**-0.080**	0.487
Ga[a]	0.151	0.000	0.143	0.193	0.899	0.000
Ge	<MDL	<MDL	<MDL	<MDL	<MDL	<MDL
As	**0.594**	0.002	**1.588**	**0.455**	**0.562**	0.000
Se	**0.542**	**0.000**	**2.076**	**0.808**	**0.647**	0.000
Br	**0.626**	**0.000**	**0.986**	**0.211**	**0.879**	0.000
Rb	<MDL	<MDL	<MDL	<MDL	<MDL	<MDL
Sr[a]	0.005	0.000	-0.010	0.039	0.306	0.000
Cd	<MDL	<MDL	<MDL	<MDL	<MDL	<MDL
Sn	**0.774**	**0.000**	**0.852**	**0.128**	**1.096**	0.000
Sb	**0.729**	**0.000**	**1.588**	**0.390**	**1.200**	0.000
Ba	0.451	0.000	1.960	0.754	0.607	0.829
Tl	<MDL	<MDL	<MDL	<MDL	<MDL	<MDL
Pb	0.103	0.000	0.802	0.555	0.817	0.496
Bi	N/A	N/A	N/A	N/A	N/A	N/A

NA = internal standard did not pass QAQC

ND = under MDL

[a] Element concentration was extremely close to MDL, however not under; could result in some noise/unreliability with measurement.

Table 9e.2 Summer ICPMS comparison for IMPROVE PM2.5 vs MOUDI PM1.8.
(IMPROVE = f(MOUDI))

Element	RSQ	RSQ SE	Slope	Slope SE	Intercept/ Average	Intercept SE
Li	<MDL	<MDL	<MDL	<MDL	<MDL	<MDL
S	**0.471**	**0.375**	**1.607**	**0.472**	**1.226**	0.489
K	N/A	N/A	N/A	N/A	N/A	N/A
Ti	<MDL	<MDL	<MDL	<MDL	<MDL	<MDL
V	**0.816**	**0.000**	**1.189**	**0.157**	**0.045**	0.000
Mn	**0.617**	**0.001**	**1.070**	**0.436**	**0.209**	0.000
Fe	**0.911**	**0.008**	**0.677**	**0.190**	**0.253**	0.198
Ga	0.243	0.000	1.940	0.949	1.022	0.000
Ge[a]	<MDL	<MDL	<MDL	<MDL	<MDL	<MDL
As	**0.654**	**0.000**	**0.856**	**0.316**	**0.423**	0.000
Se	**0.691**	**0.000**	**0.707**	**0.131**	**0.750**	0.000
Br	**0.524**	**0.001**	**1.278**	**0.338**	**0.492**	0.357
Rb	<MDL	<MDL	<MDL	<MDL	<MDL	<MDL
Sr[a]	**0.782**	**0.000**	**1.896**	**0.278**	**0.727**	0.000
Cd	<MDL	<MDL	<MDL	<MDL	<MDL	<MDL
Sn	<MDL	<MDL	<MDL	<MDL	<MDL	<MDL
Sb	<MDL	<MDL	<MDL	<MDL	<MDL	<MDL
Ba	**0.486**	**0.000**	**1.344**	**0.383**	**0.716**	0.000
Tl	<MDL	<MDL	<MDL	<MDL	<MDL	<MDL
Pb	**0.757**	**0.000**	**1.830**	**0.403**	**0.555**	0.000
Bi	N/A	N/A	N/A	N/A	N/A	N/A

NA = internal standard did not pass QAQC

<MDL = concentration lower than MDL

[a] Element concentration was extremely close to MDL, however not under; could result in some noise/unreliability with measurement.

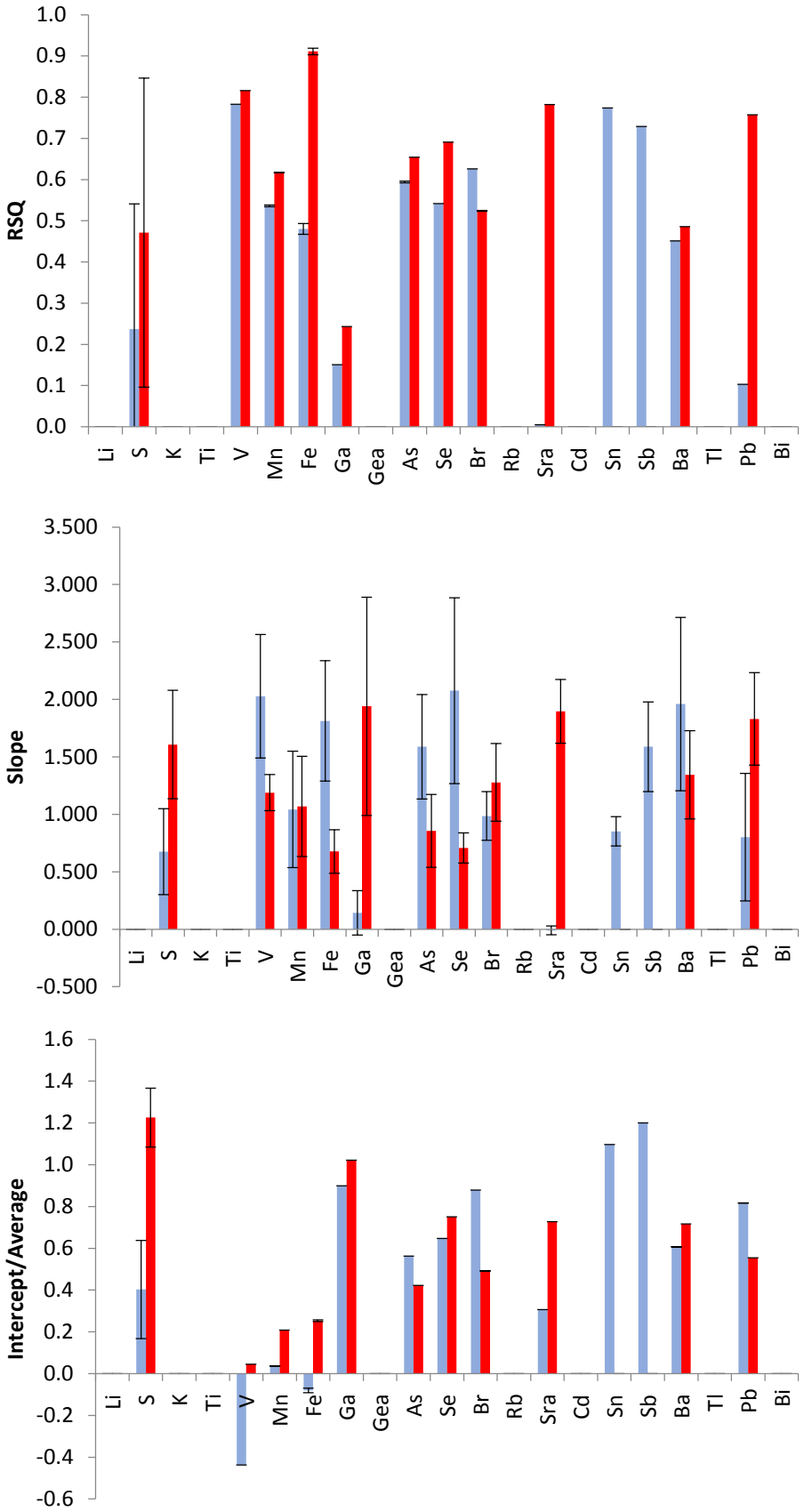

Figure 9e.1 Comparison between IMPROVE PM2.5 and MOUDI PM1.8 (IMPROVE= f(MOUDI)) analyzed by ICPMS for Winter (blue bars) and Summer (red bars) showing RSQ, slope, intercept/average and their uncertainties for each (error bars).

10. Regression Analysis

Sections 8 and 9 lay out the core of the data collected. This section takes the complete XRF data set and organizes it into a logical progression that leads to the ultimate conclusions.

The following tables represent a series of comparisons in order to determine which elements are comparable between which samplers. All of the elements analyzed by XRF were under investigation for this section of the study. For the IMPROVE sampler and RDI the cut point was at 2.5µm while the MOUDI was at 1.8µm. The first tier of comparisons began by comparing the two IMPROVE (PM2.5) samplers (ROSNA vs RONSA), as well as the two RDIs (PM2.5) (3a vs 7a) for both the winter and summer sampling events. If an element's correlation coefficient (R^2) was larger than 0.5 and slope was between the values of 0.5 and 2, that element passed the comparison. If a specific element passed it then moves on to the next tier of comparisons. Tables 10a.1-4 show the first tier of comparisons.

The second tier looked at the comparison of elements between the MOUDI (PM1.8) versus the IMPROVE (PM2.5) as well as the RDI (PM2.5) versus IMPROVE (PM2.5) for both the winter and summer sampling events. In order for an element to be analyzed, it must have passed both the IMPROVE vs IMPROVE and RDI vs RDI comparison from the Tier one comparison. Tables 10b.1-6 show the second tier of comparisons.

The third tier took the elements that were deemed passable in both the MOUDI vs IMPROVE and the RDI vs IMPROVE comparisons from Tier two in order to compare the MOUDI (PM1.8) versus RDI (PM2.5) analysis.

10a. Tier One Comparison

Comparison of ambient particulate matter (PM2.5) collected on two IMPROVE samplers (ROSNA = f(RONSA)) in the winter and summer, 2013 sampling events. Values shown in bold correlate to the elements in the specified sampling period that passed the comparison test.

Table 10a.1 Winter PM2.5 comparison between two IMPROVE samplers.

(ROSN = f(RONS)

Element	RSQ	SE RSQ	SLOPE	SE SLOPE	INTERCEPT/AVG	SE Intercept /AVG
Na	**0.979**	**0.017**	**1.180**	**0.032**	**-0.003**	0.068
Mg	**0.906**	**0.005**	**1.063**	**0.063**	**0.167**	0.093
Al	**0.948**	**0.003**	**0.908**	**0.039**	**0.017**	0.052
Si	**0.959**	**0.006**	**0.895**	**0.034**	**0.043**	0.042
P	**0.856**	**0.000**	**0.989**	**0.075**	**0.049**	0.000
S	**0.997**	**0.003**	**1.061**	**0.010**	**-0.021**	0.928
Cl	**0.991**	**0.009**	**0.993**	**0.018**	**-0.006**	0.016
K	**0.996**	**0.001**	**1.019**	**0.011**	**0.004**	0.025
Ca	**0.966**	**0.002**	**0.964**	**0.034**	**-0.005**	0.020
Ti	**0.927**	**0.000**	**0.951**	**0.050**	**0.030**	0.000
V	<MDL	0.000	<MDL	0.000	<MDL	0.000
Cr	0.218	0.000	0.536	0.188	0.522	0.000
Mn	0.645	0.000	0.806	0.111	0.265	0.000
Fe	**0.968**	**0.005**	**0.969**	**0.033**	**-0.001**	3.106
Ni	<MDL	0.000	<MDL	0.249	<MDL	0.000
Cu	**0.877**	**0.001**	**1.033**	**0.072**	**0.020**	0.000
Zn	**0.968**	**0.001**	**1.047**	**0.035**	**-0.014**	0.000
As	<MDL	0.000	<MDL	0.176	<MDL	0.000
Se	0.221	0.000	0.527	0.184	0.545	0.000
Br	**0.923**	**0.000**	**0.925**	**0.050**	**0.084**	0.000
Rb	<MDL	<MDL	<MDL	<MDL	<MDL	<MDL
Sr	<MDL	<MDL	<MDL	<MDL	<MDL	<MDL
Zr	<MDL	<MDL	<MDL	<MDL	<MDL	<MDL
Pb	0.255	0.001	0.599	0.114	0.455	0.000

Table 10a.2 Summer PM2.5 comparison between two IMPROVE samplers.

(ROSN = f(RONS).

Element	RSQ	SE RSQ	SLOPE	SE SLOPE	INTERCEPT/AVG	SE INTERCEPT /AVG
Na	**0.898**	**0.089**	**0.954**	**0.061**	**0.102**	0.086
Mg	**0.798**	**0.019**	**0.800**	**0.076**	**0.181**	0.098
Al	0.550	0.008	0.391	0.067	0.475	0.091
Si	0.445	0.024	0.346	0.073	0.513	0.088
P	<MDL	<MDL	<MDL	<MDL	<MDL	<MDL
S	**0.847**	**0.048**	**0.837**	**0.067**	**0.188**	0.074
Cl	**0.952**	**0.049**	**1.020**	**0.043**	**0.083**	0.080
K	**0.844**	**0.007**	**0.822**	**0.067**	**0.149**	0.087
Ca	**0.651**	**0.009**	**0.565**	**0.078**	**0.359**	0.088
Ti	0.476	0.001	0.338	0.067	0.545	0.000
V	0.344	0.000	0.564	0.147	0.431	0.000
Cr	0.013	0.000	0.016	0.026	0.483	0.000
Mn	0.037	0.000	0.133	0.128	0.727	0.000
Fe	0.471	0.010	0.315	0.063	0.565	0.069
Ni	0.109	0.000	0.134	0.072	0.694	0.000
Cu	0.394	0.000	0.423	0.099	0.496	0.000
Zn	**0.613**	**0.001**	**0.644**	**0.097**	**0.210**	0.000
As	<MDL	0.000	<MDL	0.161	<MDL	0.000
Se	0.371	0.000	0.581	0.143	0.213	0.000
Br	**0.808**	**0.000**	**0.830**	**0.076**	**0.163**	0.000
Rb	<MDL	<MDL	<MDL	<MDL	<MDL	<MDL
Sr	<MDL	<MDL	<MDL	<MDL	<MDL	<MDL
Zr	<MDL	<MDL	<MDL	<MDL	<MDL	<MDL
Pb	0.069	0.001	0.215	0.150	0.609	0.000

Table 10a.3 Winter PM2.5 comparison between two RDI samplers.

(7a = f(3a)

Element	RSQ	SE RSQ	Slope	SE SLOPE	Intercept/Average	SE INTERCEPT /AVG
Na	**0.984**	**0.007**	**0.733**	**0.025**	**0.177**	**0.026**
Mg	0.480	0.007	0.514	0.143	0.859	0.126
Al	**0.915**	**0.007**	**0.830**	**0.068**	**-0.053**	**0.090**
Si	**0.681**	**0.043**	**0.829**	**0.152**	**0.617**	**0.125**
P	0.007	0.002	-0.085	0.262	0.928	0.314
S	**0.703**	**0.023**	**0.803**	**0.139**	**0.082**	**0.160**
Cl	**0.998**	**0.005**	**0.786**	**0.009**	**0.061**	**0.018**
K	**0.876**	**0.006**	**0.667**	**0.067**	**0.169**	**0.082**
Ca	**0.925**	**0.006**	**0.964**	**0.073**	**0.195**	**0.069**
Ti	**0.944**	**0.001**	**0.894**	**0.058**	**0.019**	**0.093**
V	**0.905**	**0.000**	**0.760**	**0.066**	**-0.031**	**0.000**
Cr	**0.875**	**0.000**	**0.864**	**0.087**	**-0.114**	**0.000**
Mn	**0.713**	**0.000**	**0.666**	**0.113**	**1.547**	**0.000**
Fe	**0.925**	**0.012**	**0.928**	**0.071**	**-0.037**	**0.086**
Co	0.044	0.001	-0.740	0.925	1.990	0.000
Ni	0.005	0.000	-0.150	0.592	1.727	0.000
Cu	**0.919**	**0.001**	**0.865**	**0.069**	**0.206**	**0.107**
Zn	**0.825**	**0.001**	**0.865**	**0.107**	**0.020**	**0.097**
Se	**0.794**	**0.000**	**0.800**	**0.109**	**0.228**	**0.000**
Br	**0.667**	**0.000**	**0.707**	**0.133**	**0.227**	**0.119**

Table 10a.4 Summer PM2.5 comparison between two RDI samplers.

(7a = f(3a)

Element	RSQ	SE RSQ	SLOPE	SE SLOPE	INTERCEPT/AVG	SE INTERCEPT /AVG
Na	**0.635**	**0.118**	**0.607**	**0.119**	**0.323**	**0.176**
Mg	0.046	0.043	0.236	0.278	0.698	1.006
Al	0.028	0.366	0.264	0.399	0.718	0.000
Si	0.014	0.321	0.177	0.379	0.826	1.484
P	0.004	0.004	0.033	0.134	0.964	0.262
S	**0.747**	**0.119**	**0.649**	**0.098**	**0.290**	**0.000**
Cl	**0.861**	**0.048**	**0.839**	**0.076**	**0.084**	**0.000**
K	0.424	0.068	0.596	0.207	0.373	0.000
Ca	0.221	0.122	0.517	0.040	0.491	0.000
Ti	0.043	0.013	0.298	0.362	0.690	1.445
V	0.070	0.001	0.320	0.302	0.571	0.000
Cr	0.017	0.002	0.204	0.000	0.793	0.000
Mn	0.198	0.018	0.570	0.001	0.597	0.000
Fe	0.061	0.313	0.396	0.002	0.612	0.000
Co	0.329	0.015	1.055	0.118	0.392	0.000
Ni	0.136	0.002	0.603	0.001	0.552	0.000
Cu	0.351	0.001	0.996	0.000	0.077	0.000
Zn	0.221	0.005	0.517	0.001	0.482	0.000
Se	0.098	0.001	0.418	0.002	0.640	0.000
Br	**0.814**	**0.003**	**0.747**	**0.000**	**0.231**	**0.000**

The following summarizes the elements in each of the sampling periods that passed Tier One review.

IMPROVE PM2.5 vs IMPROVE PM2.5

Winter Elements – Na, Mg, Al, Si, P, S, Cl, K, Ca, Ti, Fe, Cu, Zn, Br

Summer Elements – Na, Mg, S, Cl, K, Ca, Zn, Br

RDI PM2.5 vs RDI PM2.5

Winter Elements – Na, Al, Si, S, Cl, K, Ca, Ti, V, Cr, Mn, Fe, Cu, Zn, Se, Br

Summer Elements – Na, S, Cl, Br

10b. Tier Two Comparison

The following shows a comparison of ambient particulate matter collected by MOUDI (PM1.8) versus IMPROVE (PM2.5) (IMPROVE = f(MOUDI)) in the winter and summer, 2013 sampling events. Values shown in bold font identify the elements in the specified sampling period that passed the comparison test.

Table 10b.1 Winter MOUDI PM1.8 vs IMPROVE PM2.5.
(IMPROVE = f(MOUDI))

Element	RSQ	SE RSQ	SLOPE	SE SLOPE	INTERCEPT/AVG	SE Intercept /AVG
Na	**0.970**	**0.017**	**1.582**	**0.076**	**0.206**	**0.127**
Mg	0.004	0.014	-0.015	0.069	0.478	0.205
Si	0.008	0.001	-0.078	0.240	0.810	0.328
P	**0.500**	**0.001**	**1.050**	**0.294**	**0.325**	**0.000**
S	**0.870**	**0.020**	**1.062**	**0.114**	**-0.261**	**0.130**
Cl	**0.963**	**0.017**	**1.770**	**0.097**	**-0.588**	**0.153**
K	**0.936**	**0.005**	**1.070**	**0.078**	**-0.068**	**0.084**
Ca	0.137	0.010	0.533	0.371	0.797	0.320
Ti	0.015	0.001	-0.128	0.287	1.004	0.384
Fe	0.051	0.023	0.302	0.361	0.589	0.401
Cu	0.137	0.001	-0.040	0.028	0.231	0.081
Zn	0.362	0.002	0.410	0.151	0.054	0.192
Br	**0.761**	**0.001**	**0.951**	**0.148**	**0.521**	**0.000**

Table 10b.2 Summer MOUDI PM1.8 vs IMPROVE PM2.5.
(IMPROVE = f(MOUDI))

Element	RSQ	SE RSQ	SLOPE	SE SLOPE	INTERCEPT/AVG	SE INTERCEPT /AVG
Na	**0.879**	**0.070**	**1.293**	**0.133**	**0.026**	**0.132**
Mg	**0.869**	**0.012**	**1.167**	**0.126**	**0.034**	**0.019**
S	**0.749**	**0.047**	**0.670**	**0.108**	**0.078**	**0.141**
Cl	**0.945**	**0.036**	**1.582**	**0.106**	**-0.177**	**0.133**
K	**0.624**	**0.008**	**1.181**	**0.254**	**-0.071**	**0.115**
Ca	**0.633**	**0.009**	**1.357**	**0.287**	**0.027**	**0.182**
Zn	<MDL	<MDL	<MDL	<MDL	<MDL	<MDL
Br	**0.551**	**0.001**	**0.592**	**0.148**	**0.332**	**0.183**

Comparison of ambient particulate matter collected by RDI 3a (PM2.5) versus IMPROVE (PM2.5) (IMPROVE = f(RDI))in the winter and summer, 2013 sampling events. Values shown in bold correlate to the elements in the specified sampling period that passed the comparison test.

Table 10b.3 Winter RDI 3a PM2.5 vs IMPROVE PM2.5.

(IMPROVE = f(RDI 3a))

Element	RSQ	SE RSQ	SLOPE	SE SLOPE	INTERCEPT/AVG	SE INTERCEPT /AVG
Na	**0.940**	**0.024**	**1.525**	**0.107**	**-2.111**	**0.181**
Al	0.900	0.004	0.443	0.041	0.132	0.069
Si	0.659	0.018	0.320	0.064	-0.194	0.122
S	**0.690**	**0.032**	**1.120**	**0.208**	**-0.087**	**0.276**
Cl	0.978	0.013	0.768	0.032	0.028	0.275
K	**0.909**	**0.006**	**1.099**	**0.096**	**0.001**	**0.088**
Ca	0.868	0.004	0.440	0.047	-0.204	0.074
Ti	0.950	0.000	0.262	0.017	-0.065	0.000
Fe	**0.927**	**0.006**	**0.509**	**0.040**	**0.029**	**0.061**
Cu	**0.889**	**0.000**	**0.560**	**0.055**	**-0.600**	**0.172**
Zn	**0.882**	**0.001**	**0.711**	**0.072**	**-0.559**	**0.156**
Br	**0.810**	**0.000**	**1.393**	**0.187**	**-1.805**	**0.450**

Table 10b.4 Winter RDI 7a PM2.5 vs IMPROVE PM2.5.

(IMPROVE = f(RDI 7a))

Element	RSQ	SE RSQ	SLOPE	SE SLOPE	INTERCEPT/AVG	SE INTERCEPT /AVG
Na	**0.955**	**0.020**	**1.134**	**0.068**	**-1.323**	**0.103**
Al	0.931	0.003	0.388	0.029	0.048	0.057
Si	0.899	0.010	0.378	0.035	-0.039	0.068
S	**0.585**	**0.036**	**0.972**	**0.227**	**-0.060**	**0.300**
Cl	**0.975**	**0.014**	**0.602**	**0.027**	**0.077**	**0.267**
K	**0.897**	**0.006**	**0.802**	**0.075**	**0.126**	**0.084**
Ca	0.800	0.005	0.422	0.058	-0.074	0.067
Ti	0.946	0.000	0.239	0.016	-0.052	0.000
Fe	**0.955**	**0.005**	**0.496**	**0.030**	**-0.031**	**0.039**
Cu	**0.917**	**0.000**	**0.512**	**0.043**	**-0.388**	**0.000**
Zn	**0.835**	**0.001**	**0.671**	**0.083**	**-0.507**	**0.127**
Br	**0.643**	**0.001**	**1.087**	**0.224**	**-1.172**	**0.319**

Table 10b.5 Summer RDI 3a PM2.5 vs IMPROVE PM2.5.

(IMPROVE = f(RDI 3a))

Element	RSQ	SE RSQ	SLOPE	SE SLOPE	INTERCEPT/AVG	SE INTERCEPT /AVG
Na	**0.917**	**0.072**	**1.298**	**0.109**	**-0.569**	**0.137**
S	**0.556**	**0.078**	**0.604**	**0.150**	**0.192**	**0.179**
Cl	**0.817**	**0.081**	**0.524**	**0.069**	**-0.158**	**0.142**
Br	**0.577**	**0.001**	**1.065**	**0.253**	**-1.285**	**0.403**

Table 10b.6 Summer RDI 7a PM2.5 vs IMPROVE PM2.5.

(IMPROVE = f(RDI 7a))

Element	RSQ	SE RSQ	SLOPE	SE SLOPE	INTERCEPT/AVG	SE INTERCEPT /AVG
Na	0.375	0.197	0.920	0.329	-0.144	0.392
S	**0.638**	**0.071**	**0.745**	**0.155**	**0.094**	**0.169**
Cl	0.483	0.137	0.403	0.116	0.005	0.210
Br	0.367	0.001	3.593	0.274	-0.504	0.360

The following elements in each sampling period passed Tier Two review:

MOUDI PM1.8 vs Improve PM2.5

Winter Elements – Na, P, S, Cl, K, Br
Summer Elements – Na, Mg, S, Cl, K, Ca, Br

RDI 3a PM2.5 vs Improve PM2.5

Winter Elements – Na, S, K, Fe, Cu, Zn, Br
Summer Elements – Na, S, Cl, Br

RDI 7a PM2.5 vs Improve PM2.5

Winter Elements - Na, S, Cl, K, Fe, Cu, Zn, Br
Summer Elements – S

10c. Tier Three Comparison

Comparison of ambient particulate matter collected by RDI (PM2.5) versus MOUDI (PM1.8) (RDI = f(MOUDI))in the winter and summer, 2013 sampling events. Values shown in bold correlate to the elements in the specified sampling period that passed the comparison test.

Table 10c.1 Winter RDI 3a PM2.5 vs MOUDI PM1.8.

(RDI 3a = f(MOUDI))

Element	RSQ	SE RSQ	SLOPE	SE SLOPE	INTERCEPT/AVG	SE INTERCEPT /AVG
Na	0.894	0.020	2.926	0.089	-1.434	0.163
S	**0.688**	**0.011**	**0.982**	**0.028**	**0.240**	**0.089**
K	**0.800**	**0.006**	**0.932**	**0.076**	**0.158**	**0.110**
Br	**0.612**	**0.001**	**1.110**	**0.245**	**-1.646**	**0.425**

Table 10c.2 Winter RDI 7a PM2.5 vs MOUDI PM1.8.

(RDI 7a = f(MOUDI))

Element	RSQ	SE RSQ	SLOPE	SE SLOPE	INTERCEPT/AVG	SE INTERCEPT /AVG
Na	0.908	0.018	2.689	0.061	-0.865	0.095
S	**0.533**	**0.011**	**0.815**	**0.020**	**0.296**	**0.082**
Cl	0.955	0.009	0.330	0.101	0.314	0.171
K	**0.773**	**0.007**	**0.673**	**0.081**	**0.264**	**0.097**
Br	**0.591**	**0.001**	**0.955**	**0.220**	**-1.169**	**0.320**

Table 10c.3 Summer RDI 3a PM2.5 vs MOUDI PM1.8.

(RDI 3a = f(MOUDI))

Element	RSQ	SE RSQ	SLOPE	SE SLOPE	INTERCEPT/AVG	SE INTERCEPT /AVG
Na	**0.855**	**0.055**	**0.727**	**0.083**	**-0.340**	**0.127**
S	0.554	0.097	0.498	0.187	0.376	0.215
Cl	**0.904**	**0.029**	**0.271**	**0.024**	**-0.045**	**0.058**
Br	0.313	0.001	0.786	0.323	-0.900	0.526

Table 10c.4 Summer RDI 7a PM2.5 vs MOUDI PM1.8.

(RDI 7a = f(MOUDI))

Element	RSQ	SE RSQ	SLOPE	SE SLOPE	INTERCEPT/AVG	SE INTERCEPT /AVG
S	**0.659**	**0.071**	**0.782**	**0.156**	**0.130**	**0.165**

Under the relatively clean conditions of this study, the following elements in each sampling period passed Tier Three review:

MOUDI vs RDI 3a
Winter –S, K, Br
Summer – S, Na, Cl

MOUDI vs RDI 7a
Winter – S, K, Br
Summer – S

Under higher loading conditions or longer sampling times, a great number of elements may pass these tests.

11. RDI-MOUDI size distribution comparison

Figures 11.1, 11.2, 11.3, and 11.4 show the size distributions of the RDI compared to the MOUDI for the element/season combinations that passed the Tier 3 comparison in Section 10c. The MOUDI size distributions peak in the classic size range of the accumulation mode, whereas the RDI shows a bimodal distribution. Although the peak in the particle size distribution shifts between seasons and elements, the MOUDI mono-modal and the RDI bimodal distributions persist in all three comparisons. In addition, the valley in the RDI size distribution is consistently located only in the 0.34-0.56 um size bin, indicating a possible flaw in this sampling stage of the RDI.

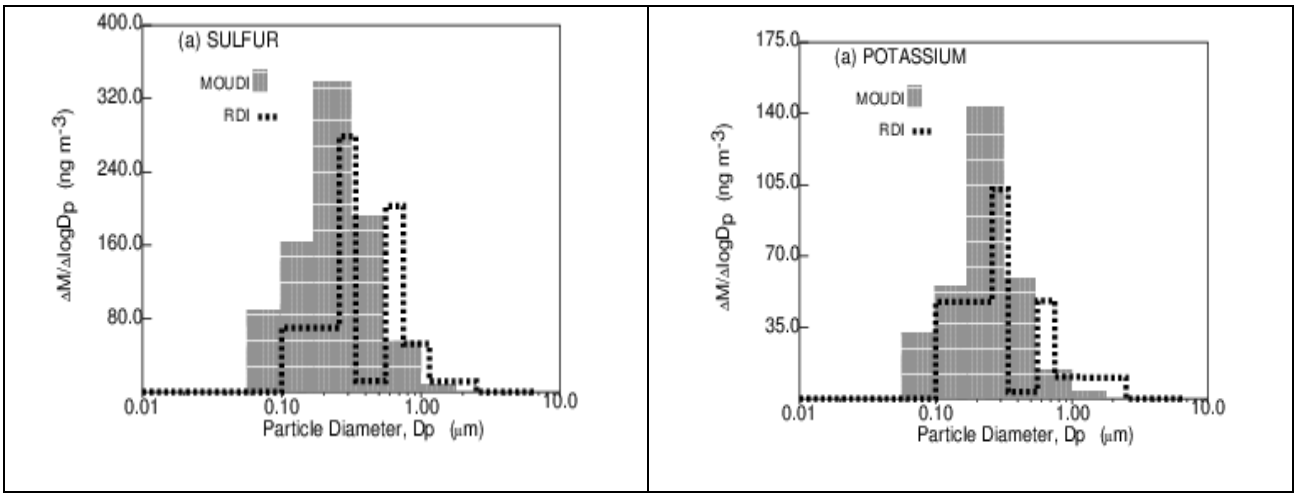

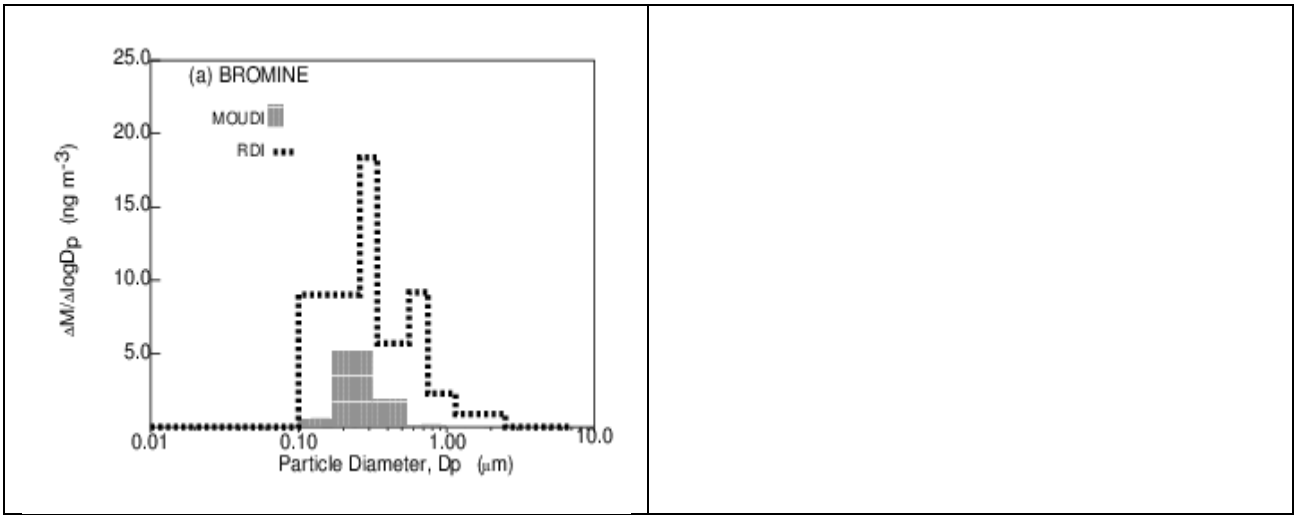

Figure 11.1. Winter RDI 3a (dashed black dots) size distribution compared to MOUDI (grey block) size distributions for elements S, K, and Br.

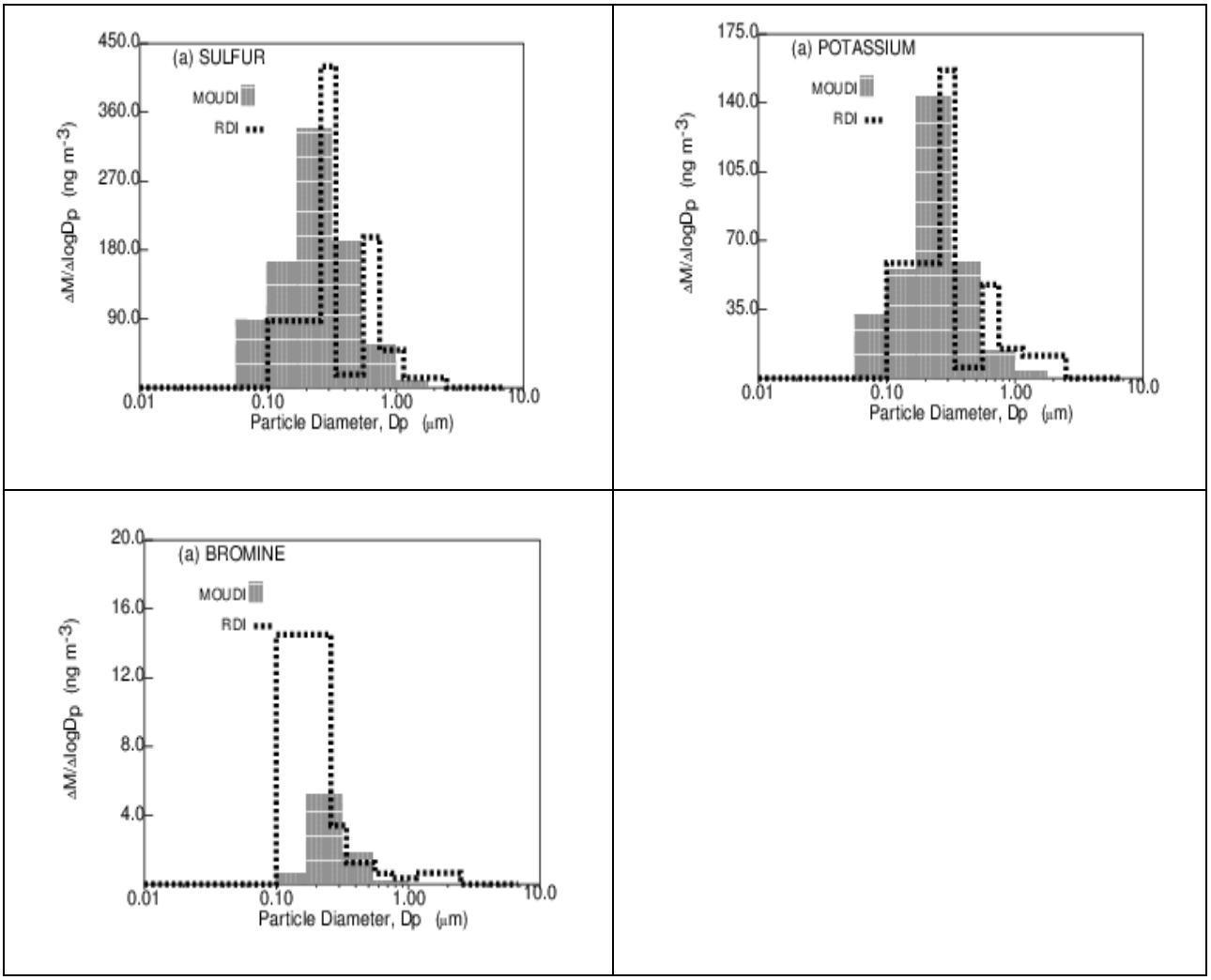

Figure 11.2 Winter RDI 7a (black dash dots) size distribution compared to MOUDI (grey blocks) size distributions for elements S, K, and Br.

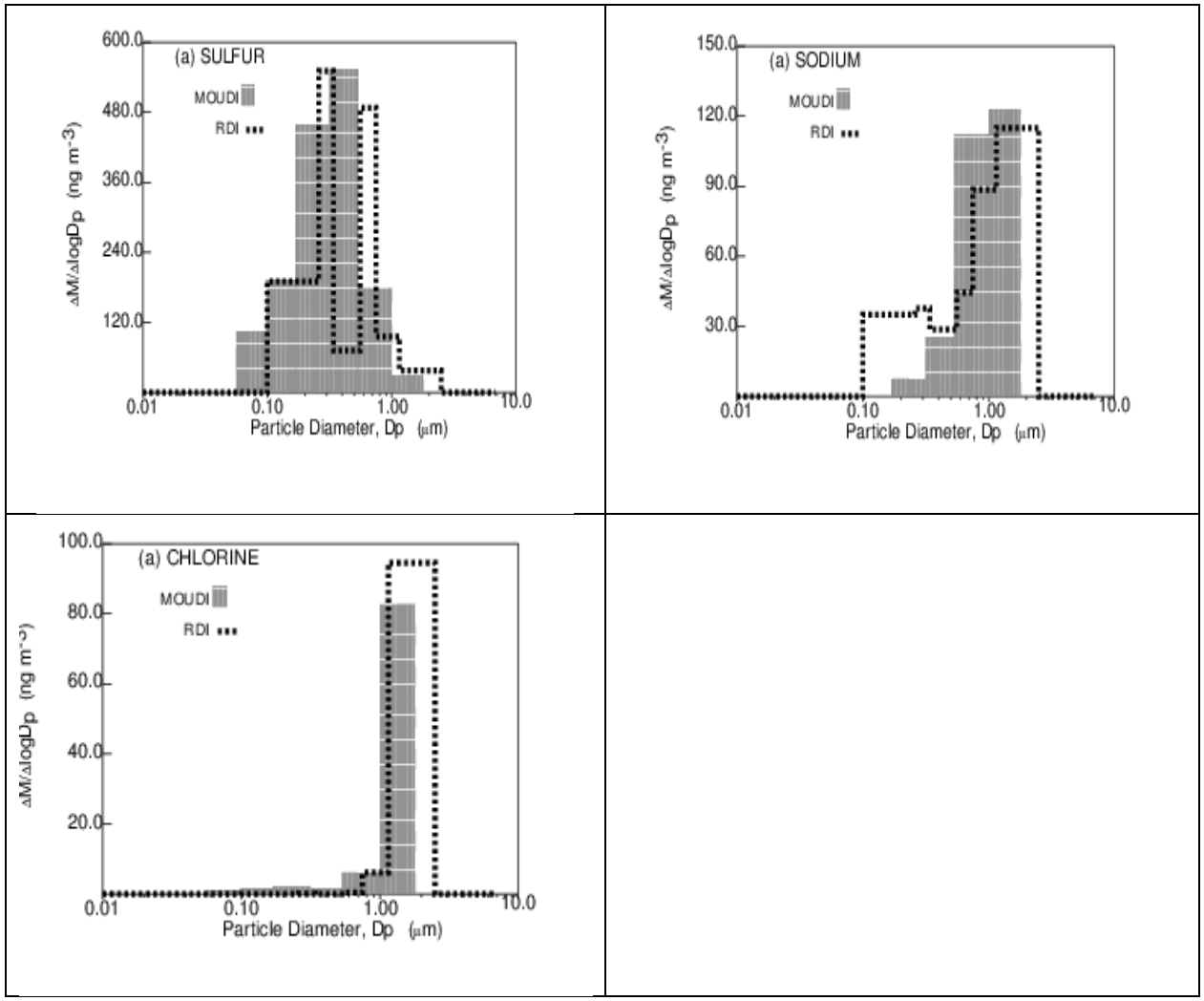

Figure 11.3. Summer RDI 3a (black dashed dot) size distribution compared to MOUDI (grey block) size distributions for elements S, Na, Cl.

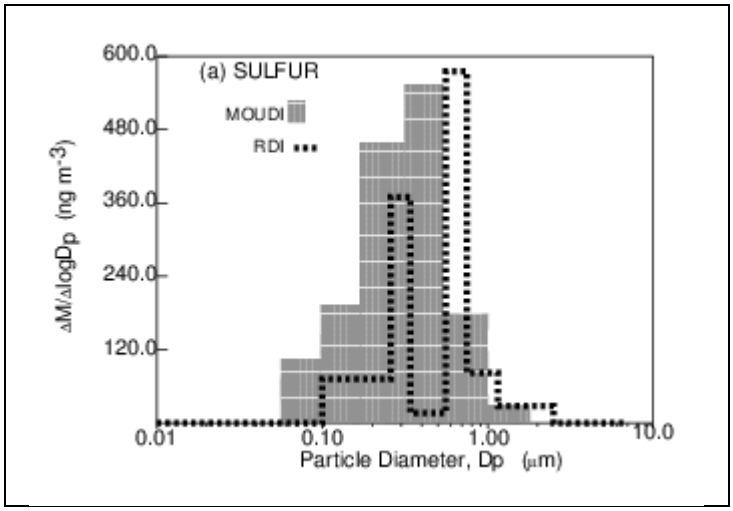

Figure 11.4 Summer 7a (dashed black dots) size distribution compared to MOUDI (grey block) size distributions for element S.

To test whether the RDI size distributions shown in Figures 11.1 - 4 are realistic, given the measured collection efficiency distribution, we calculated the minimum possible PM on Stage 6 from the PM collected on Stage 5 of the RDI (Raabe et al., 1988). Figure 10.5 shows the measured and curve-fit collection efficiency for Stage 5. Assuming the smooth size distribution measured by the MOUDI samplers, the minimum mass on Stage 6 (0.34 – 0.56 µm) of the RDI is 54% of the mass on Stage 5 (0.56 – 0.75 µm). For sulfur, the actual mass on Stage 6 of the RDI was measured to be only 7% in Winter and 8% in Summer of the Stage 5 measurements, again suggesting a collection or analysis problem on that stage in both RDI samplers.

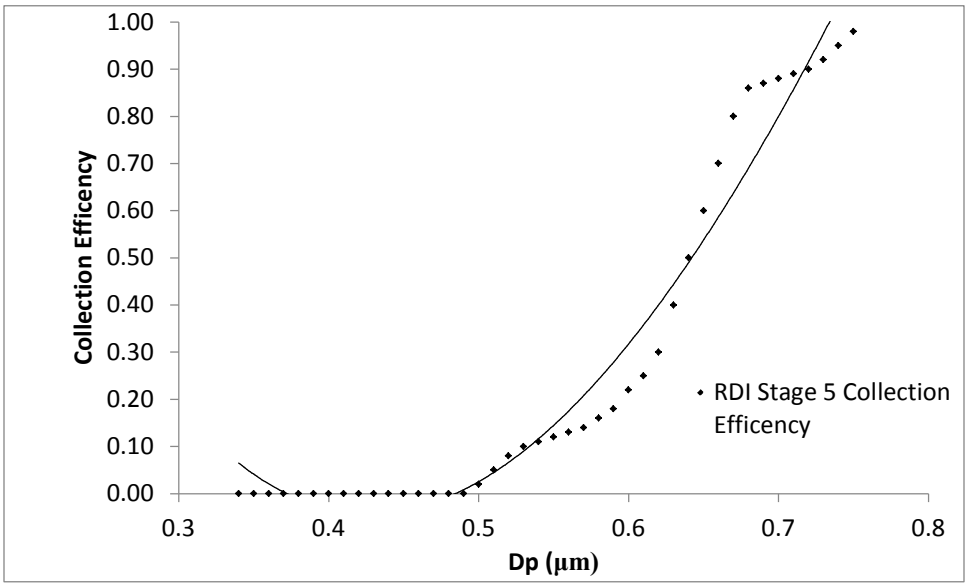

Figure 11.5. Collection Efficiency for Stage 5 of the RDI from Raabe et al., 1988. Dots are measurements; solid line is curve fit.

12. Conclusions

The following table summarizes the characteristics of each instrument:

Table 12.1. Instrument Summary

Characteristic	**IMPROVE**	**MOUDI**	**RDI**
Size Distribution	PM2.5; sharp size cuts from prior studies	6 size cuts below 1.8 um; sharp size cuts from prior studies; particle bounce problem suspected for particles larger than 1.8 um	6 size cuts below 2.5 um; broader size cuts from prior studies; particle bounce problem not yet studied
Temporal Resolution	Stated as 1-day under low concentration conditions but MDL analysis in current study suggests longer times may be needed	2-days under low concentration conditions but MDL analysis in current study suggests longer times may be needed	A few hours depending on operating conditions but MDL analysis in current study suggests longer times may be needed
Operating Cost	Modest due to filter handling and XRF analysis of each filter	High due to stage handling and XRF analysis of each stage	Low due to automated operation
XRF Precision	High	High	High
Sampler Precision	Typically high but known problems in dry dusty environments	High in prior studies for ICP/MS	High in winter, low in summer
Seasonal Sampler Accuracy for PM2.5	----	Moderate for XRF in both summer and winter. High for ICPMS in summer and winter	Moderate in winter, low in summer
Size Distribution	----	Plausible	Not plausible due to a problem in Stage 4 or 5.
*Validated PM2.5 Elements**	Taken as the Standard	Winter: Na, P, S, Cl, K, Br Summer: Na, Mg, S, Cl, K, Ca, Br	RDI-3 Winter: Na, S, K, Fe, Cu, Zn, Br RDI-7 Winter: Na, S, Cl, K, Fe, Cu, Zn, Br RDI-3 Summer: Na, S, Cl, Br RDI-7 Summer: S

* Under the low atmospheric PM concentrations of this study, these elements passed Tier 2 review (see section 10 for details). Under higher loadings, a greater number of elements may pass review.

The following conclusions and recommendations result from this work:

1) **RDI PM2.5**
20 elements were above the stated S-XRF MDLs for the RDI sampler in both winter and summer. Despite this, the RDI3 sampler precisely measured only 7 elements (35%) in the winter and 4 elements (20%) in the summer; the RDI7 sampler reliably measured 8 elements (40%) in winter and 1 element (5%) in summer. The RDI instruments appear to have a bias problem for some elements in that the temporal patterns generally match those of the other instruments but the magnitudes are wrong (e.g., Na in Figure 9d1; Si in Figure 9d12). This is likely not a flow rate calibration problem because other elements (e.g., sulfur, chlorine and potassium in Figures 9d3-5) match quite well.

2) **RDI Size Distributions**
Despite passing precision tests and accuracy tests for PM2.5, the size distributions reported by the RDIs were unrealistic in both the winter and summer seasons. The RDI size distribution was shown to be qualitatively implausible since size distributions with a gap around 0.2μm are generally not observed in the atmosphere. In addition, using the size-dependent deposition efficiency measurements of Raabe and coworkers (1988), it was shown that the gap in the size distribution measurements at this stage are implausible, indicating a leak or other problem associated with this stage. Deposition problems on this stage will likely influence deposition on downstream stages adversely affecting their readings. The gap in the size distribution is likely not a results of loss of particles in the sampler. As a result, particle mass is still conserved leading to reasonable results for PM10 and PM2.5 for some elements.

3) **IMPROVE PM2.5**
The stated MDLs for the IMPROVE sampler and XRF analysis technique are optimistic. 18 elements were measured above stated MDLs in winter and 19 elements were measured above MDLs in summer. Of these, 14 elements (78%) passed precision tests between the two co-located IMPROVE samplers for the winter and 8 elements (42%) passed the precision test between the two IMPROVE samplers for the summer. This leads to the conclusion that the actual IMPROVE sampler + XRF MDLs are greater than stated and that more elements are actually below MDL than would be expected based on the stated MDL values. XRF appears to be quite precise so the disagreement is due to sampler performance differences. This is a known shortcoming of the IMPROVE sampler (Hyslop and White, 2011).

4) **MOUDI XRF PM1.8**
18 elements were above the stated XRF MDLs for the MOUDI sampler in winter and 19 elements were above the MDLs during the summer. Of these, 6 elements (33%) passed the precision tests between a co-located MOUDI + XRF and IMPROVE + XRF sampler during the winter and 7 elements (37%) passed the precision tests between the MOUDI + XRF and IMPROVE + XRF sampler during the summer. The MOUDI PM1.8 size fraction should be comparable to the IMPROVE PM2.5 because the elements are from high temperature sources so should have negligible mass in the 1.8 to 2.5 μm size range. This lack of agreement may reflect the need for appropriate size-resolved correction factors to account for XRF response to different particle diameters on different impactor stages (Formenti et al., 2009). No size-resolved MOUDI + XRF corrections were applied in the current study.

5) **MOUDI ICP/MS PM1.8**
13 elements were above the stated ICP-MS MDLs for the MOUDI sampler in winter and 11 elements were above the MDLs during the summer. Of these, 8 elements (62%) passed the precision tests between a co-located MOUDI + ICPMS and IMPROVE + ICPMS sampler during the winter and 10 elements (91%) pass the precision tests between a MOUDI + ICPMs and IMPROVE + ICPMS sampler during the summer. The closer agreement between the expected MDLs and the actual performance of the co-located samplers suggests that the stated MOUDI + ICP-MS MDLs are more realistic than the stated MOUDI + XRF MDLs, but still somewhat optimistic.

6) **MDLs**
Under the low concentration conditions present during this study, none of the instruments could reliably measure 100% of the elements that were above stated MDLs for either XRF or ICP-MS. Investigators should assess their MDLs and consider longer collection times under low concentration conditions.

13. References

Barone, J.B., T.A. Cahill, R.A. Eldred, R.G. Flocchini, D.J. Shadoan, and T.M. Dietz. A multivariate statistical analysis of visibility degradation at four California cities. Atmospheric Environment. 12:2213-2221 (1978).

Bench, G., Grant, P., Ueda, D., Cliff, S., Perry, K., Cahill, T. (2002), The Use of STIM and PESA to Measure Profiles of Aerosol Mass and Hydrogen Content, Respectively, across Mylar Rotating Drum Impactor Samples, Aerosol Science and Technology, 36, 642–651.

Bukowiecki, N., A. Richard, M. Furger, E. Weingartner, M. Aguirre, T. Huthwelker, P. Lienemann, R. Gehrig, and U. Baltensperger (2009), Deposition Uniformity and Particle Size Distribution of Ambient Aerosol Collected with a Rotating Drum Impactor. Aerosol Science and Technology, 43:891–901.

Cahill, T.A. Proton microprobes and particle-induced x-ray analytical systems. Annual Reviews Nuclear and Particle Science. 30:211-252 (1980).

Cahill, T.A., B.H. Kusko, L.L. Ashbaugh, J.B. Barone, R.A. Eldred, and E.G. Walther. Regional and local determinations of particulate matter and visibility in the southwestern United States during June and July, 1979. Symposium on Plumes and Visibility. Grand Canyon, AZ, 1980. Atmospheric Environment. 15:2011-2016 (1981).

Cahill, T.A., C. Goodart, J.W. Nelson, R.A. Eldred, J.S. Nasstrom, and P.J. Feeney. Design and evaluation of the drum impactor. Proceedings of International Symposium on Particulate and Multi-phase Processes. Teoman Ariman and T. Nejat Veziroglu, Editors. Hemisphere Publishing Corporation, Washington, D.C. 2:319-325. (1985).

Cahill, Thomas A., Marcelle Surovik, and Ian Wittmeyer. Visibility and aerosols during the 1986 carbonaceous species methods comparison study. Aerosol Science and Technology. 12:149-160 (1990).

Cahill, Thomas A. and Paul Wakabayashi. Compositional analysis of size-segregated aerosol samples. Chapter in the ACS book Measurement Challenges in Atmospheric Chemistry. Leonard Newman, Editor. Chapter 7, Pp. 211-228 (1993).

Cahill, Thomas A., Kent Wilkinson, and Russ Schnell. Composition analyses of size-resolved aerosol samples taken from aircraft downwind of Kuwait, Spring, 1991. Journal of Geophysical Research. Vol. 97, No. D13, Paper no. 92JD01373, Pp. 14513914520, September 20 (1992).

Cahill, T.A., P, Wakabayashi, T. James. Chemical State of Sulfate at Shenandoah National Park During Summer 1991 Nuclear Instruments and Methods in Physics Research B: Beam Interactions with Materials and Atoms, 109/110 (1996) 542-547.

Cliff, S.S. (2005), Quality Assurance Analysis of Filter Samples Collected during the Lake Tahoe Atmospheric Deposition Study using Synchrotron X-Ray Fluorescence (LTADS s-XRF QA). Final report for Agreement No. 03-344, 2005, available at http://www.arb.ca.gov/research/abstracts/03-344.htm.

EPA (2011) Acceptable criteria for performance testing, Environmental Protection Agency. 40 CFR 23, Part 136, Appendix B, Fed. Regist. July 1, 2011. http://www.gpo.gov/fdsys/pkg/CFR-2011-title40-vol23/pdf/CFR-2011-title40-vol23-part136-appB.pdf

Feeney, P.J., T.A. Cahill, R.G. Flocchini, R.A. Eldred, D.J. Shadoan, and T. Dunn. Effect of roadbed configuration on traffic derived aerosols. Journal of the Air Pollution Control Association. 25:1145-1147 (1975).

Flocchini, Robert G., Thomas A. Cahill, Danny J. Shadoan, Sandra J. Lange, Robert A. Eldred, Patrick J. Feeney, Gordon W. Wolfe, Dean C. Simmeroth, and Jack K. Suder. Monitoring California's aerosols by size and elemental composition. Environmental Science and Technology. 10:76-82 (1976).

Formenti, P., Nava, S., Prati, P., Chevaillier, S., Klaver, A., Lafon, S., and Chiari, M. (2010), Self-attenuation artifacts and correction factors of light element measurements by X-ray analysis: Implication for mineral dust composition studies. J. Geophys. Res.: Atmos. 115(D1).

Hering, Susanne V., Bruce R. Appel, W. Cheng, F. Salaymeh, Steven H. Cadle, Patricia A. Mulawa, Thomas A. Cahill, Robert A. Eldred, Marcelle Surovik, Dennis Fitz, James E. Howes, Kenneth T. Knapp, Leonard Stockburger, Barbara J. Turpin, James J. Huntzicker, Xin-Qui Zhang, and Peter H. McMurry. Comparison of sampling methods for carbonaceous aerosols in ambient air. Aerosol Science and Technology. 12:200-213 (1990).

Herner, Jorn D., Peter G. Green, and Michael J. Kleeman (2006), Measuring the trace elemental composition of size-resolved airborne particles. Environ. Sci. Technol. 40.6: 1925-1933.

Hyslop, Nicole P., and Warren H. White (2011), Identifying sources of uncertainty from the inter-species covariance of measurement errors. Environ. Sci. Technol. 45:4030-4037.

Knochel, A. (1990), TXRF, PIXE, SYXRF; Principles, Critical Comparison and Applications, Fresenius' Journal of Analytical Chemistry, 337, 614-621.

Lundgren, D. A. (1967), An Aerosol Sampler for Determination of Particle Concentration as a Function of Size and Time, Journal of the Air Pollution Control Association, 17, 225-229.

Malm, W.C., Sisler, J.F., Huffman, D., Eldred, R.A. and Cahill, T.A.. Spatial and seasonal trends in particle concentration and optical extinction in the United States. Journal of Geophysical Research, VOL. 99, No. D1, 1347-1370, January 20, 1994

Motallebi, Nehzat, Robert G. Flocchini, Leonard O. Myrup, and Thomas A. Cahill. A principal component analysis of visibility and air pollution in six California cities. Atmosfera. Pp. 127-141 (1990).

MSAM - Development of a Modular System for Acidic Deposition Monitoring, ARB Contract No. A132-102, July, 1993

Method 6020 Inductively Coupled Plasma-Mass Spectrometry, in SW-846 Test methods for evaluating solid waste, physical/chemical methods, S. Waste, Editor. 1994, U.S. EPA: Washington, D.C.

Perry, Kevin D., Thomas A. Cahill, Russell C. Schnell, and Joyce M. Harris. Long-range transport of anthropogenic aerosols to the NOAA Baseline Station at Mauna Loa Observatory, Hawaii. 1999 Journal of Geophysical Research Atmospheres. Vol. 104, No. D15, Pages 18,521-18,533.

Perry, Kevin, Cahill, T.A., Eldred, R. A., Dutcher, D.D, Gill, T.E. Long-range transport of North African dust to the eastern United States. 1996 Journal of Geophysical Research-Atmospheres, 102, D10, 11,225-11,238.

Perry K. D., Cliff, S. S. and Jimenez-Cruz, M.P. (2004), Evidence for Hygroscopic Mineral Dust Particles from the Intercontinental Transport and Chemical Transformation Experiment, Journal of Geophysical Research, 109, 23-28, doi:10.1029/2004JD004979.

Raabe, O.G., Braaten, D.A., Axelbaum, R.L., Teague, S.V., and Cahill, T.A. (1988), Calibration Studies of the DRUM Impactor, Journal of Aerosol Science, 19, 183-195.

Standard Operation Procedures (SOPs)

for

Rotating Drum Impactor (RDI) sampler operation and data analysis

Prepared by

Yongjing Zhao, Yuee Pan, and Steven S. Cliff

(Air Quality Research Center, University of California-Davis)

Kevin Perry

(Department of Atmospheric Sciences, University of Utah)

Reviewed by

Richard A. VanCuren

(Air Quality Research Center, University of California-Davis)

Version 1.0

(November 8, 2012)

Table of Contents

1. General Statement A-3
2. Standard Operation Procedure for Uploading Drum Cartridge A-4
2.1 Materials and tools A-4
2.2 Cleaning and checking RDI cartridge A-4
2.3 Uploading Mylar substrates on RDI wheel A-4
2.4 Coating the Mylar substrate mounted on RDI drums A-4
2.5 Device Photos A-4
3. Standard Operation Procedure for Downloading Drum Cartridge A-9
3.1 Materials and tools A-9
3.2 Downloading Mylar substrates from the RDI wheels A-9
3.3 Device Photos A-10
4. Standard Operating Procedure for Analyzing RDI Samples at the Advanced Light Source (ALS) A-16
5. Standard Operation Procedure for Deriving Elemental Concentrations from S-XRF Spectra A-18
5.1 Initial System Setup/Check A-18
5.2 Data Reduction Procedure Outline A-18
5.3 Analyzing peaks using WinAxilBatch A-18
6. Standard Operation Procedure for Installing RDI Sampler in Field A-19
6.1. Unpack A-19
6.2 Structure of the sampler A-21
6.3 Setup sampler A-221
6.4. Start sampling A-26
6.5 Stop sampling and change the cartridge 30

1. General Statement

Since the Rotating Drum Impactor (RDI) sampler is a research based aerosol sampler, currently there is no operation manual available. Any person who is going to use it for scientific research must be hand-on trained by qualified personnel before he/she can work on it independently. All Standard Operation Procedures (SOPs) provided in this document is not for training purpose but the procedures for qualified operators to follow either in field deployments or samples/data analysis in laboratory for quality assurance and control (QA/QC) purpose.

In case that the RDI is deployed in a remote field site where qualified personnel are not available, it is strongly recommended that the person who is going to install the RDI sampler onsite needs to well understand the SOP#6 "Standard Operation Procedure for Installing RDI Sampler in Field" before starting the installation and needs to communicate with qualified personnel during the installation if any concerns arise. For this purpose, the SOP#6 is written in more detail than the other SOPs. In this case, only installation can be done without qualified personnel present, but all other procedures (uploading and downloading Mylar substrates, analysis of RDI samples and XRF data) are still to only be performed by qualified personnel.

When the new RDI cartridges are shipped to the site or the sampled cartridges are shipped back from the field sites, it is strongly recommended to use a commercial shipping carrier, such as UPS or FedEx. DO NOT take them as checked bags when flying commercial airlines because they may be damaged if a safety inspection were to occur.

2. Standard Operation Procedure for Uploading Drum Cartridge

2.1 Materials and tools

a. One Nalgene wash bottle with 100% methanol
b. One box of KIMTECH wipes (see Photo 2-1)
c. One customer-made RDI drum-wheel holding stand (see Photo 2-2)
d. One roll of ¾" wide Magic tape (see Photo 2-3)
e. Eight pre-cut 3/4" wide and 7-1/2" long Mylar substrates.
f. Solution of 2% Apiezon L (a vacuum grease) in Toluene
g. One ¼" OD X 3" long stainless steel (SS) bar or one #1 Phillips screw driver
h. One ceramic roller with mated coating solution reservoir (see Photo 2-4)
i. Several clean ¼" - ½" wide paper strips
j. One RDI cartridge with 8 drum-wheels (see Photo 2-5)
k. One pump and one vacuum hose with fitting to the RDI cartridge outlet port
l. One 20 liter/min flowmeter with a cartridge inlet coupler (see Photo 2-6)
m. One preprinted paper tag One preprinted paper tag
n. Orifice spacing check adapter (customer made, Photo 2-7)
o. One Lab table or desk with at least 24"x24" surface area.

2.2 Cleaning and checking RDI cartridge

a. Record the cartridge number on the preprinted paper tag.
b. Clean the orifices in drum cartridge with dry clean paper strips.
c. Check the orifice spacing at each stage using the spacing check adapter (see Photo 2-7).
d. Connect the pump to the cartridge outlet port, connect the flow meter to the cartridge inlet port, and measure the flow rate. The flow rate should be in the range between 14.5 and 16.7 liter/min, which varies with cartridge. Record it on the preprinted paper tag.
e. Clean RDI drums, cartridge, table surface, and drum-wheel holding stand with 100% methanol.

2.3 Uploading Mylar substrates on RDI wheel

a. Attach one RDI drum to the drum-wheel holding stand (see Photo 2-2).
b. Mount one clean Mylar substrate on the RDI drum-wheel and tape both ends of the Mylar substrate on the RDI drum surface with the magic tape.
c. Mount 8 RDI drums for each cartridge.

2.4 Coating the Mylar substrate mounted on RDI drums

(It is recommended that this job be performed under a laboratory venthood of any size or in a well-ventilated area.)

a. Clean the ceramic roller with mated coating solution reservoir with 100% methanol and air-dry for at least 5 min. (see Photo 2-4)
b. Fill the coating solution reservoir with the 2% Apiezon L/toluene solution until about 1/8" of roller wheel is submerged in the solution.
c. Insert the ¼" SS bar into the center hole of the Mylar coated RDI drum-wheel. The RDI wheel can rotate freely around the ¼" SS bar.
d. Rotate the ceramic roller wheel about 1-turn, a thin film of the Apiezon/toluene solution can be seen on roller surface.
e. Attach the RDI wheel surface with Mylar substrate to the surface of the coating roller-wheel and rotating the RDI wheel about 2-turns slowly, the ceramic coating wheel rotates together with the RDI drum-wheel and coats a film of Apiezon L solution on the Mylar substrate.
f. Place the coated RDI wheels in the cartridge, leaving the uploaded cartridge in the vent-hood or a well-vented area to let the toluene evaporate from the coating solution, which leaves a thin film of Apiezon coating on the Mylar substrate.
g. About 1-2 hours after coating, place the cylinder lids on all 8 stages of the RDI cartridge, cover the inlet port of the cartridge with a plastic cap, and record the coating date on the preprinted paper tag.
h. Collect the unused Apiezon L solution in waste container and treat the chemical waste according to University procedure if the work is performed in UC Davis (see link below for details http://safetyservices.ucdavis.edu/ps/cls/clsm)

2.5 Device Photos

Photo 2-1. KIMTECH wipes

Photo 2-2. Drum-wheel holder

Photo 2-3. Magic tape

Photo 2-4. Ceramic roller

Photo 2-5a. RDI cartridge with covers open

Photo 2-5b. RDI cartridge with cover closed

Photo 2-6. Flow meter with coupler

Photo 2-7. Orifice checking adapter

3. Standard Operation Procedure for Downloading Drum Cartridge

3.1 Materials and tools

a. One Nalgene wash bottle with 100% methanol
b. One box of KIMTECH wipes (see Photo 3-1)
c. One Drum-wheel holding stand (see Photo 3-2)
d. One roll of ¾" wide Magic tape (see Photo 3-3)
e. Eights customer-made plastic frames to mount the Mylar substrates (Available @ www.DrumAir.com, see Photo 3-4)
f. One pump and one vacuum hose with fitting to the cartridge outlet port.
g. One flow meter of 20 liter/min with a cartridge inlet coupler (see Photo 3-5)
h. One customer-made substrate frame holder (see Photo 3-6)
i. One thin permanent marker pen
j. One customer-made plastic archive box for mounted sample frames (availanle @ www.DrumAir.com, see Photo 3-7)
k. One stainless steel scalpel (see Photo 3-8).
l. One Lab table or desk with at least 24"x24"surface area.

3.2 Downloading Mylar substrates from the RDI wheels

a. Clean the plastic frames, the frame holder, lab table surface, and RDI drum-wheel holding stand with the 100% methanol. Wait for at least 10 minutes for the Methanol to air-dry.
b. Record the sampling site name, starting and ending dates/times, stage number, RDI cartridge number, and flow rate on the white side of each of the eight plastic frames using the permanent mark pen (label in normal direction from left to right, see Photo 3-9.).
c. Flip the plastic frame over and mark an arrow on the blue side of the plastic frame pointing in the same direction as the label on the white side. This arrow denotes the start and progression of the ambient sampling period when the Mylar substrate is mounted to the blue side of the frame (i.e., when reading the recorded information on the white side, sample progression is left to right).
d. Place the plastic frame on the frame holder with blue side facing up, ensuring the arrow direction is from right to left as viewed from the top (see Photo 3-6)
e. Place the sampled RDI drum-wheel on the drum-wheel holding stand (see Photo 3-2).
f. Carefully cut the tape between each end of the Mylar substrate on the RDI drum-wheel with a scalpel.
g. Remove the sampled Mylar substrate off the RDI drum-wheel carefully with right hand on starting edge and left hand on the ending edge.
h. Place the Mylar substrate on the plastic frame on the frame holder, the direction from starting point to ending point should be the same as the arrow mark. The deposit on the Mylar substrate should be facing up.

i. After ensuring the Mylar substrate is laying flat on the plastic frame, affix both starting and ending edges of the Mylar substrate to the plastic frame using Magic tape (see Photo 3-10).
j. Place the mounted frames in the plastic archive box (see, Photo 3-11).
k. Replace downloaded RDI drum-wheel in the cartridge and cover the stage.
l. Repeat to download al 8 stages.
m. Measure the flow rate using the pump and the flow meter. If the flow rate change compared to the value priori deployment is less than 10%, the RDI samples are acceptable.
n. Affix the paper tag inside the plastic archive box (see Photo 3-11).
o. Close the archive box firmly and store it on the lab shelf. Freezer is not required to store the RDI samples...

3.3 Device Photos

Photo 3-1. KIMTECH wipes

Photo 3-2. Drum-wheel holder with a sampled drum-wheel

Photo 3-3. Magic tape

Photo 3-4. Plastic frame

Photo 3-5. Flow meter with cartridge inlet coupler

Photo 3-6. Frame holder

Photo7. Plastic archive box

Photo 3-8. Stainless Steel scalpel

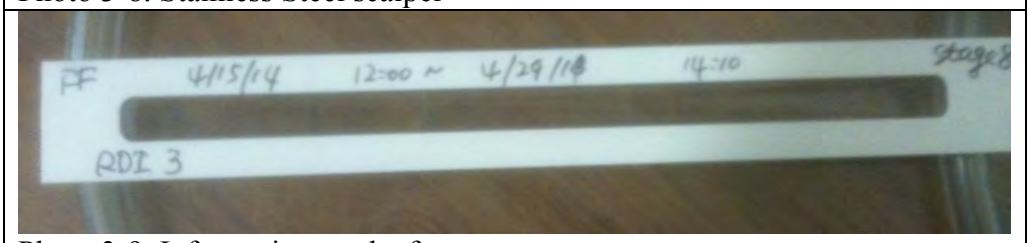

Photo 3-9. Information on the frame

Photo 3-10. Sampled Mylar substrate on the plastic frame

Photo 3-11. Archive box with frames and tags

4. Standard Operating Procedure for Analyzing RDI Samples at the Advanced Light Source (ALS)

1. Contact ALS operations personnel at least 24 hours in advance of arrival to schedule key-enable procedure for the beamline.
2. Upon arriving at ALS, turn on Helium gas flow for hutch and N_2 gas for Ion chamber prior to opening beam shutter.
3. Setup sample chamber on the beamline table (see Photo 4-1)
4. Perform initial alignment of the chamber to the X-ray beam by aligning the sample chamber entrance and exit windows with the X-ray ion chamber window on a straight line (see Diagram 1)
5. Setup camera to monitor inside the chamber.
6. Setup stepper motor and stepper motor controller.
7. Install detector to the sample chamber.
8. Leak check the sample chamber.
9. Using a phosphor strip, perform final alignment of the X-ray beam to the substrate central position in the sample chamber (see Photo 4-2).
10. Adjust horizontal and vertical collimating slits to the center of the X-ray beam.
11. Set the X-ray beam size (vertical slit width = 500 micron).
12. Turn on ionization chamber voltage supply and set the I_0 amplifier gain at $x10^6$. The ionization chamber measures incident beam intensity.
13. Analyze calibration standards.
14. Run QA check using the QA sample (e.g. Trin4 reno strip) and communicate with the data analyst who analyzes the QA XRF data, compares the results with the average of the previous data, and determines if the current QA check is passed (see SOP#5).
15. Start analyzing samples after the QA check is passed.

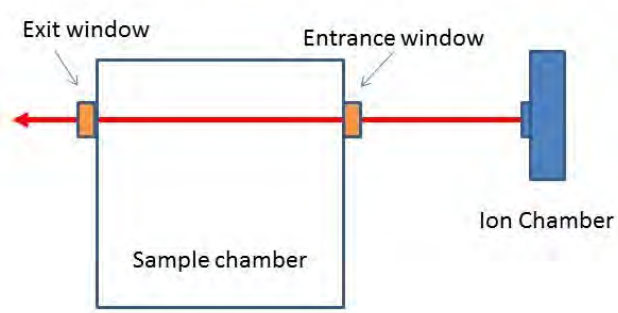

Diagram 1. Initial alignment of the X-ray beam

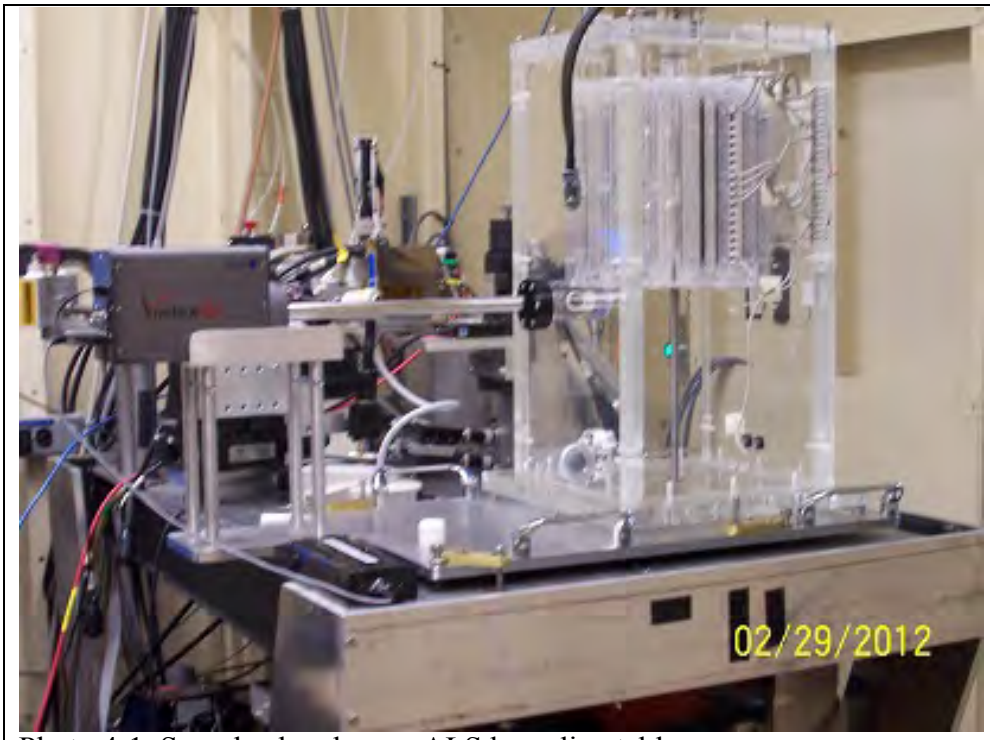

Photo 4-1. Sample chamber on ALS beamline table

Photo 4-2. X-ray alignment with a phosphor strip

5. Standard Operation Procedure for Deriving Elemental Concentrations from S-XRF Spectra

Data reduction of S-XRF spectra collected at ALS currently consists of the following procedures:

5.1 Initial System Setup/Check

1. Check the energy calibration using WinAxil.
2. Analyze the K-line standards and Pb using WinAxilBatch.
3. Perform the system calibration for the K-line elements and Pb.
4. Create a .CAL file for the current calibration and transfer it to a FORTRAN computer system.
5. Analyze the QA-Trin4 reno strip (reanalyzed at ALS for the current period) using WinAxilBatch.
6. Compare the current QA-Trin4 renos strip to previous runs on an element-by-element basis to ensure consistency from run to run.

5.2 Data Reduction Procedure Outline

1. Analyze the peaks using WinAxilBatch exporting the data to a .xls file. It is more efficient to analyze an entire set of strips simultaneously.
2. Convert the .xls file to a .csv file. The first column must have the filename only without the path. This can be accomplished with a macro in Excel.
3. Transfer the .csv file to a computer system that has FORTRAN capabilities.
4. Convert the .csv file to a .asr file using the program 'csv2asrCHPC'.
5. Move the .asr files to an appropriate directory.
6. Create a batch file for each strip. The batch file has the filename, particle size correction info, particle loading correction info, and the conversion constant.
7. Copy the .CAL into a filename called latest.cal.
8. Copy the batch .txt file into a filename called input.txt.
9. Run the xrfCHPC program.
10. Load the resultant .txt files into Excel or equivalent.
11. Align the data for each stage. Label the data unit info (i.e., ng/m^3 or ng/cm^2 depending on conversion constant).
12. Perform QA on the data set.
13. Eliminate missing or extraneous elements. Can be accomplished with an Excel macro.

5.3 Analyzing peaks using WinAxilBatch

WinAxilBatch requires the user to input a model that will be used for fitting the data. We currently use a model called Vortex.Afm. The .Afm model can only be created or modified using WinAxil. The model tells WinAxil which elements to look for, the energy calibration and how to perform the background subtraction.

6. Standard Operation Procedure for Installing RDI Sampler in Field

This is an 8-Stage Rotating Drum Impactor (RDI) particle sampler made by the University of California-Davis, which uses coated Mylar substrates to collect atmospheric aerosols continuously for up to 6 weeks with an ambient sampling time resolution of 4hr/mm. The nominal cut points of the 8 stages are: 10.0-5.0, 5.0-2.5, 2.5-1.15, 1.15-0.75, 0.75-0.56, 0.56-0.34, 0.34-0.26, and 0.26-0.09 μm aerodynamic diameter.

NOTE: It is critical to the success of the experiment that the sampling cartridge NEVER be opened. This cartridge has been prepared in a clean lab to assure experimental integrity. Opening this cartridge will compromise the sample. In the event that the cartridge is inadvertently opened, you MUST record this information for accurate data interpretation. Please contact us if you have questions!

6.1. Unpack

Unpack all units from shipping containers and compare with the list below. Save all packing items, as these will be useful for return shipment. Leave the plugs used to maintain cartridge cleanliness in place until that component gets connected to system.

Packing List (see Photo 6-1):

1. One grey sampler field case, with electronics and rotation mechanism
2. One stack coupler to sampler case
3. One power cord
4. One black vacuum hose with quick connect for pump onsite
5. One eight-stage cartridge.
6. One PM10 inlet head with a glass jar
7. One Inlet stack (1-3/4” metal tube)
8. One pair of support stands

RDI case

Stack coupler

Power cord	Vacuum hose
Cartridge	Inlet stack
PM10 head with glass jar	"L" shape Support stands

Photo 6-1. Packing list

In case there are any questions or problems, please contact:

Yongjing Zhao at (U.S.) 530-219-9014 or send e-mail to yjzhao@ucdavis.edu

Steve Cliff at (U.S.) 530-867-2037 or e-mail (sscliff@ucdavis.edu)

6.2 Structure of the sampler

The assembled sampler without cartridge is shown in Photo 6-2. Please follow this SOP carefully to reduce the chance of problems.

Photo 6-2. Assembled RDI sampler

6.3 Setup sampler

1. To install the "L" shape support frame on the back of the gray Pelican box, place the sampler on its side and attach the two support frames to the RDI case as show Photo 6-3.

Photo 6-3. Attach the "L" shape support frame to RDI case

2. Secure the support frame on a flat surface at the site (see the RDI case orientation in Photo 6-2). Ideally, some support for the back of the sampler will

be available. This will reduce the chance of tip-over during high winds. Bolting or screwing the feet to a table or roof structure will also help support the sampler. One should not rely solely on a freestanding sampler.

3. Screw in the cylindrical stack coupler to the top of the sampler case. Make sure coupler is firmly seated to prevent water entry to the sampler case. See Photo 6-4, the red circle.

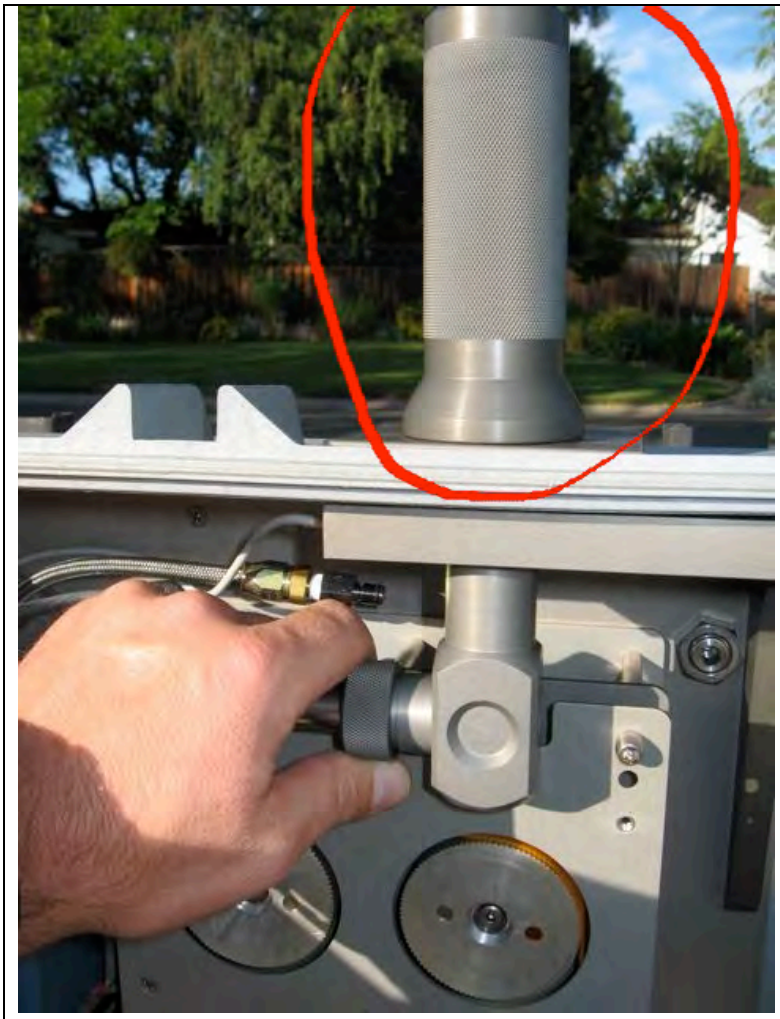

Photo 6-4. Attach the Cylindrical stack coupler to RDI case

4. Insert the inlet stack (long tube) into the stack coupler from top (see Red circle in Photo 6-5) and insert the manifold "T" into the inlet stack from bottom (see yellow circle in Photo 6-5), so that the stack is between the coupler and the manifold. DO NOT insert "T" into stack coupler until the inlet stack is seated in the coupler. Make sure the stack is well seated in the coupler during this procedure. If successful, the inlet stack is fully engaged with the manifold, which connects the inlet stack to the sampler cartridge inside the case.

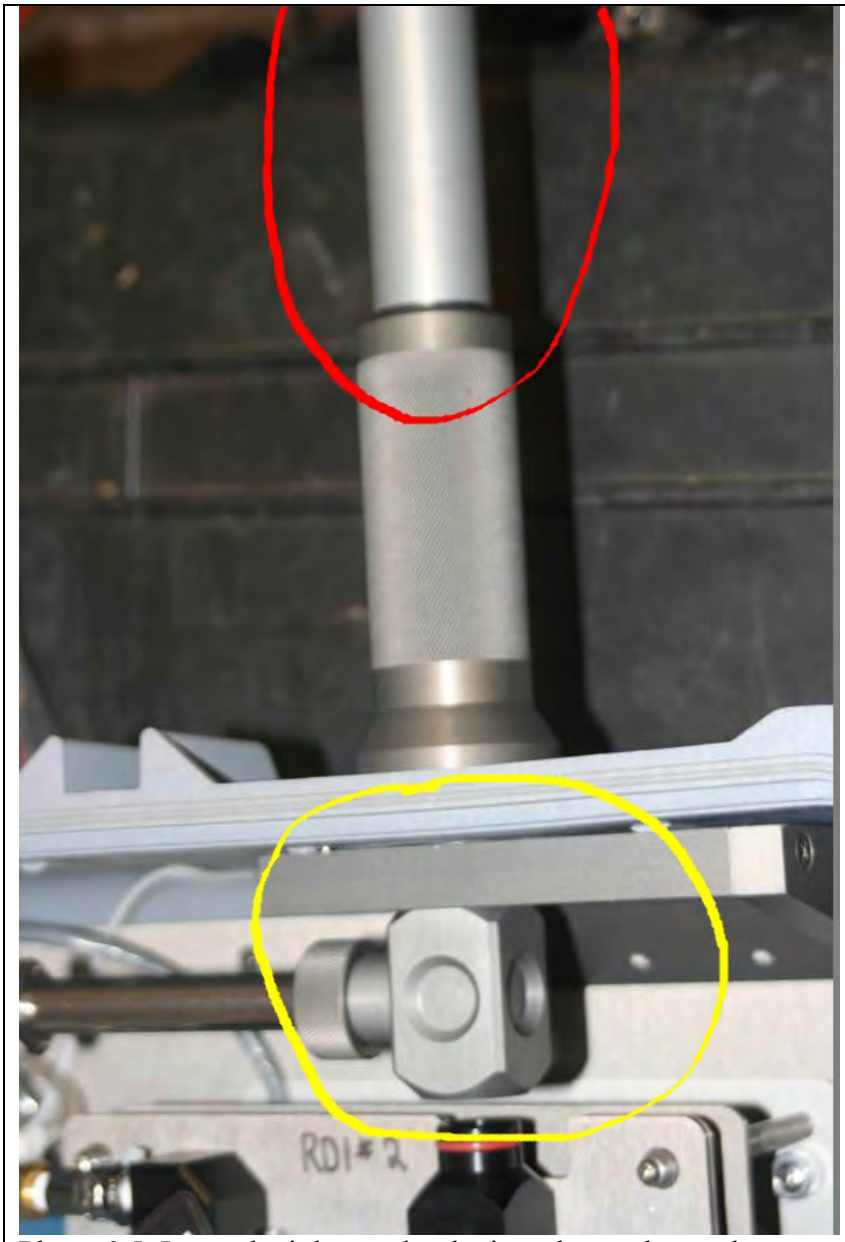

Photo 6-5. Insert the inlet stack tube into the stack coupler

5. Remove white cap (see red circle in Photo 6-6) and install sample cartridge into sampler. Start with the cartridge holes (see yellow circles in Photo 6-6) aligned with the pins at the top of the sampler while holding the bottom of the cartridge (see green circle in Photo 6-6). Rotate cartridge down until the cartridge is seated on the drive plate of the sampler. Magnets couple the drive plate and cartridge (i.e., be careful not to pinch you hand between these plates!)

Photo 6-6. Install cartridge into RDI sampler

6. Seat the manifold "T" onto the sample cartridge (see Photo 6-7a). Install braided stainless steel pump line to cartridge and fully seat quick connector until a *click* is heard (see Photo 6-7b).

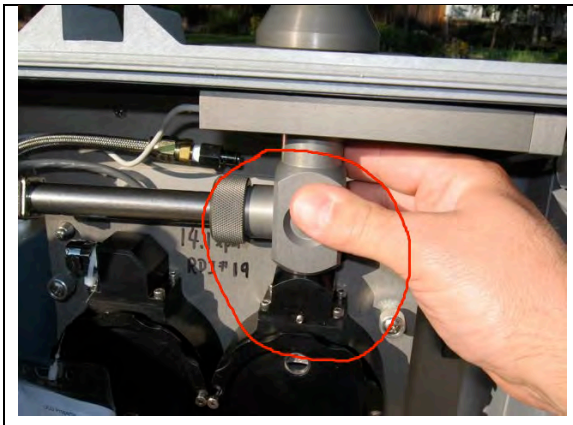

Photo 6-7a. Seat Manifold "T"

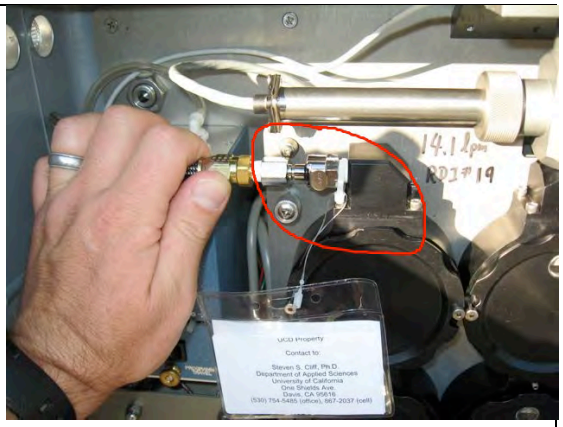

Photo 6-7b. Install pump line

7. *Gently* tighten the 6 outer screws on the sample cartridge as show in Photo 6-8. These screws only prevent the cartridge from falling out should the sampler tip over and need not be over-tightened.

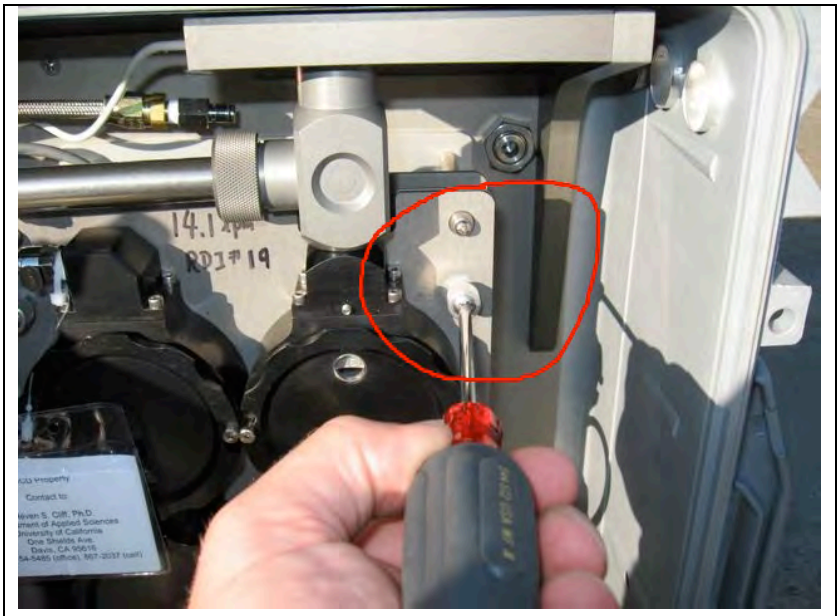

Photo 6-8. Tighten screws

8. Install the PM10 head on the inlet stack. Fully seat the PM10 head onto the sampling stack, about 4-5cm (see yellow circles in Photo 6-9). Gently but firmly screw jar onto black coupler (see red circle in Photo 6-9). This jar collects any condensation to prevent water entry to the sampler.

Photo 6-9. Install PM10 head

9. Connect vacuum pump to the sampler with the black vacuum hose.

10. Connect the power cord to sampler on the bottom and plug the power to AC power (the sampler is configured to run on voltages between 100-250 VAC at 50 or 60 Hz).

11. Provide separate power to the pump, but do not turn on pump power.

12. Protect the pump against rain, sun, etc. as necessary.

6.4. Start sampling

1. Open the RDI lid, set the dial speed to position (see red circle in Photo 6-10) according to Table 6-1, and set the rocker switch at the middle "OFF" position (see yellow circle in Photo 6-10).

Table 6-1

Dial Position	**0**	**1**	**2**	**3**	**4**	**5**	**6**	**7**
Duration (weeks)	**96**	**48**	**24**	**12**	**6**	**3**	**1.5**	**0.75**

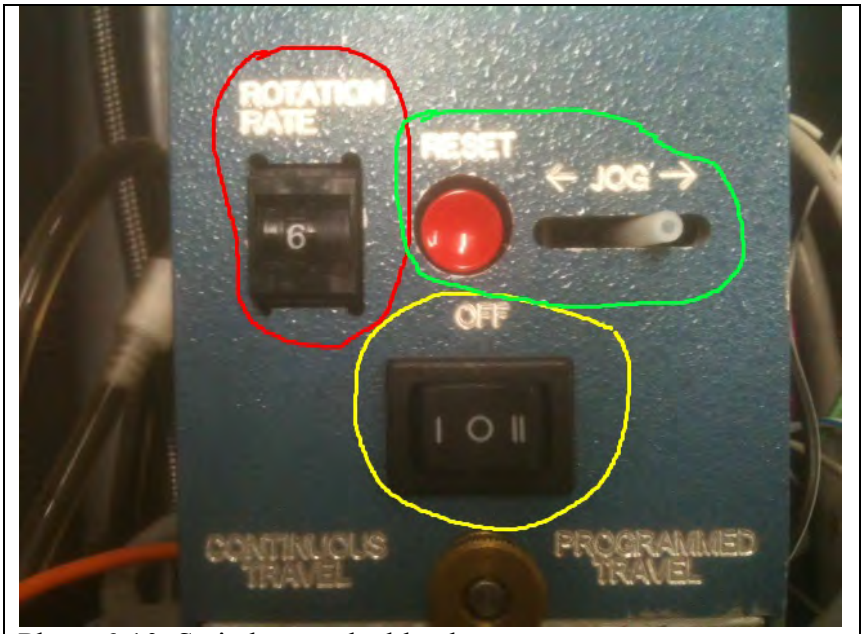

Photo 6-10. Switches on the blue box

2. Replace the fuse from the storage baggie to the black fuse holder (orange wires from 12V batteries lead to the fuse holder, see red circle in Photo 6-11). The fuse unit opens by pushing the two sides together and unscrewing. Once the fuse is replaced, a multiplexing program will start from which you should hear cycling and see a green LED flash every 2-3 seconds (see green circle in Photo 6-11).

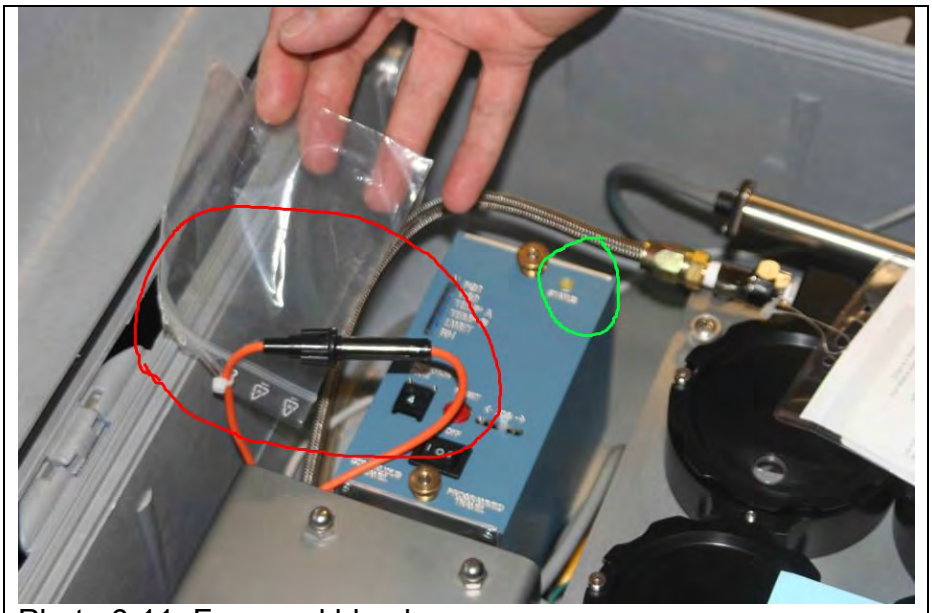
Photo 6-11. Fuse and blue box

3. There are 21 delineation marks on each drum-wheel (see Photo 6-12a) and the large space between 21 and 0 is not used for sampling because the two ends of the Mylar substrate are affixed with tape in this area. The drum-wheel position can be observed at the stage 1 site window (see red circle in Photo 6-12b).

Stage 1 is the upper right hand cylinder that is directly connected to the manifold "T." The position of the drum wheel is changed by depressing the red "RESET" for approximately 1 second until a "click" is heard and then moving the "<JOG>" handle to left or right while continuing to depress the red reset button (see green circle in Photo 6-10).

Photo 6-12a. Drum-wheel with 21 marks

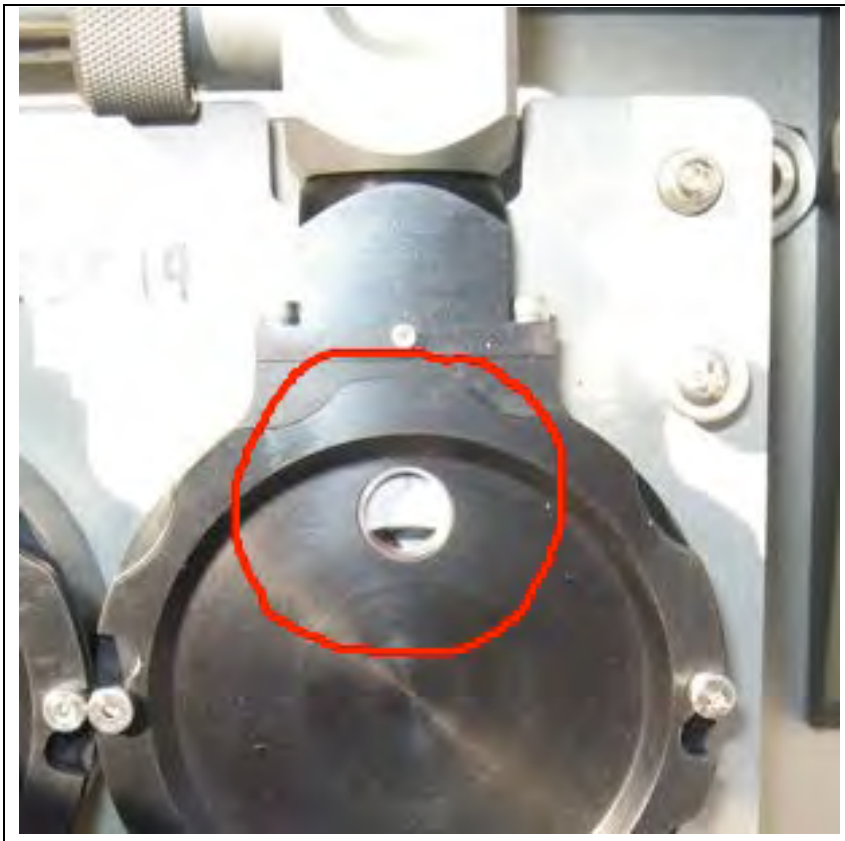

Photo 6-12b. Stage 1 Window

4. Move the drum-wheel position in the Stage 1 window to the middle between scales 21 and 0 as described in step 3. Remove the PM10 head (a reversed procedure in Photo 6-9) and connect a 20 liter/min flow meter on top of the 1-3/4" OD sampling stack. Turn on the pump, measure the flow rate for field audit, and TURN OFF the pump quickly. Because this procedure may cause contamination on the Mylar substrate, the shorter of the flow measurement, the lower of the contaminations.

5. Compare the field audit flow rate with the lab measured value recorded on the preprinted paper tag. If the field audit is lower the lab value over 5%, check all connections of the air flow (sampling stack to "T" manifold, "T" manifold to cartridge, vacuum hose to cartridge, vacuum hose to RDI case, and vacuum hose to pump) and fix the leak. Repeat Step 4 to audit the flow rate again until the audit value agrees with the lab value within 5%.

6. Replace the PM10 head back on the sampling stack (see Photo 6-0)

7. Move the drum-wheel position in the Stage 1 window to slightly greater than scale "0" (about 1-2 mm over "0") as the start position. NOTE: The total sampling time is set by the rotation rate and the length of the substrate. Therefore, the starting position should be close to, but not before "0" on ANY site window to provide the maximum sampling period possible. All stages are not aligned perfectly and thus one should confirm that the starting position is within specifications.

8. Move the black rocker switch from the middle "OFF" position to the left "CONTINUE TRAVEL" position (see yellow circle in Photo 6-10). Sampling rotation is started as soon as the RESET button is *reset* (by no longer depressing it). Record this start time and observe the drum position at 5 min and 23 seconds later (i.e., 323 seconds). This is critical: If the program started successfully, the drums will move ahead approximately 2 mm at this time. You should observe this carefully as the movement is small and this is your confirmation that the program has started. A stopwatch is useful to know when the movement will occur. Watch the site window at approximately 5 minutes past *reset* to verify movement. The *reset* procedure can be repeated if this initial movement is not confirmed.

9. Once program start is confirmed, "**power on" the pump,** and **record start date/time as well as the site information** on the preprinted paper tag (recommended to use local time in MM/DD/YY hh:mm format. If local time is not used, make a note after the time such as "UT", "PST", etc.

10. During the sampling period, check that rotation is correctly taking place according to the sampling duration. For example, total sampling interval for the 6-week duration is theoretically 42 days and there are 21 delineation marks on the drum-wheel. Thus, each day should advance about 0.5 delineation mark. If the expected rotation is not observed, a ***reset*** by depressing the red "RESET" button may be needed. Please contact UC Davis (see info on at the end of this SOP) for technical support before the "reset" procedure. NOTE: If it is necessary to *reset* the device after initial sampling on a new cartridge, there is ambient aerosol sample on the substrate if the pump has been started. Therefore, do not *reset* to "0" position, but leave in current position and record this position. The 2 mm movement at 323 seconds will provide the new start position.

11. Record unusual events as many as possible, such as power failures, stop and restart times, etc. Although the RDI sampler is equipped with a battery-powered data logger with an internal clock that monitors and records the RDI operation status (T, RH, pressure for flow rate, and drum-wheel position). The field not is still useful for RDI sample/data analysis.

6.5 Stop sampling and change the cartridge

1. Stop aerosol collection by turning off the pump (no pump, no particles).
2. To stop sampling, remove the fuse from the fuse holder (see Photo 6-11). Store the fuse in the shipment storage baggie (see Photo 6-11).

3. Remove the cartridge by:
    a. Remove the braided stainless steel pump line (see Photo 6-7b)
    b. Remove the manifold "T" by carefully slipping up into the inlet stack (from position in Photo 6-7a to position in Photo 6-5).
    c. Loosen the 6 screws on the cartridge (see Photo 6-8).
    d. Pull up cartridge starting from the bottom by rotating out using the connector tube at the bottom as a handle (See Photo 6-6).
    e. Replace white cap on cartridge (see Photo 6-6).
4. To continue sampling with next cartridge, follow the initial set-up directions of Steps 5-7 in ***Section 6.3*** of this SOP. Specifically, (1) put the new cartridge in place, (2) re-insert the braided pump line, (3) *loosely* tighten the 6 screws, and (4) move down the "T" manifold.
5. To start a new sampling interval, follow the steps in ***Section 6.4*** of this SOP.

In case of any question or problem, contact:

Yongjing Zhao at 530-219-9014 or e-mail to yjzhao@ucdavis.edu

Steve Cliff at 530-867-2037 or e-mail to sscliff@ucdavis.edu

Appendix B. MOUDI SOP

Sample Loading

a) Gloves (nitrile) should be worn for all sample handling operations. Wash your hands, and then rinse your working tweezers with DI/Methanol/Hexane. Prepare a clean surface of annealed aluminum foil. Use clean foil to seal all open holes in the impactor and cyclone as you work. Disconnect the MOUDI from the pump.

b) The impactors can either be loaded from the upper stages working down or from the bottom stages working up. Either method works, but do not open more than one stage at a time to avoid confusion. Note that the AIHL-design cyclone should remove all particles that would otherwise be collected on stages 0-4. These stages should be loaded with unweighed foil substrates at the beginning of each intensive operation period, but they do not have to be changed within the IOP.

c) Open the impactor at each sample stage in succession to expose the impaction plate. Remove the impaction plate with your “clean hand” and place it on the annealed aluminum surface. Note that the body of the impactor has silicone grease on it. Avoid placing the impaction stage in a silicone grease deposit. Remove the hold-down ring from the impaction plate using either the fingers of your clean hand or a solvent-rinsed screwdriver.

d) Open the petri dish containing the sample substrate using your “clean hand”. Any contamination on the petri dish greatly increases the chance of sample contamination later. Use your dirty hand to hold the base of the tweezers. Use the tweezers to move the sample substrate on to the impaction plate. Close the petri dish with your clean hand and place the hold-down ring loosely on the impaction plate with your clean hand.

e) It is important that the top of the sample substrate and hold-down ring be level with the top of the impaction plate during sampling. The distance between the jet orifice and the impaction plate is small, especially in the lower stages, and uneven Teflon substrates may cause flow imbalances. Push the hold-down ring onto the impaction plate slowly, keeping the sample substrate centered and flat. Inspect the sample to make sure that there are no large wrinkles (foil substrates) and that the top of the hold down ring is level with the top of the impaction plate. If these conditions are not met, try removing the hold down ring and repositioning the substrate. Note that Teflon substrates will tear at the outer ring if they are subjected to too much stress. Proceed carefully. If a tear occurs, replace the filter and try again. Be sure to record which substrate IDs were actually loaded in the log sheets.

f) Replace the impaction plate on the body post using your clean hand. Rotate the impaction plate to find the position at which the magnets have the strongest attraction. Assemble the impactor at this stage, and proceed to the next stage. Continue until all stages are loaded.

g) Open the MOUDI after filter holder by unscrewing the outer ring surrounding the body. Place the bottom half of the filter holder in the upright orientation in your “dirty” hand and use tweezers to place the afterfilter on top of the backing screen. Reattach the bottom half of the filter holder to the top half and tighten the outer ring to seal the holder.

h) Check the impaction substrates loaded in stages 0-5. Replace substrates that have a heavy loading pattern with foil substrates that have been baked at 550C for 48 hours. Inspect o-rings for damage and verify that all stages turn freely when reassembled. Lubricate as necessary.

Flow Check and Sampler Operation

a) Place the MOUDI back in the rotating cabinet and activate the rotate switch for a few seconds to lock it in place. Attach the cyclone to the top of the impactor, and reconnect the pressure gages.

b) Turn on the pump for a few seconds and adjust the valve so that the top pressure gage is at the setpoint. Check the lower setpoint. If it is within 10% of the pre-sampling value (checked at UC Davis) then the MOUDI is ready for operation. Seal the cyclone with clean foil until you are ready to sample.

c) When the sample period begins, remove the foil covering the inlet to the cyclone and start the pump. Activate the rotate switch to allow for uniform deposition. Adjust the MOUDI setpoint, and make appropriate notes in the log sheets. Check the MOUDI pressure drops at the start and finish of each sampling period. Also note the weather conditions.

Sample Unloading

a) At the end of the sample period, make a note of the time and final pressure readings, and turn off the pumps. Cover the open holes with clean foil, and move the impactor to your clean working area.

b) Follow general procedures for loading the sampler in reverse order. Impactor can be reloaded with a new set of substrates as it is unloaded, but be careful to not get confused. Use substrates in numerical order and keep good notes in the log sheets.

c) Seal collected samples in petri dish using Teflon tape, and store in freezer as soon as possible.

Teflon Filter Extraction for ICP-MS

Standard Operating Procedure

Prepared by

Walter Ham and Michael Kleeman

Reviewed by

Michael Kleeman

Effective Date: August 25, 2009

Appendix C. MOUDI ICPMS SOP

Table of Contents

1. Purpose and Application C-3
2. Summary of the Method C-3
3. Definitions C-3
4. Health and Safety Warnings C-3
5. Cautions C-3
6. Interferences C-3
7. Personnel Qualifications C-4
8. Equipment and Supplies C-4
9. Procedural Steps C-4
10. Data and Records Management C-5
11. Quality Assurance and Quality Control C-6
12. References C-7

1. PURPOSE AND APPLICABILITY

Extract airborne particulate matter collected on Teflon filters so that it can be analyzed by inductively coupled plasma mass spectrometry (ICP-MS) for 23 elements (Li, Na, Mg, Al, P, S, K, Ca, Ti, Mn, Fe, Cu, Zn, Ga, Ge, As, Se, Br, Rb, Sr, Sn, Sb, and Ba). Applicable to stretched membrane Teflon filters (R2PJ047) in size fractions of PM10 or smaller.

2. SUMMARY OF THE METHOD

Extract filters with 75% acetone/25% 1N HNO_3. Soncate for 30 minutes. Decant fluid into auto-sampler vials. Analyze samples using ICP-MS (Agilent 7500ce).

3. DEFINITIONS

DI = de-ionized water

MilliQ = ultra-pure water supply

ICP-MS = inductively coupled plasma mass spectrometry

4. HEALTH AND SAFETY WARNINGS

Wear gloves, safety glasses, and lab coat for all lab procedures. Avoid direct contact with any organic solvent.

5. CAUTIONS

All cutting boards, scalpels, Teflon weights, and other materials must be thoroughly cleaned before use. This involves scrubbing with an aqueous detergent, rinsing thoroughly with milli-Q (at least three times), followed by a methanol and a hexanes rinse, and finally drying for several hours. Trace measurements can be easily compromised by contamination. Refrigerate extracted samples before running on ICP-MS.

6. INTERFERENCES

High Li background is common on ICP-MS due to desorption from sampling cones. Minimize this background via ICP-MS tuning, without sacrificing sensitivity to other

elements as Li is not expected to contribute significantly to atmospheric particulate matter. The sensitivity of ICP-MS to some elements (e.g., Na, Mg) is low; bverify concentrations by comparison to results obtained via ion chromatography.

7. PERSONNEL QUALIFICATIONS

Basic knowledge of inorganic chemistry, training in lab procedures.

8. EQUIPMENT AND SUPPLIES

Teflon Filters (R2PJ047) 2 μm pore size. Order from Gelman or other supplier.

Avery Copier Labels #5351

Teflon-coated tweezers

Teflon cutting board

Razor or scalpel

Pipette with 200 μl tips

Acetone (Fisher Ultima grade)

Nitric acid (Fisher Trace Metal grade), prepeared as a 1N solution in milli-Q

De-ionized water (pure) – 18.2 MΩ water (i.e., "mQ") obtained from a ultra-filtration system, after allowing water to run for several minutes when valve is first opened.

Set of standards containing elements of interest (Spex2A, Rare earth, custom mix)

15mL polypropylene vials (Corning)

50mL polypropylene vials (Corning)

9. PROCEDURAL STEPS

A. Sample extraction

1. Solvent wash all tools (Teflon cutting board, half moon, o-ring, scalpel, scissors, etc.) under the hood using DI, methanol, and hexane. Allow the tools to dry before starting. Cut Teflon filters down the middle using the Teflon cutting board, cutting half moon and o-ring. Cut the outer filter ring on each side of this incision with scissors so that each

half of the filter is still supported by its outer ring. If only ½ of the filter is present (i.e. ½ removed for IC analysis) but the entire outer ring is present, cut the outer filter ring so that the remaining ½ filter is supported in a taut manner. Place half the Teflon filter with its supporting outer ring in a 50 mL Corning vial with an appropriate label.

2. Add 30 mL of a 75% acetone / 25% 1N HNO_3 solution to each 50 mL Corning vial. The acetone will remove PM from the Teflon filter while the 1N HNO_3 solution will keep the extracted metals in solution. Place the vials in a rack and place in a sonicator for 30 minutes. The sonicator water level should be even with the 30 mL mark on the Corning vials.

3. Following sonication, remove each vial from the rack and dry it with a KimWipe. This prevents sonicator water from being transferred into the sample analysis vials. Transfer the extract into new appropriately labeled 50 mL Corning vials.

4. Add 50µL of 1mM Tb internal standard to the extract, and load into the heated nitrogen blowdown system.

5. Concentrate extracts (primarily by removing acetone) to approximately 5mL. These vials will be loaded into the ICP-MS auto-sampler and the extract will be analyzed directly in its current state, and the Tb internal standard will be used to quantify the exact concentration factor (i.e., initial volume:final volume).

B. ICP-MS Analysis

1. Turn on the cooling water, argon gas, oxygen, and then the plasma.

2. While the instrument is warming up, verify that it is sensitive, steady, well-resolved, mass-accurate, has low noise, and is properly 'tuned' for low occurrence of doubly-charged ions ($Ce^{2+}/Ce^{+}<1.5\%$), and very low molecular ions ($CeO/Ce<0.4\%$).

3. Samples will be analyzed for about 6 minutes each, covering at least one isotope for all the elements of interest (plus other masses as needed to check for possible interferences and / or stability).

4. In between each sample, the probe tip that touches the samples is rinsed in a vial of clean 75/25 extraction fluid for a total cycle time of about 10 minutes per tube.

10. DATA AND RECORDS MANAGEMENT

1. Before field campaigns, all teflon filters are weighed, and are transported to the field at <0 deg C in plastic petri dishes, sealed with teflon tape, and labeled with unique sample IDs (e.g., "EPA-T47-xxxx", where xxxx is a four-digit sample code).

2. All samples and blanks collected in the field are recorded onto sample logs, which include the unique filter ID, filter material, the type of collector used, the duration of the collection, and any additional notes relevant to future analysis.

3. All containers used will also be labeled with the sample ID, including the 50mL and 15mL Corning vials used for extraction and as autosampler vials.

4. Unique sample IDs are entered into ICP-MS sequence files, which will automatically be stored in the master database created by the software, and output onto raw results files. All raw output files and chromatograms are stored on the PC interfaced to the ICP-MS, and backed up onto optical storage media after each ICP-MS run (typically 50-100 samples).

5. Processed results files will be stored individually and synthesized into a spreadsheet containing all other chemical analyses. These files will be backed up onto optical storage media.

11. QUALITY ASSURANCE AND QUALITY CONTROL

Every set of ten samples will contain at least one blank and one external standard, used to quantify instrument drift (if any).

a) Instrument blanks – a 1N nitric acid solution will be analyzed directly.

b) Extraction blanks – filters directly out of the box will be extracted identically to field samples (in 75% acetone / 25% 1N HNO_3, sonicated for 30 minutes, followed by nitrogen blowdown).

c) Field blanks – filters treated identically to field samples (pre-weighed, loaded into petri dishes, transported to the field, loaded into sampling equipment, and extracted). The only difference is that the pumps on the equipment will be not activated.

2. Three calibration curves are developed based on three external standards at range of concentrations. Calibration curves are generated once at the beginning of a run, and will only be considered acceptable if the linear regression of ICP-MS response to concentration has an r2 value of at least 0.99. Instrument drift is monitored by running a mid-level standard every tenth sample. Several elements are present in more than one external standard, and can therefore be used to validate calibrated concentrations. The three external standards include:

a. Spex2a, at the following concentrations: 20, 50, 100, 200, 500, and 1000 pptr

b. A mix of more prevalent metals, at the following concentrations: 20, 100, 200, 500 pptr, and 1, 2, 5, 20, and 100 ppb.

c. A mix of non- and major metals, including Si, P, S, Na, Mg, K, and Ca, at the following concentrations: 200, 500, 1000, and 2000 ppb.

3. At least 10% of all field samples will be re-run on a different day, and analytical precision based on these replicate samples will be reported.

12. REFERENCES

Derrick, M and Moyers, J. "Precise and Sensitive Water Soluble Ion Extraction Method for Aerosol Samples Collected on Polytetrafluorethylene Filters," Anal Lett. 14 (1981) 1637-1652.